DSPACE

https://dspace.org/

Characterisation of the quality of the Main Seam at the Ngwabe Shaft of the Zululand Anthracite Colliery, Northern KwaZulu-Natal

Mbonambi, Ntuthuko Blessing

2021

https://hdl.handle.net/10539/33027

Downloaded from a DSpace repository. https://dspace.org/



Characterisation of the quality of the Main Seam at the Ngwabe Shaft of the Zululand Anthracite Colliery, Northern KwaZulu-Natal

June 2021

Ntuthuko Blessing Mbonambi

Student number 0705285k

Supervisors:

Professor Gillian Drennan

Doctor Phillip John Hancox

Professor Nicola Wagner

Declaration

I, Ntuthuko Blessing Mbonambi (Student number: 0705285k), am a student registered for the degree: MSc Economic Geology, in the year 2021. I hereby declare the following:

• I am aware that plagiarism (the use of someone else's work without their permission and/or without acknowledging the original source) is wrong;

• I confirm that ALL the work submitted for assessment for the above degree is my own unaided work except where I have explicitly indicated otherwise;

• I have followed the required conventions in referencing the thoughts and ideas of others; and

• I understand that the University of the Witwatersrand may take disciplinary action against me if there is a belief that this is not my own unaided work or that I have failed to acknowledge the source of the ideas or words in my writing.

Signature:  Date: 21 June 2021

Supervisor: Date:

Supervisor: Date:

Supervisor: Date:

Acknowledgements

I want to thank the Almighty God for giving me the opportunity to enrol and study in this programme. All praise and glory be unto Him alone.

To my supervisors, Professor Gillian Drennan, Doctor Phillip John Hancox, and Masters Programme coordinator Professor Judith Kinnaird. Thank you very much for your guidance, for sharing your geological knowledge and helping me with the skills necessary to become a competent geologist. Your expertise, work ethic and professionalism are of a high standard and I have learnt a lot from each of you. I appreciate all the support you gave me.

To Professor Nicola Wagner of the University of Johannesburg, and her assistant in the Geology Department; thank you for allowing me to use your resources to complete petrographic analyses, for the guidance you gave and for availing yourself when needed.

To my wife Yonela Mbonambi; thank you so much for your support and continuous encouragement towards me working on and completing this programme.

To the Ogunshola family; thank you very much for the support you have demonstrated towards me.

I would also like to thank the Zululand Anthracite Colliery mine for all the support, the resources and the time off work they gave me to carry out and complete this study.

I would also like to thank my family at large for their continuous support and prayers encouraging me to do well.

Abstract

The Nongoma Coalfield in KwaZulu-Natal is currently one of the least well-known coal deposits in South Africa, yet it is of critical importance as it contains the best quality anthracite in South Africa. The coalfield is still set to remain the country's major source of anthracite and high-quality metallurgical source for local industry. Coal rank increases from west to east within the Karoo Basin in South Africa. Coal maturity stages include peat, lignite, bituminous and anthracite.

Previous work has focused mainly on the structural controls of the coal deposits of the Nongoma Coalfield; no work has been undertaken on quantifying the nature of the seams - particularly the principal economic Main Seam.

Thirteen channel samples were collected for this research at several localities at Section 30 of the Ngwabe Shaft at Zululand Anthracite Colliery. Here the Main Seam may be divided into three plies: (i) Coal mainly Bright, Dull (CBD), (ii) Coal mainly Dull, Bright (CDB) and (iii) Coal Bright (CB). Proximate, washability and petrographic (maceral analyses and vitrinite reflectance) analyses were conducted on each ply, thereby allowing for the first description of the physio-chemical and petrographic constituents of the Main Seam in the Nongoma Coalfield.

The proximate analyses indicate that the CBD, CDB, and CB plies are characterised by low Inherent Moisture of 1.4-4.2%, Ash of 7.6-20.7%, Volatile Matter of 5.1-6.8%, and a high Fixed Carbon content of 71.4-84.5%. The Total Sulphur analysis revealed low values of Total Sulphur ranging from 0.74-1.62%. The maceral analysis reflected that the CBD, CDB, and CB plies are rich in inertinite and vitrinite, with no liptinite content. The basal CB ply and the top CBD ply exhibits the same maximum reflectance

value (5.17%), but the minimum reflectance values recorded for the CB ply (2.40%) and the CBD ply (2.03%) are different. The CBD ply has the highest percentage of mineral matter, mainly sulphides (2.3-3.8%), clay (3.2-8.0%), quartz (0.2-1.0%), and carbonates (0-5.6%). The CB ply reflects the lowest percentage of mineral matter, mainly sulphides (0.8-2.8%), clay (0.2-1.6%), and carbonates (0-0.2%). Quartz is not present in the CB ply.

The Main Seam is overlain by two well-defined marker horizons, namely the Upper anthracite marker and the Wave rippled cross laminated marker. The Upper anthracite marker occurs 45m above the Main Seam and is a thin shaly anthracite seam. The Wave ripple marker lies some 80m above the Main Seam. Because this horizon is slightly calcareous it has a distinctive appearance when weathered. This marker is very useful in defining target areas in this structurally complex environment. In most areas the roof consists of competent sandstones, and the floor comprises siltstones and carbonaceuous shale.

In conclusion, this research has shown that the Main Seam in Section 30 of the Ngwabe Shaft is comprised of high quality anthracite and that the CDB ply would be the best ply to be targeted should selective mining be considered in the future.

Table of Contents

Declaration 2
Acknowledgements 3
Abstract 4
Table of Contents 6
List of Figures 9
List of Tables 12
Acronyms and Abbreviations 13
Chapter 1 15
Introduction 15
Location of the study area 16
Regional geology 21
Local geology of the study area 27
A drill core long: NG-108 28
Stratigraphy 35
Delta sequence 36
Shelf deposits 36
Prodelta deposits 38
Wave-ripple cross-lamination 38
Interbeds of laminated siltstone and medium-grained sandstone 40
Medium to coarse-grained sandstone with traction current-formed structures 41
Distributary mouth bars 42
Coarse-grained sandstone interlaminated with shale showing vertical bioturbation burrows 42
Interdistributary bay sequence 43
Coarse-grained sandstone interbedded with shale and siltstone 43
Distributary channel deposit 44
Coarse-grained, cross-laminated, whitish sandstone 44
Fluvial sequence 44
Channel deposits 45
Medium-grained sandstone in lower angle horizontal stratification 45
Flood basin deposits 46
Fine-grained siltstone interlaminated with shale 46

Coal seams 47
Chapter 2 49
Research Methodology 49
Introduction 49
Channel sampling 49
Petrographic analysis 53
Sample preparation 53
Petrographic analysis – methodology 53
Proximate analysis 54
Inherent Moisture (IM) content 54
Volatile Matter (VM) 54
Ash content 55
Fixed Carbon (FC) 55
Total Sulphur analysis 56
Washability analysis 56
Chapter 3 57
Introduction 57
Coal quality 57
Proximate analysis 57
Total Sulphur analysis 58
Washability analysis 59
Prime product calculations 60
Middlings product calculations 60
Channel Sample 30B 61
Channel Sample 30AI 69
Channel Sample 30D 77
Petrography analysis 85
Maceral analysis 85
Vitrinite reflectance 90
Chapter 4 94
Discussion and Conclusion 94
Conclusion 100
References 102

Appendices

1: Geological Log Drill hole NG-108 113
2: NG-108 Core photos 172
3: Coal quality data and Proximate analysis data..... 177
4: Washability data 178
5: Petrographic data analyses and Maceral group analyses..... 183
6: Reflectance of vitrinite analysis (RoV%) histograms 184

List of Figures

Figure 1: Map showing the distribution of the coalfields of South Africa and the lithostratigraphic units that host them (Hancox and Götz, 2014)..... 17

Figure 2: A topographic map showing the regional locality of the ZAC mining Operations, with reference to the nearby tribal authority areas and the Hluhluwe-uMfolozi Game Reserve (www.golder.com)..... 18

Figure 3: A topographic map showing the regional locality of the ZAC mining operations:
The Ngwabe Shaft, the Deep E Shaft, and the Outcrop Shaft (www.golder.com)..... 20

Figure 4: Generalised stratigraphic sequence of the Karoo Supergroup fill of the Nongoma Graben in the Msebe area, Nongoma *Coalfield* (Hatherly and Sexton, 2013) 24

Figure 5: A geological map depicting the structural setting of the study area (ZAC Geologists)..... 26

Figure 6: A generalised geological section of the ZAC mines showing the 14 lithological units (ZAC Geologists)..... 28

Figure 7: A photograph of a drill core from a drill hole NG-108 located 300m from the Section 30 where channel samples were collected..... 29

Figure 8: A detailed Main Seam log from the drill hole NG108 30

Figure 9: Google Earth image showing the position of the shafts and drill hole NG-108 34

Figure 10: A sedimentary log depicting facies and their depositional environment (Whateley, 1980) 36

Figure 11: Measured stratigraphic profiles of the Karoo Supergroup showing coarsening-upward and fining-upward depositional trends and interpreted depositional environment (Turner and Whateley, 1983)..... 37

Figure12: Wave-ripple cross-lamination in drill hole NG-108 (an example of unit 1 of ZAC stratigraphy)..... 39

Figure 13: Medium-grained sandstone with interbeds of laminated siltstone (an example of unit 2 and some part of unit 11of the ZAC stratigraphy)..... 40

Figure 14: Medium- to coarse-grained sandstone (an example of unit 3, unit 5, unit 7, and unit 9 of the general stratigraphy of ZAC) 41

Figure 15: Course-grained sandstone interlaminated with shale showing vertical bioturbation burrows 42
Figure 16: Very fine-grained sandstone interbedded with shale and siltstone in drill hole NG-108 43
Figure 17: Coarse-grained, cross-laminated, whitish sandstone..... 44
Figure 18: Medium-grained sandstone with lower angle horizontal stratification (source: NG-108)..... 45
Figure 19: Fine-grained siltstone interlaminated with shale 46
Figure 20: Ngwabe Shaft Section 30 layout showing the location where the channel Sampling was conducted……..50
Figure 21: An example of the coalface where channel sampling was conducted for this Study (Photo by Blessing at the coalface in Section 30) 51
Figure 22: Graphical representation of the Ash Yield and RD Yield washability result of the CBD ply of the CS30B..... 65
Figure 23: Graphical representation of the Ash Yield and RD Yield washability result of the CDB ply of the CS30B..... 65
Figure 24: Graphical representation of the Ash Yield and RD Yield washability result of the CB ply of the CS30B. 65
Figure 25: The densimetric and ash yield curves of the prime product of the CBD ply of the Channel Sample 30B 66
Figure 26: The densimetric and ash yield curves of the prime product of the CDB ply of the Channel Sample 30B 67
Figure 27: The densimetric and ash yield curves of the prime product of the CB ply of the Channel Sample 30B 69
Figure 28: Graphical representation of the Ash Yield and RD Yield washability result of the CBD ply of the CS30AI..... 73
Figure 29: Graphical representation of the Ash Yield and RD Yield washability result of the CDB ply of the CS30AI..... 73
Figure 30: Graphical representation of the Ash Yield and RD Yield washability result of the CB ply of the CS30AI 73
Figure 31: The densimetric and ash yield curves of the prime product of the CBD ply of the Channel Sample 30AI 75
Figure 32: The densimetric and ash yield curves of the prime product of the CDB ply of the Channel Sample 30AI 76

Figure 33: The densimetric and ash yield curves of the prime product of the CB ply of the Channel Sample 30AI 77
Figure 34: Graphical representation of the Ash Yield and RD Yield washability result of the CBD ply of the CS30D 81
Figure 35: Graphical representation of the Ash Yield and RD Yield washability result of the CDB ply of the CS30D 81
Figure 36: Graphical representation of the Ash Yield and RD Yield washability result of the CB ply of the CS30D 81
Figure 37: The densimetric and ash yield curves of the prime product of the CBD ply of the Channel Sample 30D 82
Figure 38: The densimetric and ash yield curves of the prime and middlings product of the CDB ply of the Channel Sample 30D 84
Figure 39: The densimetric and ash yield curves of the middlings product of the CB ply of the Channel Sample 30D 85
Figure 40(A-F): Photomicrographs of different maceral determined within the Main Seam 90
Figure 41: Unimodal distribution of the vitrinite reflectance of the CBD, CDB, and CB plies of the Main Seam 93

List of Tables

Table 1: Results of proximate analysis for the CBD, CDB and CB plies (source: Appendix 2)..... 58
Table 2: Results of Total Sulphur analysis for CBD, CDB, and CB..... 59
Table 3: A generic table used to calculate prime and middlings products at an ash yield of 8.5% 60
Table 4: Washability analyses of the CBD, CDB, and CB plies of the Channel Sample 30B (source: Appendix 4)..... 62
Table 5: The prime and middlings products results of the CBD ply of the Channel Sample 30B..... 66
Table 6: The prime and middlings products results of the CDB ply of the Channel Sample 30B..... 66
Table 7: The prime and middlings products results of the CB ply of the Channel Sample 30B..... 68
Table 8: Washability analyses of the CBD, CDB, and CB plies for Channel Sample 30AI 70
Table 9: The prime and middlings product results of the CBD ply of the Channel Sample 30AI..... 74
Table 10: The middlings product results of the CDB ply of the Channel Sample 30AI 75
Table 11: The prime and middlings products results of the CB ply of the Channel Sample 30AI..... 76
Table 12: Washability analyses of the CBD, CDB, and CB plies for Channel Sample 30D 78
Table 13: The middlings product and waste results of the CBD ply of the Channel Sample 30D 82
Table 14: The prime and middlings products results of the CDB ply of the Channel Sample 30D 83
Table 15: The middlings product and waste results of the CB ply of the Channel Sample 30D 84
Table 16: Results of the maceral group analysis of the CBD, CDB and CB plies within the Main Seam (source: Appendix 5)..... 88
Table 17: Vitrinite reflectance analysis results of the CBD, CDB and CB plies..... 92

Acronyms and Abbreviations

ASTM	American Society for Testing and Materials
CB	Coal Bright
CBD	Coal mainly Bright, Dull
CDB	Coal mainly Dull, Bright
cm	Centimetre
FC	Fixed Carbon
g/cm³	grams per cubic centimeter
IM	Inherent Moisture
ISO	International Standards Organisation
KZN	KwaZulu-Natal
MJ/kg	Megajoules per kilogram
MKB	Main Karoo Basin
m	Metre
mm	Millimetre
mmf	Mineral Matter Free basis
PN	Pyritic Nodular

PY	Pyritic Stringer
RD	Relative Density
RoV%	Reflectance of Vitrinite
SACS	South African Committee for Stratigraphy
SANS	South African National Standard
TS	Total Sulphur
VM	Volatile Matter
UJ	University of Johannesburg
Vol%	Volume Percentage
ZAC	Zululand Anthracite Colliery

Chapter 1

Study Aim and Objective

The aim of this research report is to characterise the Main Seam in the Ngwabe Shaft located in the Nongoma Coalfield. The Main Seam comprises three plies: (i) the Coal mainly Bright, Dull (CBD), (ii) Coal mainly Dull, Bright (CDB) and (iii) Coal Bright (CB). The objective of this research report is to investigate the coal quality and petrography of each ply to determine which ply within the Main Seam in the Ngwabe Shaft is of best quality, and that can be targeted should selective mining be considered in the future.

Introduction

Coal mining started on a commercial basis in South Africa in 1857 (Eberhard, 2011). Currently, South Africa is the 7th largest producer of coal in the world (WCA, 2019). Coal remains the primary source of domestic power generation, cement manufacturing and steel production (Ward and Suárez-Ruiz, 2008). South Africa is also the only country in the world that operates commercial coal-to-liquids synfuel plants of which coal resources are part of the major feedstock (Burton et al., 2018.). The production of steel is highly dependent on coal; about 60% of steel production uses coal. Therefore, metallurgical coal, in this case anthracite, is vital in steel and petrochemical making processes (McHugh, 2017). The Zululand Anthracite Colliery (ZAC) is acknowledged as the sole producer of prime anthracite in South Africa (Board, 2018). The ZAC's unique qualities are the highest ranking, least ash and least volatile anthracite produced in South Africa. However, the qualities of this coal deposit are largely unknown because of the paucity of research that has been conducted on this coalfield.

Location of the study area

According to Hancox and Götz (2014) there are 19 coalfields in South Africa, located mainly in the Gauteng, Mpumalanga, Limpopo, Free State, KwaZulu-Natal (KZN) and Eastern Cape provinces (Figure 1). The study area for this research report is within the Nongoma Coalfield in KZN.

The ZAC is located within the Nongoma Coalfield, Northern KZN in South Africa. It falls within the magisterial districts of Nongoma and Mahlabatini. The Hluhluwe-uMfolozi Game Reserve is situated to the east of the ZAC (Figure 2). The ZAC is situated approximately 48km north-east of Ulundi; approximately 32km east of Mahlabatini; 36km south-west of Hlabisa, and 42km south of Nongoma.

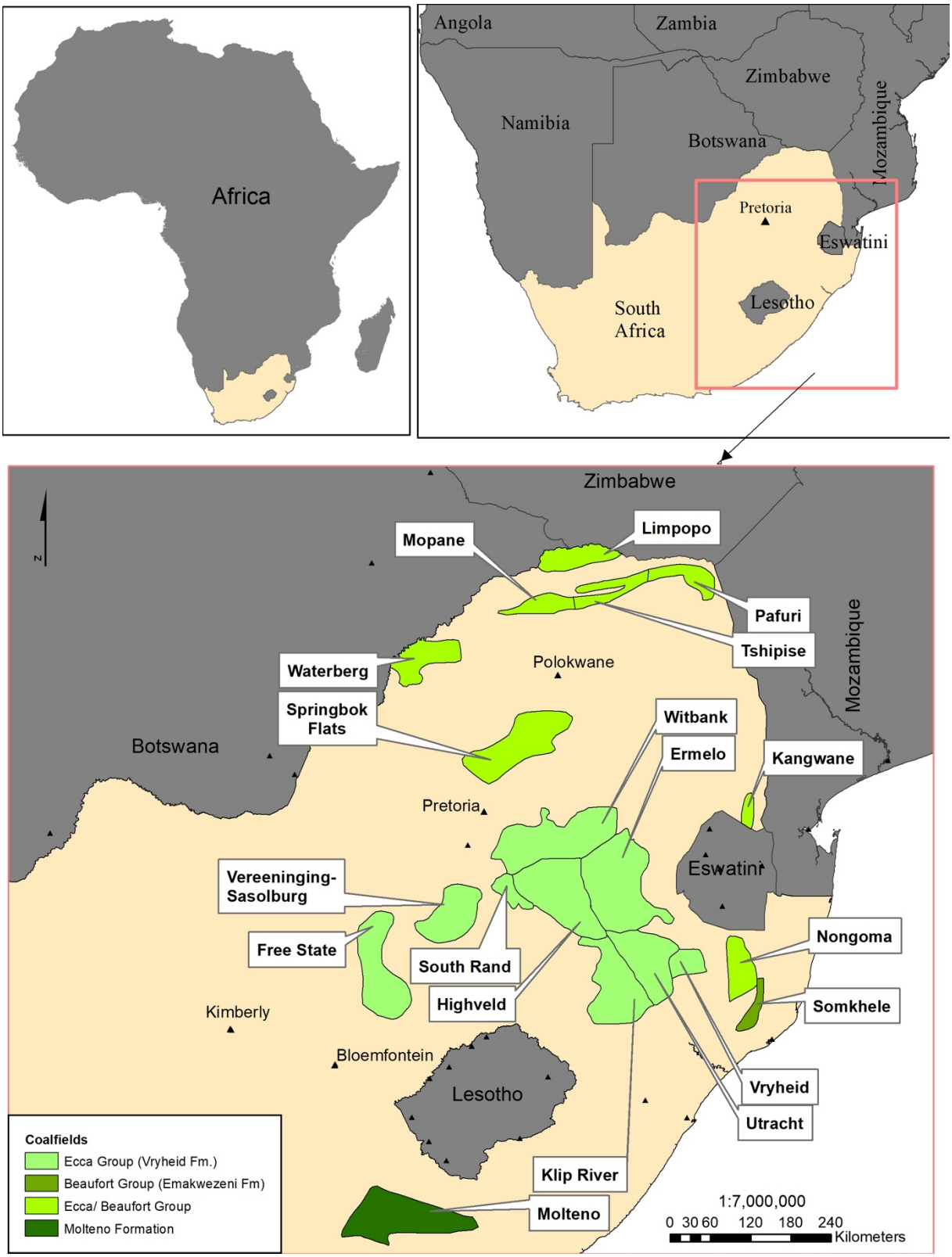


Figure 1: Map showing the distribution of the coalfields of South Africa and the lithostratigraphic units that host them (Hancox and Götz, 2014).

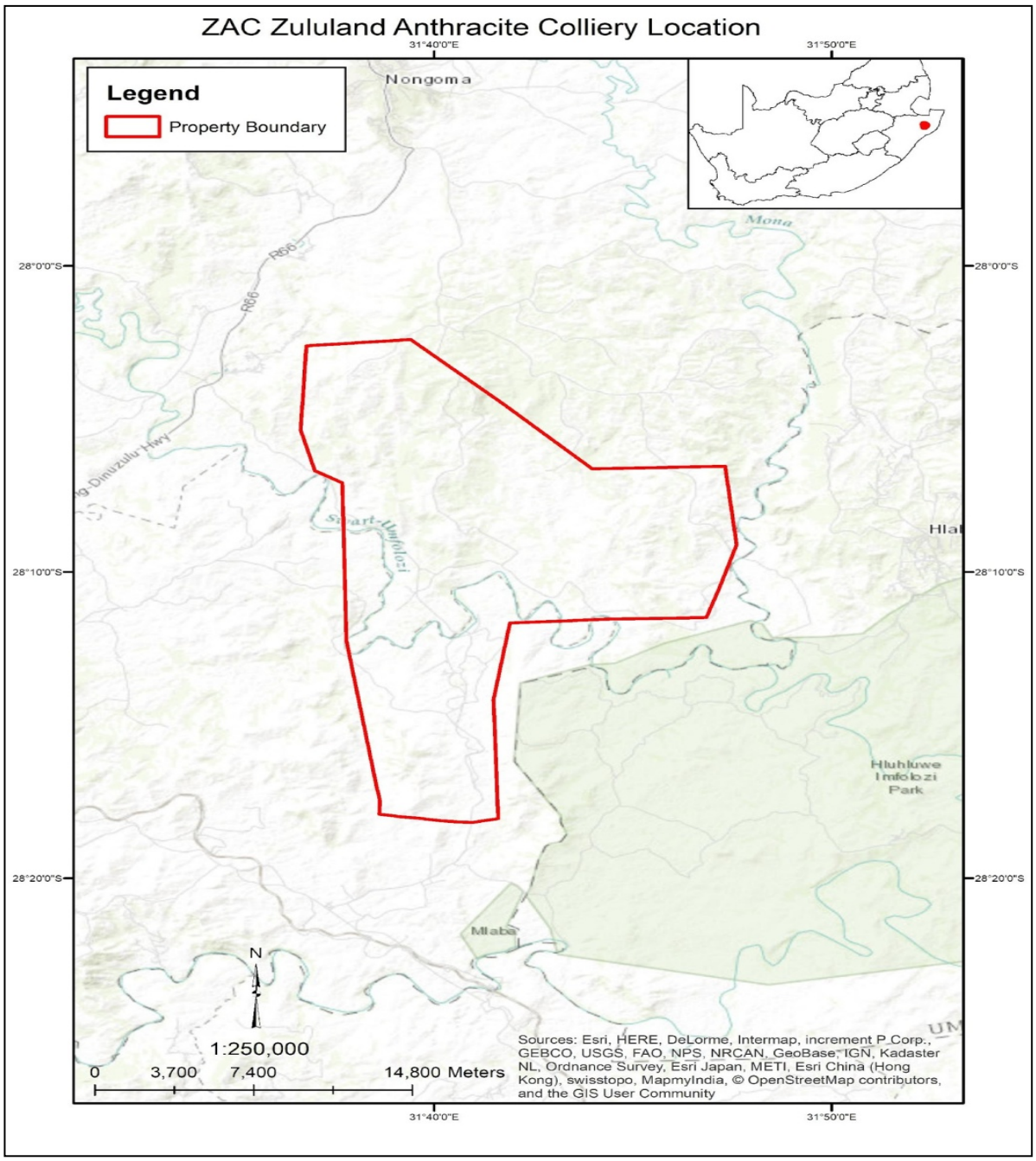


Figure 2: Topographic map showing the regional locality of the ZAC mining operations, with reference to the nearby tribal authority areas and the Hluhluwe-uMfolozi Game Reserve (*www.golder.com).*

Coal mining at the ZAC occurs in three main shafts: Ngwabe Shaft, Deep E Shaft and Outcrop Shaft (Figure 3). The Ngwabe and Deep E shafts are known as 'high seam' shafts with seam thickness varying between 2-3m. The Outcrop Shaft is known as the 'low seam' with a seam thickness ranging from 0.8-1.2m. The variability in seam thickness is because high coal seams are confined within the graben, whereas thin coal seams are confined towards the edges of the basin margin where there was less vegetation for thick coals to form (Whateley, 1980). The ZAC is the only operating mine in the Nongoma Coalfield, producing a prime and middlings anthracite product from the Main Seam - mainly for the metallurgical industry. The prime peas produced at the ZAC are used by electrode paste, calcium carbide and ferrochrome producers, whereas its prime nuts are used by ferrochrome and steel producers and for domestic heating purposes. The prime duff is used by mineral sands producers and in ferrochrome direct current furnaces, while middlings are used by local and international sinter pellets producers (WCA, 2019).

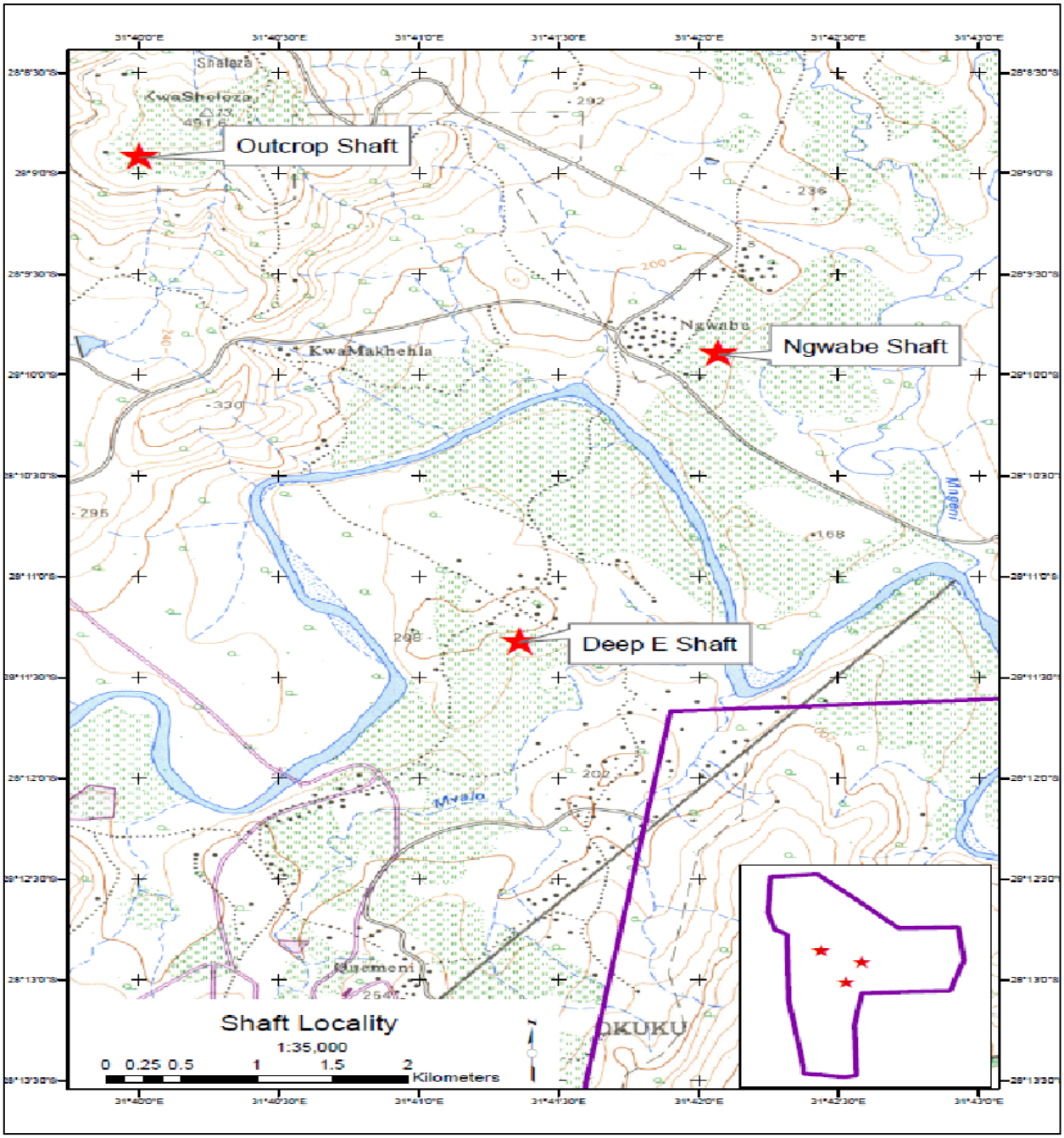


Figure 3: A topographic map showing the regional locality of the ZAC mining operations: the Ngwabe Shaft, the Deep E Shaft, and the Outcrop Shaft (www.golder.com).

Regional geology

The South African coal deposits of economic value are preserved in the Karoo Supergroup (Snyman and Botha, 1993). Coal deposits contained in the Karoo basin are within the Lower Permian Vryheid Formation and the Triassic Molteno Formation; however only coals within the Vryheid Formation are of economic value (Cadle et al., 1993).

The main Karoo Basin of South Africa is a Late Carboniferous–Middle Jurassic retroarc foreland fill developed in front of the Cape Fold Belt in relation to subduction of the palaeo-Pacific plate underneath the Gondwana plate (Catuneanu et al., 1998). The Karoo sedimentary fill corresponds to a first-order sequence with the basal and top contacts marking profound changes in the tectonic setting, i.e. from extensional to foreland and from foreland to extensional, respectively. The flexural behaviour to this retroarc foreland model was proposed in explaining the deposition within the proximal and distal parts of the basin (Catuneanu et al., 1998). This flexural foreland basin theory is included in later studies of the depositional environments of the sub-Saharan Karoo age basin (Catuneanu et al., 2005).

The Karoo Supergroup in South Africa is subdivided into five main groups, namely: Dwyka, Ecca, Beaufort, Stormberg and Drakensberg (SACS, 1980). The Dwyka Group is composed of diamictite, fluvioglacial pebbly sandstone, conglomerate, varved shales and mudstones with dropstone pebbles (Johnson et al., 1997). The Dwyka Group is conformably overlain by the horizontally stratified Permian Ecca Group comprising the Pietermaritzburg Formation and Vryheid Formation in which coal seams are developed (Von Brunn, 1993). Jurassic dolerite dykes and sills intrude the strata (Von Brunn, 1993).

The Ecca Group in the type-Karoo Basin of South Africa occurs between the Late Carboniferous Dwyka Group and the Late Permian-Middle Triassic Beaufort Group, occupying most of the Permian time slot for Karoo Supergroup lithologies (Catuneanu et al., 2005). In some other places the Ecca Group occupies the same time interval, but the lithostratigraphic names of the South African Dwyka and Beaufort Groups are different in neighbouring countries (Cairncross, 2001). The Ecca Group consists of a clastic sequence of sandstone, siltstone, mudstone and coal in some areas outcrop in the main Karoo Basin in South Africa, and in all other Southern Africa Karoo Supergroup localities (SACS, 1980; Catuneanu et al., 2005). This sequence of clastic sediments in the northern Karoo Basin is subdivided into the Pietermaritzburg, Vryheid and Volksrust Formation. This sequence cannot be correlated to clastic sediments to the south, although the Vryheid Formation is regarded as the time equivalent of the upper Prince Albert and Whitehill Formations. The Volksrust Formation extends horizontally into the Tierberg Formation (Catuneanu et al., 2005; Visser, 1993).

The basal Lower Permian Pietermaritzburg Formation consists of fissile, medium to dark grey, greyish olive, dark greenish grey, olive grey, greyish blue to medium bluish grey, laminated, often carbonaceous shales with subordinate sandstones, and manifest a reduction in thickness from south to north (Bordy et al., 2017). The Pietermaritzburg Formation was named after the largest city in KwaZulu-Natal (KZN) (SACS, 1980). It however does not outcrop within the northern part of the Karoo Basin. The overlying Vryheid Formation contains several coarsening-upward sequences with coals in the upper part of the sequence (Hancox and Götz, 2014). This coal-bearing sequence consists of shale and sandstone with a maximum thickness of 500m in the main Karoo Basin (SACS, 1980). A comprehensive sedimentological interpretation of the Vryheid Formation was first done by Hobday (1973) who interpreted this formation in terms of a

deltaic facies model explained in the stratigraphy section. The Volksrust Formation consists of 150-250m of dark siltstone or mudstone and lies between the Vryheid Formation and the Beaufort Group (Cairncross, 2001). The basaltic and andesitic lavas of the Drakensburg Group completely masked the Karoo Supergroup. Only the Vryheid Formation of the Ecca Group is preserved in the study area; its coal deposit is of economic value.

The coal seam contained within the Nongoma Coalfield of the Lower Ecca Group is referred to as Main Seam, and is exploited by the ZAC for steel production in domestic and international markets (McHugh, 2017). The Nongoma Coalfield stretches from east of Gluckstadt in the west, where it shares a common boundary with the Vryheid Coalfield, to a north-south trending boundary in the east where it abuts the Somkhele Coalfield (Whateley, 1980). Its southern boundary is formed by the Pongola River and it extends northwards to a common boundary with the northern extent of the Somkhele Coalfield, which then continues into Swaziland.

The Nongoma Coalfield is preserved in a graben structure (Whateley, 1980). According to Eglington (2006) tensional faulting may have been initiated in early Karoo times and therefore could have influenced deposition in the area. Major rifting was associated with the renewed plate tectonic movements during the Jurassic and Cretaceous periods, which resulted in the development of numerous north-south striking faults (Blenkinsop, 2008). The faulting displaced the coal seams into north-south trending blocks that were further subdivided by northwest-southeast striking transverse faults (Whateley, 1980). The discrete blocks caused by faulting divided the Nongoma Coalfield into a Nongoma West and Nongoma East section (Blenkinsop, 2008); each section contains distinctly different lithologies. Individual coal-bearing areas are separated from each other and coal

is not continuously developed across the coalfield. Nongoma West is unique and displayed no characteristics similar to any other coalfield in KZN. The coal here is restricted to three seams within the Vryheid Formation of the Ecca Group (Figure 4).

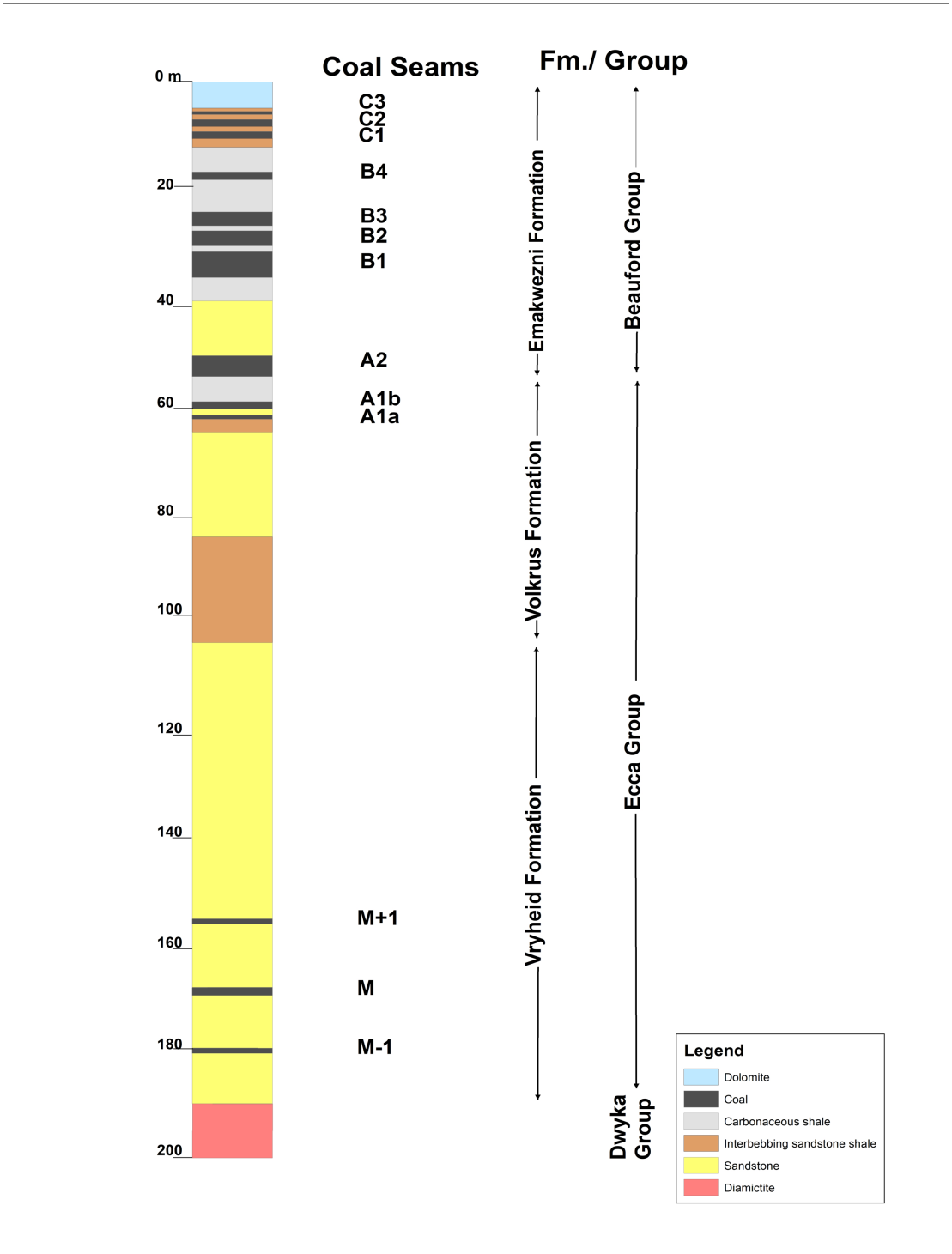


Figure 4: Generalised stratigraphic sequence of the Karoo Supergroup fill of the Nongoma Graben in the Msebe area, Nongoma Coalfield (Hatherly and Sexton, 2013).

A generalised stratigraphic profile of the Karoo Supergroup fill of the Nongoma Graben in the Masebe area of the Nongoma Coalfield is provided in Figure 4. Overlying the Nongoma Coalfield are the coals of the Emakwezini Formation within the Beaufort Group. Both the lithologies of the Vryheid and Emakwezini Formations of the Ecca and Beaufort groups, respectively, contain coal of economic value (Bordy and Prevec, 2015).

The Nongoma graben is a tectonic active zone; it is therefore geologically complex and associated with crustal weakness and high sustained heat flow which indurated the entire coalfield to produce anthracite (Eglington, 2006). The plate tectonic activities that resulted in the rifting influenced faulting, dividing the coalfield into numerous discrete blocks (Blenkinsop, 2008) (Figure 5). The seam dip within the Nongoma Coalfield ranges from 0-15^{o}. Dolerite intrusions that occurs throughout the coalfield do, in some areas, locally steepen the dip (Snyman, 1998). The faulting evident in this area is linked with a series of phases of Jurassic-aged dolerite intrusions that occurs as dykes and sills. Turner and Whateley (1983) suggest that the anthracitisation process was influenced by early phases of dolerite intrusion occurring, mainly in the form of sills in addition to an increasing regional geothermal gradient from west to east. The younger dolerite sills and dykes that were largely associated with the increased tensional faulting altered the coal where younger dolerite sills and dykes were in contact with or in close proximity to the seams (Neumann et al., 2011). This is why it remains critical to characterise the quality of the Main Seam and to identify the ply with the best coal quality.

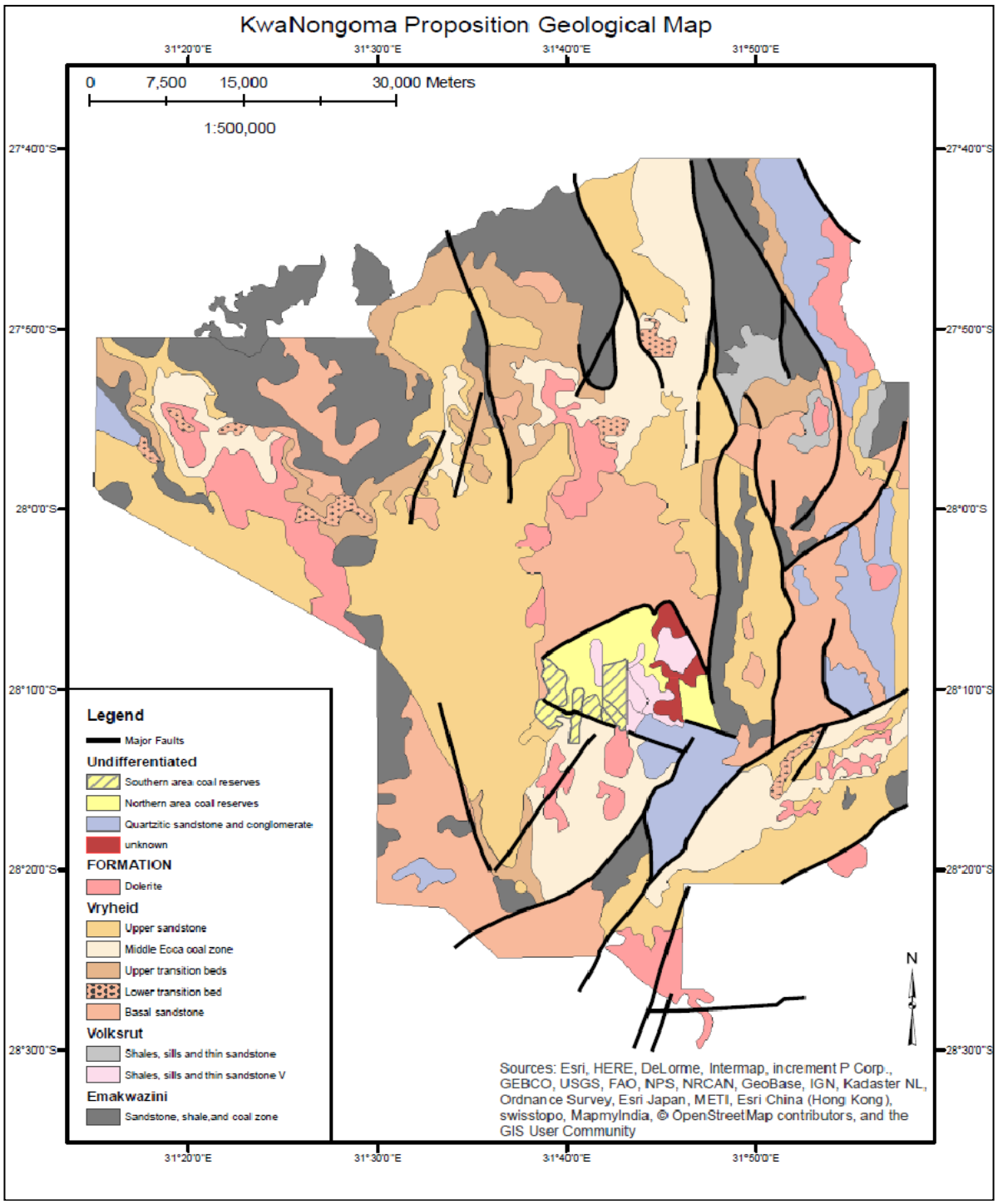


Figure 5: Geologic map depicting the structural setting of the Nongoma Coalfield (ZAC geologists).

The ZAC lies on the south-east edge of the Kaapvaal Craton at the intersection of the Namaqua Natal and Mozambique mobile belts (Turner and Whateley, 1983). It is located in the Nongoma graben structure that developed on the continental margin during post-depositional extension (Eglington, 2006). When this process occurred, thick sediment accumulated and high geothermal gradients and active intrusions took place because of the breaking-up of Gondwana; the result was a very fractured crust (Holmes, 1951; Whateley, 1980). This tectonic setting explains why the ZAC and the nearby Somkhele coal mines are believed to be the best anthracite deposits in South Africa - where regional heat and pressure play the major role in the anthracitisation process (Whateley, 1980). Furthermore, the geological setting of the ZAC is structurally complex and the strata are intersected by intrusions such as dolerite dykes and sills that formed a plumbing network of the Karoo large igneous province (Van Niekerk, 1995). Where dolerite dykes and sills and faults occur within the mining environment the coal is normally displaced.

Local geology

The geology of the ZAC comprises sedimentary successions of the lower Ecca Group (Baiyegunhi et al., 2019). Coals of economic value being exploited in the mine occur within the lower Ecca Group sedimentary sequence. The generalised stratigraphy at the ZAC (Figure 6) is subdivided into 14 lithological units; unit 10 is the Main Seam.

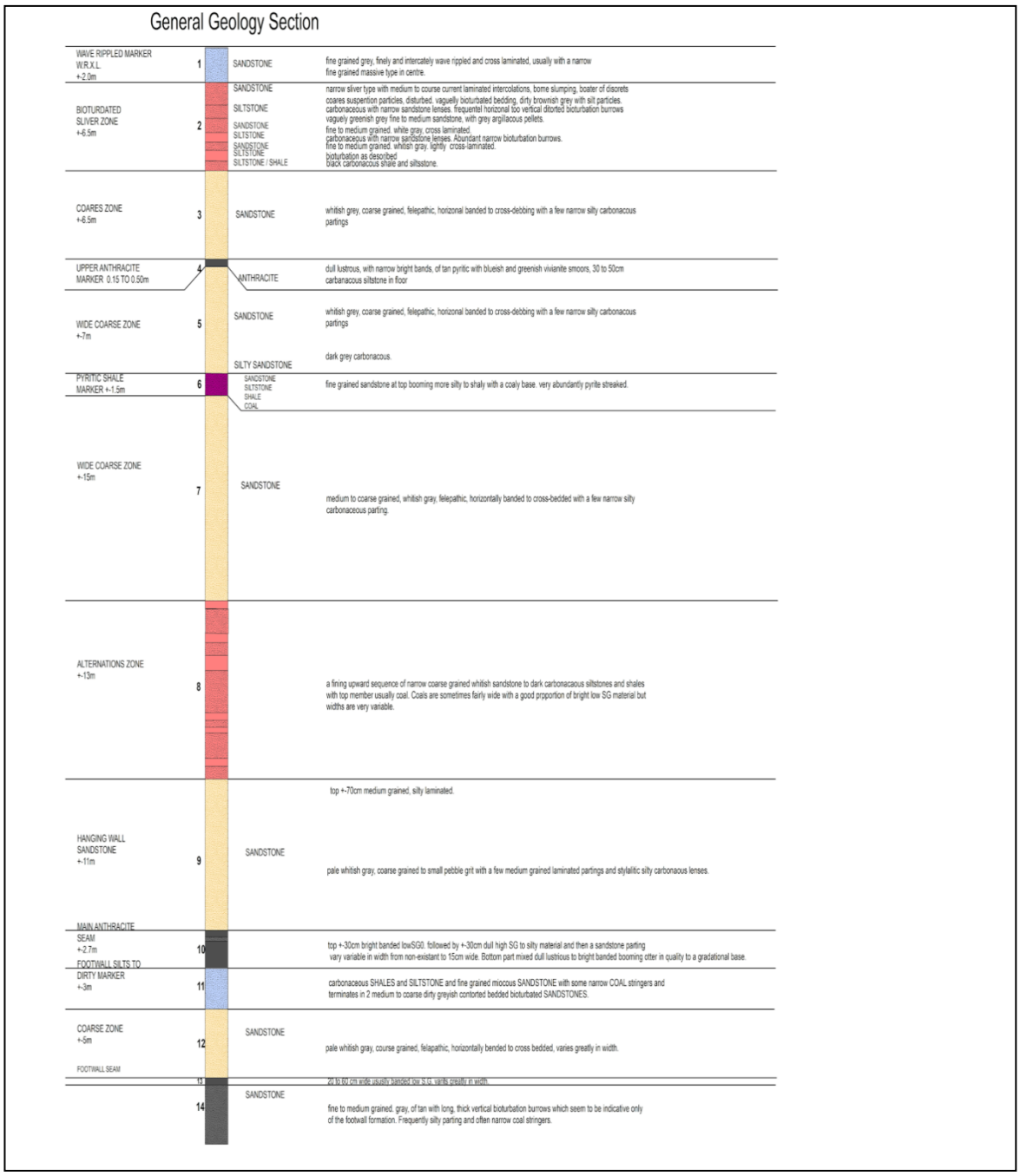


Figure 6: Generalised geological section of the ZAC mines showing the 14 lithological units (ZAC geologists).

A drill core log: NG-108

A drill hole NG-108 was drilled in the Ngwabe area to a depth of 311.86m (Appendix 1). The drill core revealed that the Nongoma Coalfield is comprised of the sedimentary units of the lower Ecca Group. The sedimentary units of the lower Ecca Group in this coalfield consist of sandstones, shales, siltstones, and coal of economic value as shown by drill

core photos in Appendix 1. Sandstones are up to 15m thick, while shales and siltstones are 3m thick. Thick dolerite intrusions occur at shallow depths (below 200m) and they can be up to 20m thick. The Main Seam is overlain by a thick sandstone unit of about 9m, and underlain by a 3m thick layer of shales interlaminated with sandstone. Mining activity at the ZAC occurs at depth between 297.60-299.77m. The Main Seam is between 2-3m thick and is made up of three plies: The CBD, CDB, and CB (Figure 7). The Main Seam was logged and a detailed log is shown below in Figure 9. Thin coal units of up to 0.30m thickness at a depth of 258.20m which are not of economic value were also noted in NG-108 (Appendix 1).

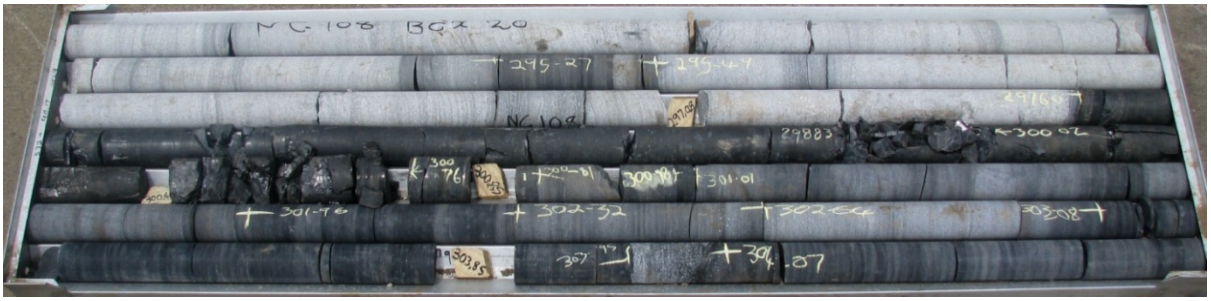


Figure 7: A photograph of a drill core from a drill hole NG-108 located 300m from Section 30 showing the roof, Main Seam, and floor of the Main Seam.

The roof rock is medium to coarse-grained, whitish, feldspathic sandstone, with cross-stratification and horizontal lamination being the dominant sedimentary structures. The floor rock is a very fine-grained, micaceous, black carbonaceous siltstone. In some areas, the floor rock is fine-grained, dark grey sandstone interlaminated with shale. The Main Seam indicating the plies that are characterised was intercepted at depth from 297.60-299.77m (Figure 8). Dolerite sills and dykes (oriented horizontal and sub-vertical, respectively) associated with faulting are prominent at the ZAC. These zones of weakness are responsible for channelling water, which eventually percolate the strata and influence weathering.

DETAILED MAIN SEAM LOG NG-108

DRILL HOLE NAME: NG-108	***SEAM NAME: MAIN SEAM***	***PAGE REF: 22 of BH Log***

PROPOSITION: NGWABE	***FARM: NGWABE***	***DISTRICT: NONGOMA***

CO-ORDINATES: Y: **-68726.02m**	***X:*****3115040.52m**	***Z:*****218.36m**

SECTION NOT TO SCALE

DEPTH FROM TO	***THICKNESS***	***% LOSS CORE***	***SECTION***	***SAMPLE NAME***	***DESCRIPTION***
295.49	***0.22***				
					Sandstone, coarse grained, feldspathic, micaceous,
					pale whitish grey, starkly planar cross-bedded with an
					erosive ±8º base.
	297.60	***1.11***			***ROOF OF MAIN SEAM***
297.60					

									Coal. Mixed, mainly bright, streaky vitrinite
									banded with scattered pellety pyrite lenses.
	297.76	***0.16***							
297.76									
									Coal. Lustrous to dull, lightly steeply jointed with
									mildly scattered pyrite streaks and a broken base.
	298.83	***1.01***							
298.83									
									Coal. Dull, jointed, slickensided, slightly broken.
								NG108/M/A	
	299.03	***0.20***						***(2.17m)***	
299.03									

								Coal. Lustrous dull, lightly vitrinite streaked with
								mildly scattered pyrite lenses.
	299.46	***0.43***						
299.46								
								Coal. Mixed, mainly bright, thickly streaky
								vitrinite banded, steeply jointed, slightly blocky broken with a
								sharp base.
	299.77	***0.31***						***FLOOR OF MAIN SEAM***
299.77								
								Carbonaceous silty mudstone, black, finely micaceous,
								laminated, fairly weak with a sharp base.

	299.82	***0.05***						

Figure 8: A detailed Main Seam log from the drill hole NG-108.

A map showing the collar position of drill hole NG-108 is provided in Figure 9. The full drill hole log and photos are presented in Appendices 1 and 2.

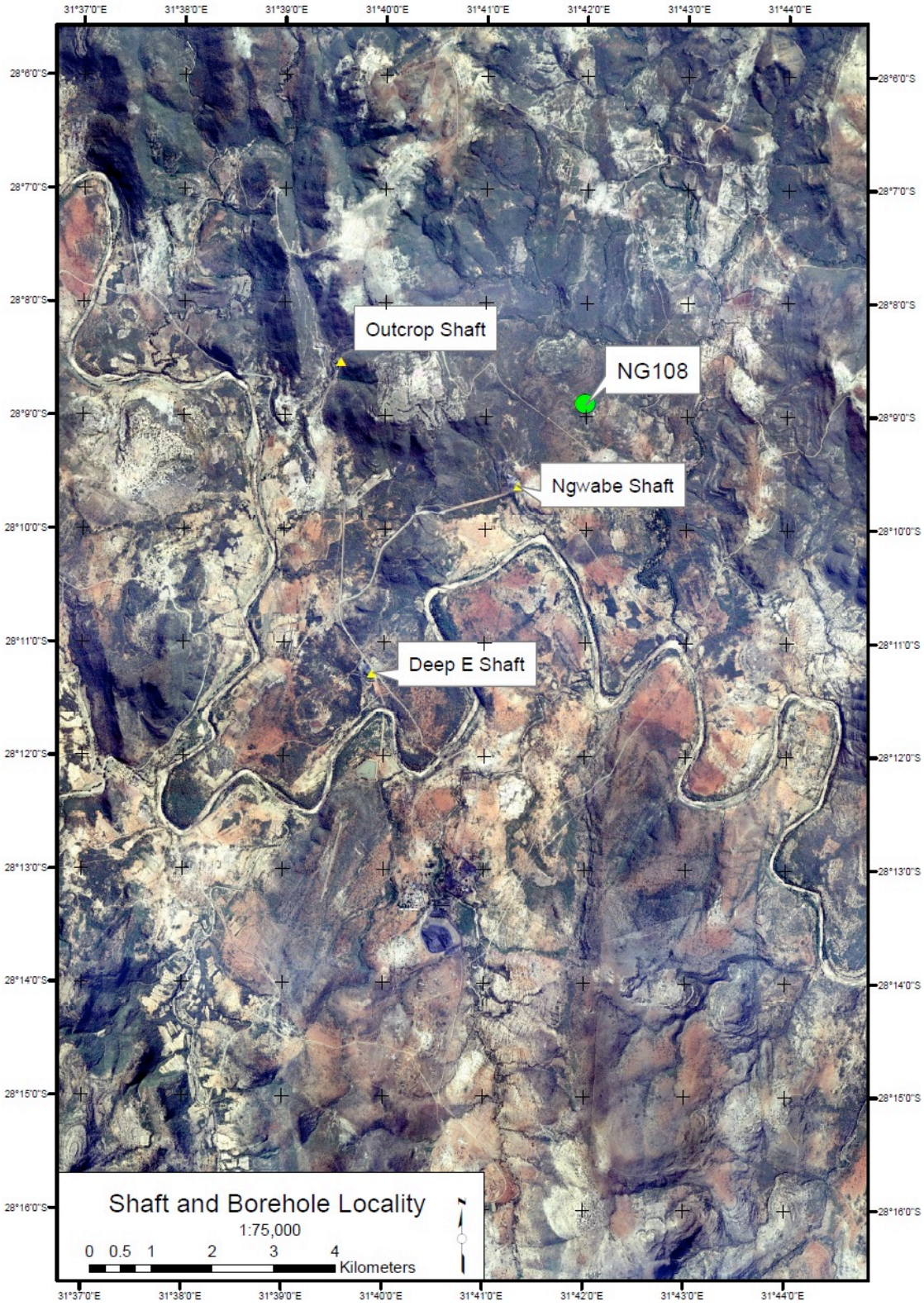


Figure 9: Google Earth image showing the position of the shafts and drill hole NG-108.

Stratigraphy

The geomorphological controls influencing sediment distribution in modern deltaic environments (Figure 10) includes: (i) sediment yield and size, and the ratio of bedload to suspended load; (ii) coastal characteristics which include river mouth processes, wave power, tidal processes, wind systems, currents, and storm frequency; (iii) shelf slope, and (iv) the tectonics of both the receiving basin and source area.

The Nongoma Graben Delta is a coarsening-upward sequence comprising five depositional environments. These include shelf deposits, prodelta, distributary mouth bar, interdistributary bay sequence, and distributary channel (Turner and Whateley, 1983) (Figure 10). The description and interpretation of each depositional environment is given below from the bottom to the top of the sequence.

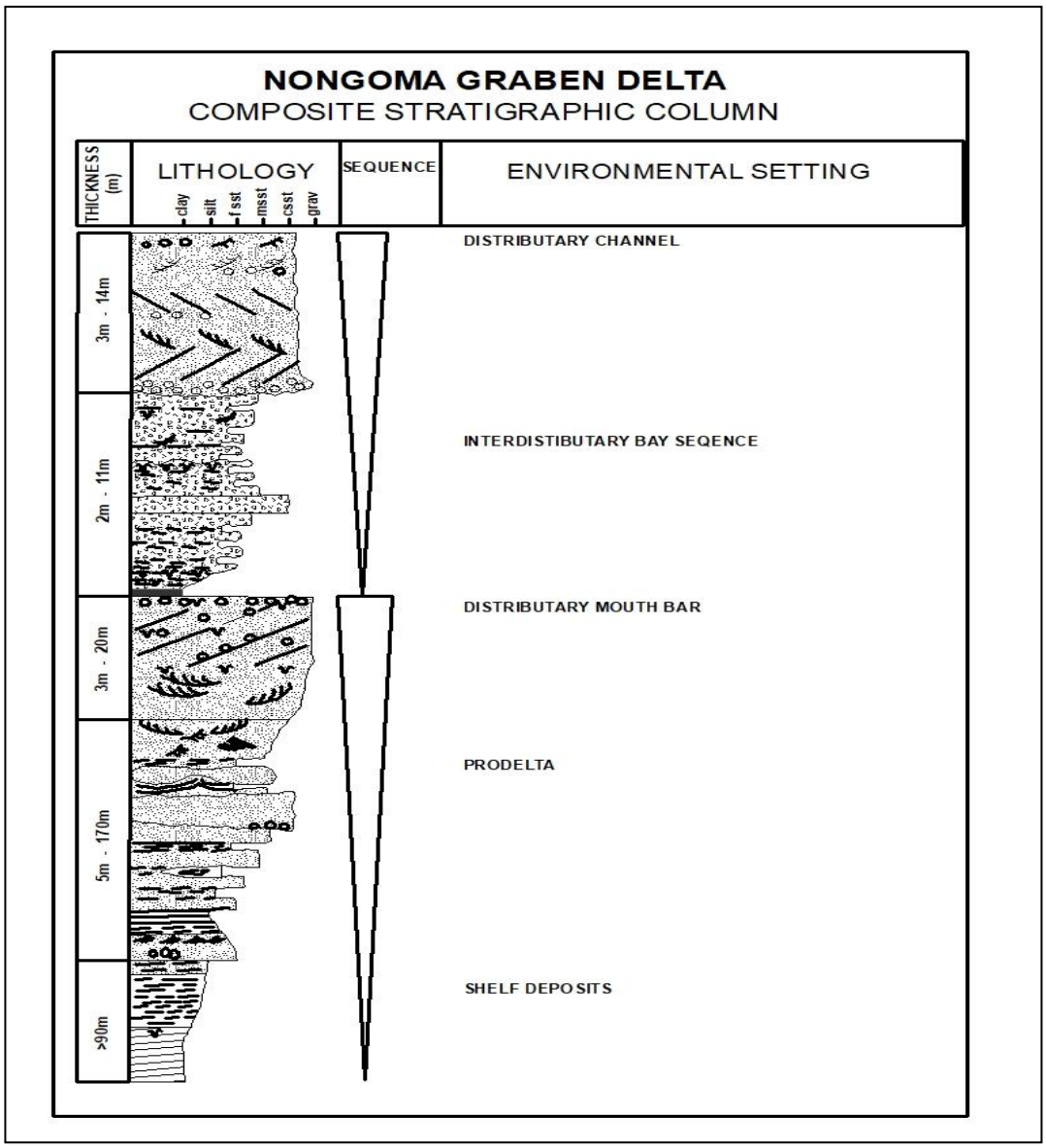


Figure 10: A sedimentary log depicting facies and their depositional environment (Whateley, 1980).

Delta Sequence

Shelf deposits

During the delta's transgressive phase in the Ngwabe Formation period and during the progradational stage in Ceza Formation times, shelf deposits accumulated (Whateley, 1980) (Figure 11).

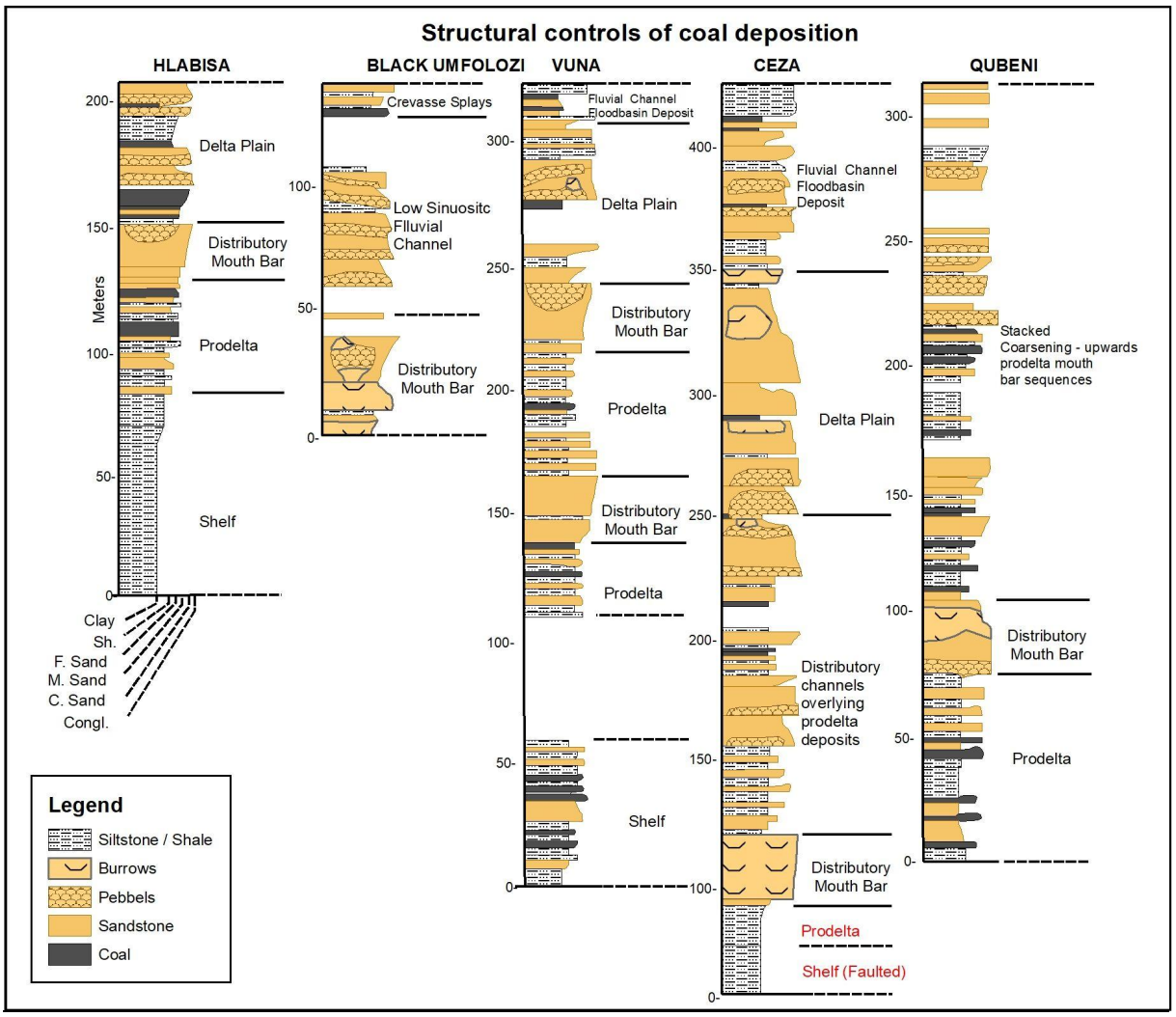


Figure 11: Measured stratigraphic profiles of the Karoo Supergroup showing coarsening-upward and fining-upward depositional trends and interpreted depositional environment (Turner and Whateley, 1983).

The shelf deposit is more than 90m thick comprising very fine-grained, dark-grey to black shale. Micaceous siltstone becomes more abundant up the sequence towards the prodelta deposits. Occasionally sand grains are present and disseminated in the shales.

The fine-grained nature of the shales suggests quiet waters and offshore conditions below effective wave base, receiving sediments mainly from suspension (Turner and Whateley, 1983). The increase in grain size from fine to silt material indicates the gradual advance of the overlying prograding delta onto the shelf area. An introduction

of a delta lobe in one area supplied more silt material into the shelf than an adjacent interlobe area (Whateley, 1980). The delta platform was then formed by shales and silty shales of the shelf deposits (Whateley, 1980).

Hypopycnal or hyperpycnal inflows are two mechanisms for the deposition of shales (Zavala and Pan, 2018). If the incoming water into the receiving basin is less dense than the water contained within the basin, the flow is referred to as hypopycnal. In such conditions the warmer river water flows into the cooler, more saline water (Zavala and Pan, 2018). The basin water keeps the incoming water and the suspended sediments afloat, and transports it far out into the basin.

Zavala and Pan (2018) state that in the case of hyperpycnal inflow, the incoming river water is denser than the basin water. Due to the turbidity currents created by density underflow, sedimentation occurred at the bottom of the prodelta slope where the slope decreases. Hyperpycnal inflow has possibly influenced the laterally extensive shales of the shelf deposits (Zavala and Pan, 2018).

Prodelta deposits

The prodelta deposits are attributed to an association of sediments that occurred randomly and incorporated wave-rippled cross-laminated sandstone (Whateley, 1980). Interbeds of laminated siltstone and medium-grained sandstone and medium to coarse-grained sandstone with traction-formed current structures.

Wave-ripple cross-lamination

This lithology comprises pale-grey to dark-grey, fine to medium-grained micaceous, ripple cross-laminated sandstone (Figure 12). This unit ranged between 2.5-6m thick and occurred as storm deposits on the upper surface of point bar channel deposits or

in the prodelta. A thick (5-15m), laterally extensive layer comprising exclusively of ripple cross-lamination exists in Sheleza (outcrop) deposits (Whateley, 1980). These sedimentary units are underlain by fine-grained floodplain deposits and overlain by fine-grained prodelta deposits. The silt material is subordinate in the ripple cross-laminated layer and is only visible as thin (1-5mm), impersistent partings between or as drapes and ripples (Whateley, 1980).

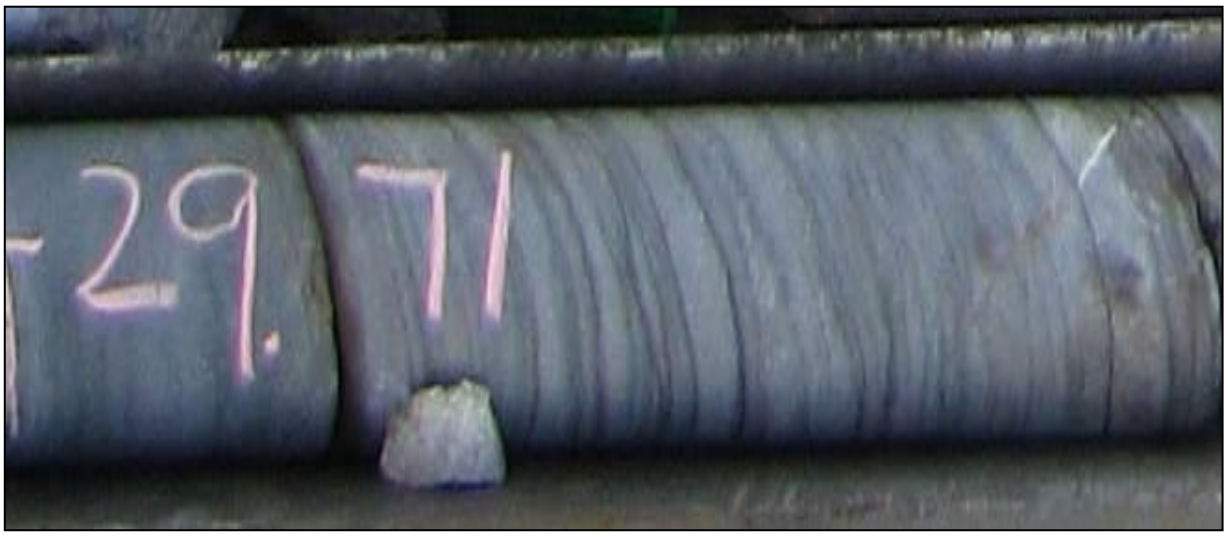


Figure 12: Wave-ripple cross-lamination in drill hole NG-108 (an example of unit 1 of the ZAC stratigraphy).

The bidirectional cross-laminations are interpreted as generated under progressive but moderate wave action (De Raaf et al., 1977). It is suggested that transgression occurred at the top of the Sheleza deposits, and that this wave-ripple cross–laminated sand is equivalent to the glauconite layer usually associated with the No.5 Seam in Mpumalanga, or the Alfred Seam of the KZN areas (Whateley, 1980). It is possible that subsidence was greater than sedimentation during this period, which permitted the finer suspension sediments to be continuously reworked by the waves and remain in suspension (Whateley, 1980).

Interbeds of laminated siltstone and medium-grained sandstone

These facies are the dominant type in the prodelta environment (Whateley, 1980). This unit is also known as the Silver Zone and is about 6.5m thick (Turner and Whateley,1983). It comprises alternating sub-layers of sandstone of about 2-20cm thick, and siltstone with shale of about 20-50cm thickness occurring occasionally at the bottom. The ratio of fine sediment and bed thickness increases upwards. Certain sandstone units in the more proximal parts of the prodelta appear to grade laterally over 15m into a single 3m, medium to coarse-grained sandstone unit (Whateley, 1980).

In the lower part of the prodelta sequence, the coarse-grained sedimentary strata are light-grey to blue-grey on exposed surfaces but dark-grey internally. The finer, interbedded sediments are generally black to dark-grey (Figure 13). Internally the medium to coarse-grained sandstones are generally structureless and poorly sorted, but the silt or the fine-grained sandstones may be laminated (Whateley, 1980).



Figure 13: Medium-grained sandstone with interbeds of laminated siltstone in drill hole NG-108 (an example of unit2 and some part of unit 11 of the ZAC stratigraphy).

These sediments reflect interbeds that formed when sediment-laden floodwaters were introduced into the receiving basin over the distributary mouth-bar sands (Whateley,

1980). The cold (denser) floodwaters flowed through hyperpycnal underflows down the prodelta slopes, and rapid sedimentation occurred at the foot of the delta as slopes declined (Zavala and Pan, 2018). Structureless beds are typical of proximal turbidites deposits (Stauffer, 1967). It is possible that they have formed by *in situ* bed movement while unconsolidated, either by current or tectonic activity. Original loss of structure during grainflow down the prodelta slope is, however, the most likely mode of formation (Whateley, 1980).

Medium- to coarse-grained sandstone with traction current-formed structures

These lithofacies, which form a zone about 15m thick, are comprised of medium- to coarse-grained, whitish-grey, feldspathic, horizontally-banded to cross-stratified sandstone with a few narrow silty carbonaceous partings (Figure 14). About 1m thick laterally extensive, fining-upward sequences are present (Whateley, 1980). These sequences comprise predominantly of parallel laminated medium- to coarse-grained sandstone which grade upward into intricately interwoven fine-grained cross-laminated sandstone (Whateley, 1980). The parallel laminated beds have a sharp, possibly erosive contact over the underlying cross-laminated beds.

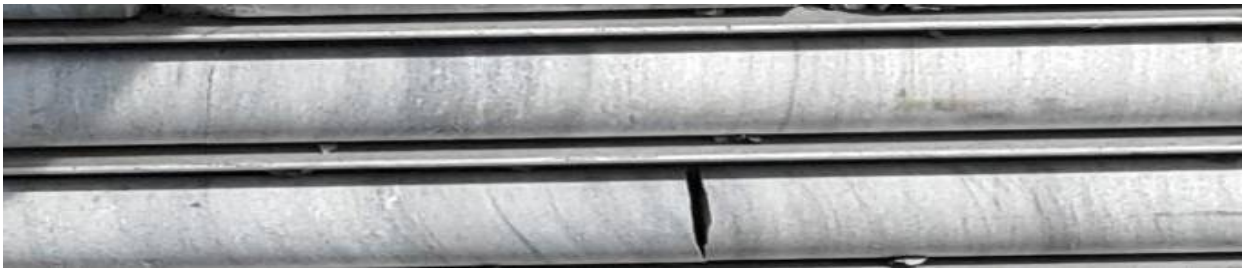


Figure 14: Medium- to coarse-grained sandstone in drill hole NG-108 (an example of unit 3, unit 5, unit 7, and unit 9 of the general stratigraphy of ZAC).

The architecture of the sediments was produced by traction currents in the sediments deposited in water above the effective wave base (Olariu and Bhattacharya, 2006).

The sandstones are interpreted as having been deposited immediately seaward of the distributary mouth bars, at the top of the prodelta association. Olariu and Bhattacharya (2006) state that the waters were fairly shallow and the basin beds were horizontal to sub-horizontal above the prodelta gradient association.

Distributary mouth bars

Coarse-grained sandstone interlaminated with shale showing vertical bioturbation burrows

The distributary mouth bar deposits comprise pale-whitish, coarse-grained, micaceous, feldspathic, sandstone often with long, thick, vertical bioturbation burrows (Figure 15). Frequently, silty partings and often narrow coal stringers are also present (Whateley, 1980). Sandstone thickness ranged between 5-20m thick. Planar cross-stratification is the most common sedimentary structure.



Figure 15: Coarse-grained sandstone interlaminated with shale in drill hole NG-108, showing vertical bioturbation burrows.

Olariu and Bhattacharya (2006) state that the distributary mouth bars are comprised of a delta lobe that developed, possibly, during the period of progradation with frequent delta shifting. At the entry point of the standing body of water, the fluvial outflow energy of the waters carrying heavy loads of sediments was reduced. Settling of sediments resulted in the choking of distributary channels. Ultimately, delta shifting resulted

(Olariu and Bhattacharya, 2006). The coarsening-upward sequence was formed as the finer sediments were carried offshore and as the progradation of the coarser sediments overlying the finer sediments occurred. The presence of bioturbation in the sandstone proves that sedimentation in shallow waters occurred, which facilitated the development of burrowing (Whateley, 1980).

Interdistributary bay sequence

Course-grained sandstone interbedded with shale and siltstone

The interdistributary bay sequence comprises very fine-grained, feldspathic greying sandstone interbedded with shale and siltstone (Figure 16). The thickness of the sequence varies between 2-11m, and it grades upwards with sandstone overlain by siltstone and shale (Whateley, 1980).



Figure 16: Very fine-grained sandstone interbedded with shale and siltstone in drill hole NG-108.

Whateley (1980) states that the alternating beds of siltstone, shale and sandstone were formed when the waters carrying heavy loads of sediments overflowed the channel banks into the interdistributary bays. Thick and thin sandstone beds bear a record of changes of the intensity of the floods in relation to the distance from the source area. Waves produced wavy laminations in sandstone, and this proves that waves were present in the interdistributary bay (Turner and Whateley, 1983).

Distributary channels deposit

Coarse-grained, cross-laminated, whitish sandstone

This unit consists of coarse-grained sandstone that is feldspathic, micaceous, and whitish in colour (Whateley, 1980). It is about 3-14m thick. Cross-lamination, and planar cross-bedding are present in the unit (Figure 17). Bioturbation is not present. An erosive contact was observed at the base of this layer which might have resulted from the incision of the channel (Whateley, 1980).



Figure 17: Coarse-grained, cross-laminated, whitish sandstone in drill hole NG-108.

The erosive contact provides evidence of channel incision into the prodelta indicating that distributary channels were deep, carried heavy loads of sediments and were of high energy, Where channel incision has occurred, interlobe deposits are formed and the erosive contact reflects channel switching (Whateley, 1980).

Fluvial sequence

This fining-upwards sequence consists of channel and floodplain deposits (Whateley, 1980). Channel deposits are subdivided into two: the lower and upper channel deposits (Whateley, 1980). The lower channel deposit is lying at the bottom of the sequence and is overlain by floodplain deposits. A very coarse-grained upper channel deposit lies on top of the erosive base, and fines-upwards encroaching on the flood basin deposits. Coals occurring at the top of the fluvial succession are up to 3m thick, while

thin coals of about 1m thick occur at the bottom of the deltaic sequence (Turner and Whateley, 1983).

Channel Deposits

Medium-grained sandstone with lower angle horizontal stratification

The lower channel deposits comprised medium-grained, feldspathic sandstone with an erosive contact at the base (Figure 18). The internal sedimentary structures present have a very low angle planar and trough cross-stratification (Whateley, 1980). The sandstone thickness varies between 2.5-20m. The sandstones are a whitish, grey to dark-grey in colour with curved streaks of carbonaceous shale or siltstone (Whateley, 1980).

The upper channel deposits comprise a fine-grained, feldspathic sandstone, that is greyish to dark-grey in colour. The thickness varies between 1-6.5m. The internal sedimentary structures (flat-bedded and wavy-ripples) are preserved on the surfaces of the sandstone.



Figure 18: Medium-grained sandstone with lower angle horizontal stratification (source: NG-108).

The sandstones of the channel deposits possibly resulted from the bedload material that was transported into the fluvial plain. It is thought that migration of dunes within the channel influenced trough cross-stratification (Whateley, 1980).

Flood basin deposits

Fine-grained siltstone interlaminated with shale

Flood basin deposits are fine-grained and have rippled, alternating siltstone and shales (Figure 19). Crevasse-splay deposits are usually cones of sandy to silty facies with both coarsening-upward and fining-upward successions (Tuner and Whateley, 1983). Coal seams are laterally persistent, encroaching in the channel and causing local coarsening-upward (Whateley, 1980).



Figure 19: Fine-grained siltstone interlaminated with shale in drill hole NG-108.

Floodplains are the areas occupied by river channels as well as the surrounding, flat, overbank areas that are subject to flooding (Whateley, 1980). Floodplain deposits are the most distal facies, consisting entirely of sediments deposited from suspension. The extent and architecture of the flood basin deposits are influenced mainly by channel shape (Turner and Whateley, 1983). During high flow stages, channels with sediment-laden waters overflow into the floodplain and deposit coarse and fine materials (Turner and Whateley, 1983). The ratio of the floodplain deposits is driven by distance from the channel, size, and the duration of flooding (Turner and Whateley, 1983).

Coal seams

Coal seams occur at the top of the fining-upward sequences and occasionally at the base of the coarsening-up sequence. The coal that is mined at the ZAC is referred to as the Main Seam. Its thickness ranges between 0.9-3m. Shale partings of about 0.2m thickness are occasionally present within the Main Seam. Perpendicular calcite cleats are present and brown-staining limonite after pyrite is visible on weathered surfaces. The Main Seam is overlain by a medium to coarse-grained, feldspathic sandstone about 9m thick, and underlain by carbonaceous, micaceous shale of about 3-5m thick. With sudden delta abandonment, ponding water on the abandoned surface would provide a suitable environment for plant growth (Turner and Whateley, 1983).

The coals are thought to be the product of *in-situ* plant growth and decay with later plants rooting themselves in the rotting vegetation of the earlier plant material (Turner and Whateley, 1983). Compaction subsidence would maintain a high water table, and the environment would have been permanently submerged. Thicker and more laterally persistent coals are located near the top of the fluvial sequences. Coal deposits forming in these areas represent a more stable environment when stream gradient and sediment input decreased, and stable high sinuous channels meandered across the floodplains (Turner and Whateley, 1983).

For such coal deposits to form, the following three stages of development must take place in the following order: (i) the formation of shallow lakes with floating peat; (ii) the formation of well-vegetated, low-lying swamps, and (iii) raised swamps resulting from the accumulation of organic material that forms an uplifted terrain with respect to the sediment substrate, and one in which clastic sediment deposition is limited (Diessel, 1992). This sequence serves as a model for the depositional environment in which

optimal formation of thick peat, and subsequently economic coal horizons, might form (Hobday, 1973 and 1977). Raised swamps can form in deltaic environments, but the above model applies specifically to those settings in which sediment input is minimised and the resultant coals are low-ash in character (Romanov, 1968; Hobday, 1973; McCabe, 1984).

Diessel (1992) states that as peat forms it incorporates inorganic clastic detritus from a variety of sources. During coalification this detritus was diagenetically altered to form a variety of authigenic mineral components such as quartz, carbonate, sulphide and clay (Whateley, 1980). These components remain behind to make up the ash content once the coal is combusted or processed (Whateley, 1980). Low ash content coals are economically advantageous as this parameter translates favourably into higher calorific values and fixed carbon (FC), better grindability and less deleterious environmental effects such as sulphur emissions (Hobday, 1973).

Temperature has been noted as one of the key influences on the rank of coal; rising temperature with increasing depth of burial increases the coal rank (Whateley, 1980). Different structural settings have varying temperatures, thus producing coals of different ranks. Whateley (1980) states that in graben structure such as the ZAC high geothermal gradients produced coal of high ranks, while in less active areas of low geothermal gradients relatively low rank coals are expected. Coals comprise microscopic organic constituents referred to as macerals (vitrinite, inertinite, and liptinite) (Richards et al., 2013). Macerals are considered to be analogous to the minerals of other rocks and they are grouped according to their petrographic characteristics.

Chapter 2

Research Methodology

Introduction

This chapter presents the methodological techniques applied in the study. In order to achieve the aim and objectives of the study, a variety of samples was acquired and coal characterisation was conducted. This chapter explains how the samples were obtained and how the samples were prepared for the different analyses.

Channel sampling

According to American Society for Testing and Materials (ASTM) channel sampling is a method used for both surface and underground coal mines to sample coal for quality monitoring and analysis (ASTM, 1986). The ASTM (1986a) standard procedure was applied for underground channel sampling to maintain quality and avoid sample contamination. A section plan depicting the spot where channel samples were collected in the Ngwabe Shaft is shown in Figure 20.

The coalface is divided into three plies: (i) Coal, mainly Bright, Dull (CBD); (ii) Coal, mainly Dull, Bright (CDB) and (iii) Coal Bright (CB). These plies are depicted in Figure 21. The total thickness of the Main Seam measured at the coalface was 2.46m. The thickness of each ply measured at the coalface does, however, vary in proportion: the CBD ply measured at 1.46m, the CDB ply at 0.75m, and the CB at 0.25m. During the channel sampling process, the Pyritic Stringer (PY) and Pyritic Nodular (PN) coal

impurities were observed within the CBD and CDB plies. The presence of both of these impurities indicated a possible compromised coal quality within the Main Seam.

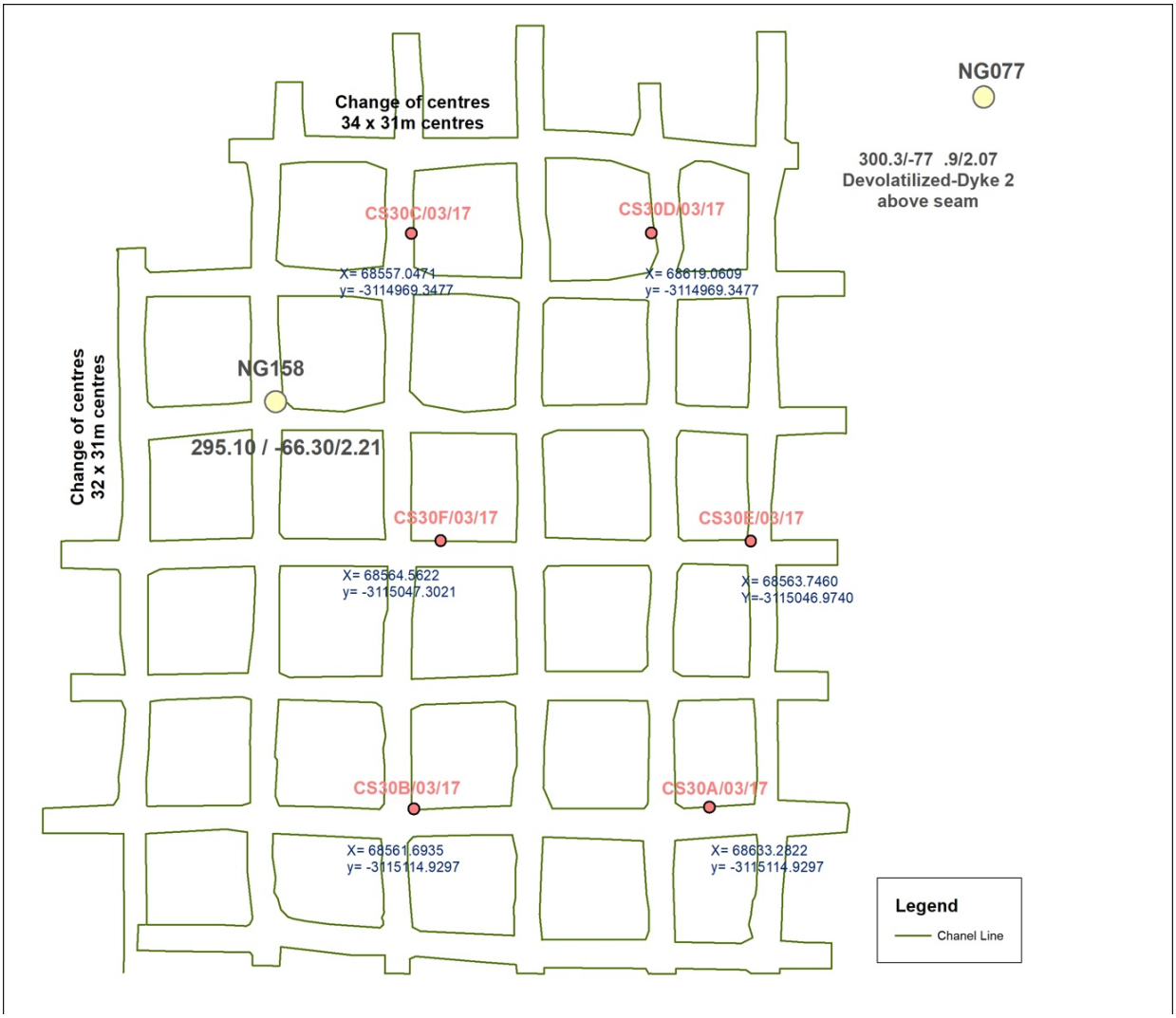


Figure 20: Ngwabe Shaft Section 30 layout showing where the channel sampling was conducted.

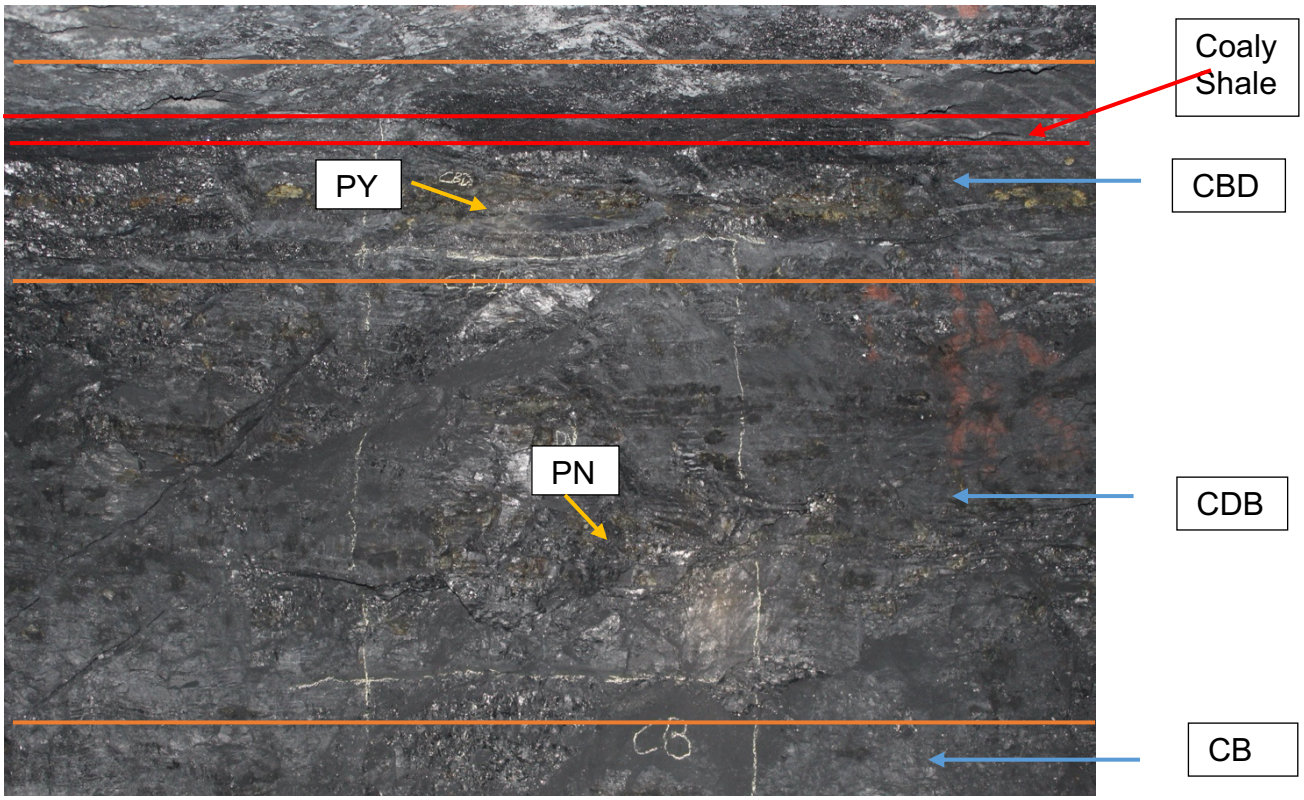


Figure 21: An example of the coalface in Section 30 where channel sampling (CBD, CDB and CB plies) was collected in this study.

The following standard procedure is used to collect channel samples of coal (ASTM, 1986):

- A freshly exposed coalface must be selected for sampling. Stick sides or a coalface with disseminated impurities such as oxidation stains must not be a target for sampling;
- The sampler can get a fresh coalface just after roof rock has been supported after the first cut;
- A coalface normal to the bedding plane must be selected for sampling;
- A hand pick must be applied to chisel the coalface at the top and bottom to produce a proper surface;
- Nylon-reinforced vinyl tarpaulin, 3m x 4m in dimension must be spread on the floor;

- Two parallel lines with 10cm spacing must be marked clearly on the coalface. Then, select the plies that should sampled. Plies that are sampled must also be clearly marked;
- Chip out the coalface between the two vertical lines drawn from bottom to top using a pick. Chipping must be at a depth of approximately 8cm; this step must then be repeated from bottom to the top of the coalface;
- The channel cut must be of uniform volume; this is achieved by carefully squaring the back of the channel;
- The entire sample must then be transferred into polyethylene-lined canvas bags or drums. Splitting for representative samples is then done in the laboratory.
- Labelled tags must be placed inside and tagged to the outside of the sample bag; each sample bag must be sealed separately;
- A full description of the coalface must be completed, with a particular emphasis on the thickness of each of the coal plies.

This procedure was used to collect the channel samples for this study.

Petrographic analysis

Coal petrography is a microscopic technique applied to characterise the proportion of macerals that comprise the coal (Lopez-Buendia et al., 2007). The macerals are separated into three groups, each of which includes several maceral types (Fan et al., 2020). The three maceral groups include: vitrinite, inertinite, and liptinite. Since coal rank is controlled by the degree of coalification, the properties of macerals vary with changes in degree of metamorphism (Gupta, 2007). The degree of coalification is determined by measuring the percent light reflectance of the macerals' vitrinite. The type of macerals is determined using a point count procedure to obtain the volume percent of the various coal macerals or fossilised plant remains. Coal petrography can also be used to determine whether contaminants are present in the coal and to detect oxidised coal in the sample (Lopez-Buendia et al., 2007).

Sample preparation

The samples were received as crushed, screened particles of +0.5 x 25mm. The samples were block-mounted following SANS ISO 7404-2 and prepared to a final 0.05 micron polish using a Struers Tegraforce polisher at the Department of Geology, University of Johannesburg (UJ).

Petrographic analysis – methodology

The polished blocks were analysed using a Zeiss Axio Imager M2m reflected light petrographic microscope fitted with a Hilgers Fossil system for vitrinite reflectance and maceral determination at a magnification of x500 under reflected white light, with oil immersion. The analyses were conducted largely following SANS ISO 7404-5 for vitrinite reflectance. A detailed maceral point count was conducted, largely following SANS ISO 7404-3. Results are reported on a volume percentage (vol%) basis.

Proximate analysis

Proximate analysis is the method used to analyse the quality of sampled coal. Parameters being examined include: inherent moisture (IM) content (%), volatile matter (VM) (%), ash content (%), and fixed carbon (FC) content (%) by difference (Rasheed et al., 2015).

Inherent Moisture (IM) content

According to Rasheed and colleagues (2015) most coals, as they are dug from the ground, have some amount of moisture associated with them. Gentle heating of coal at a temperature slightly above the boiling point of water causes a loss of weight from the sample, which is defined as moisture that is lost. The moisture content of coals range from about 5% to almost 70%. Moisture is an undesirable constituent of coals because it reduces the heating value and its weight adds to the transportation costs of coal. According to Rasheed et al. (2015) IM content is calculated as follows:

Moisture (%) = (loss in weight due to removal of moisture/weight of coal sample taken) x 100.

Volatile Matter (VM)

According to Rasheed and colleagues (2015) VM in coal refers to the components of coal, excluding moisture, which are liberated at high temperatures in the absence of air. This is usually a mixture of short and long chain hydrocarbons, aromatic hydrocarbons and some sulphur. The VM of coal is determined using rigidly controlled standards. In Australian and British laboratories this involves heating the coal sample to 900 ± 5°C (1650 ± 10°F) for seven minutes in a cylindrical silica crucible in a muffle furnace (ISO 562, 2013). American Standard procedures involve heating to 950 ± 25°C (1740 ± 45°F) in a vertical platinum crucible (ISO 562). The Australian and British

laboratory standard was used since the Zululand Anthracite Colliery (ZAC) mine laboratory also applies the same standard. VM is calculated as follows:

VM (%) = (loss in weight due to removal of VM/wt of coal sample used) x 100.

Ash content

The ash content of coal is the non-combustible residue left after coal is burnt. It represents the bulk mineral matter after carbon, oxygen, sulphur and water (including from clays) has been driven off during combustion. The analysis is fairly straightforward: the coal is thoroughly burnt and the ash material is expressed as a percentage of the original weight. According to Rasheed and colleagues (2015) ash content is calculated as follows:

Ash Content (%) = (weight of ash formed/ weight of dry coal taken) x 100.

Fixed Carbon (FC)

The FC content of the coal is the carbon that remains in the material after volatile materials are driven off (Rasheed et al., 2015). This differs from the ultimate carbon content of the coal because some carbon is lost in hydrocarbons with the volatiles (ASTM D5142, 2013). The FC is determined by removing the mass of volatiles determined by the volatility test, above, from the original mass of the coal sample. The FC is calculated by subtracting 100 from the summation of Ash, VM matter and IM, all as a percentage mass fraction on the same moisture reference base (ASTM D5142, 2013).

Total Sulphur Analysis

The Total Sulphur (TS) refers to the sum parameters of all organic and inorganic sulphur found in coal (Chour, 2012). The Total Sulphur analysis was performed to determine Total Sulphur in coal in this study.

Washability analysis

Coal beneficiation analysis is critical for: (i) assessing the quality of a coal seam; (ii) designing coal preparation plants; (iii) process modelling, and (iv) measuring the separation efficiency of process plants (Galvin, 2006). The float and sink processes are applied to separate coal from impurities such as mineral matter. In float and sink analysis a coal sample is washed either with magnetite at a larger scale (in the plant) or with zinc chloride at a smaller scale (in the laboratory). For the purpose of this study, the washability analysis was done at a laboratory scale using zinc chloride.

The medium to wash the coal samples was set at different relative densities (RDs) starting from RD of 1.35-1.75 g/cm^3 - which is a standard for the ZAC - to quantify how much yield was retained for the set RD. The raw sample was weighed first and the weight was recorded. This weight was used in calculating the volume of coal for the specific RD in order to determine the yield at that RD (Galvin, 2006).

Chapter 3

Results

Introduction

The data presented in this chapter is from the following analyses: (i) proximate analyses; (ii) Total Sulphur analysis; (iii) petrographic analyses; and (iv) washability analyses. The data presented in this chapter seek to unpack the coal quality found in the Nongoma Coalfield, specifically in the Ngwabe Shaft. Section 30 of the Ngwabe Shaft is the area where channel samples were collected (Figure 20). In total 13 channel samples were collected for this research. For the purpose of this research report, the data for three channel samples: 30B, 30AI and 30D is sufficient to draw conclusions. Coal quality characterisation in the Ngwabe Shaft is the main focus of this study.

Coal quality

The data presented in this section includes results from proximate and Total Sulphur analyses. The proximate analysis parameters that were examined include Inherent Moisture (IM) content; ash content; Volatile Matter (VM); and Fixed Carbon (FC). The Total Sulphur analysis was also performed in this study.

Proximate analysis

Proximate analysis data (Table 1) is reported on an air-dry basis. The IM content for the Coal mainly Bright, Dull (CBD) ply ranges from 1.6-2.5%. For the Coal, mainly Dull, Bright (CDB) ply it ranged from 1.4-2.6% and for the Coal Bright (CB) ply the IM content ranged from 2.9-4.2%. Ash content within the CBD ply ranged from 14.2-20.7%. For the CDB ply it ranged from 8.6-14.1%, and for the CB ply the ash content

ranged from 7.6-12.6%. In line with these values, the CB ply has the least ash content in comparison with the CDB and the CBD plies. Evidence of a high ash content is found within the CBD ply.

The VM for the CBD ply ranged from 5.5-6.3%. For the CDB ply it ranged from 5.5-6.8%, and for the CB ply the VM ranged from 4.8-5.1%. The FC for the CBD ply ranged from 71.4-78.3%. For the CDB ply it ranged from 77.4-83.3%, and for the CB ply the FC ranged from 78.1-84.4%.

Total Sulphur analysis

The Total Sulphur analysis data (Table 2) is reported on an air-dry basis. The TS content for the CBD ply ranged from 0.77-1.62%. For the CDB ply it ranged from 0.74-1.36% and for the CB ply the TS content ranged from 0.91-1.56%.

Table 1: Results of proximate analysis for the CBD, CDB and CB plies.

Proximate Analysis Results: reported on an air-dried basis					
Lab No.	**Sample Name**	**IM**	**A**	**VM**	**FC**
		%	**%**	**%**	**%**
121775	CS30E/03/17-CB	2.9	7.6	5.1	84.4
121776	CS30E/03/17-CDB	2.6	8.6	5.5	83.3
121777	CS30E/03/17-CBD	1.6	20.7	6.3	71.4
121778	CS30EI/01/17-CB	3.0	7.7	4.8	84.5
121779	CS30EI/01/17-CBD	2.1	14.2	5.5	78.3
121780	CS30DI/01/17-CB	4.2	12.6	5.1	78.1
121781	CS30EI/01/17-CDB	1.7	14.1	6.8	77.4
121782	CS30DI/01/17-CBD	2.5	19.7	5.9	71.9
121783	CS30DI/01/17-CDB	1.4	13.6	5.6	79.4

Table 2: Results of Total Sulphur analysis for the CBD, CDB and CB plies.

Total Sulphur Analysis Results: reported on an air- dried basis		
Lab No.	**Sample Name**	**TS** **%**
121775	CS30E/03/17-CB	1.03
121776	CS30E/03/17-CDB	0.74
121777	CS30E/03/17-CBD	0.77
121778	CS30EI/01/17-CB	1.56
121779	CS30EI/01/17-CBD	1.62
121780	CS30DI/01/17-CB	0.91
121781	CS30EI/01/17-CDB	1.36
121782	CS30DI/01/17-CBD	1.01
121783	CS30DI/01/17-CDB	0.98

Washability analysis

This section presents washability data for the CBD, CDB, and CB plies of the Main Seam at the ZAC. The channel samples for each ply were collected at the coalface in Section 30. The float and sink tests were conducted at the ZAC laboratory to determine the washability properties of each ply. The washability results showing the chemical properties of the CBD, CDB, and CB plies of the channel samples 30B, 30AI, and 30D are reflected in Table 4, Table 8 and Table 12, respectively.

There are two products that were can be yielded within the CBD, CDB, and CB plies of the Main Seam, namely: the prime product and the middlings product. The prime product has a low ash yield in comparison to the middlings product. The prime and middlings products have a specific ash yield of 8.5% and 8.5-15.5%, respectively. The

prime and middlings products have specific relative densities (RDs) and both products are calculated from the washability data presented in this research report. A formula to calculate RD for prime and middlings products is provided below. The prime product is the best quality compared to middlings product, and is usually obtained at an RD between 1.38-1.65 g/cm^3. The middlings product is usually obtained at an RD of 1.65-1.75g/cm^3. The results in Table 4, Table 8 and Table 12 of the washability data were used to determine the prime and middlings products for the CBD, CDB, and CB plies for each channel sample.

Table 3. A generic table used to calculate RD, prime and middlings products at an ash yield of 8.5%.

RD	Y	IM	A	VM	FC	TS
RD_1	Y_1	IM_1	A_1	VM_1	FC_1	TS_1
RD_2	Y_2	IM_2	A_2	VM_2	FC_2	TS_2
RD_p	Y_p	IM_p	8.5	VM_p	FC_p	TS_p
RD_3	Y_3	IM_3	A_3	VM_3	FC_3	TS_3
RD_4	Y_4	IM_4	A_4	VM_4	FC_4	TS_4
RD_5	Y_5	IM_5	A_5	VM_5	FC_5	TS_5
RAW	Y_r	IM_r	A_r	VM_r	FC_r	TS_r

Prime Product Calculations

α = (8.5-A_2)/ (A_3-A_2) Y_p= (Y_3-Y_2) x α + Y_2 RD_p= (RD_3-RD_2) x α + RD_2

Middlings Product Calculations

Y_m= $Y_5 - Y_p$

$RD_m = (Y_5 \text{x } RD_5 - Y_p \text{x} RD_p) / Y_m$

Note: FC=100-IM-A-VM

Channel Sample 30B

The results of the float and sink tests of the CBD, CDB, and CB plies of the channel sample 30B are presented in Table 4. The float and sink tests were conducted in a wash density of 1.35-1.75g/cm³ for all plies. Proximate and Total Sulphur analyses were also conducted for Channel Sample 30B; the results are included in Table 4. The results also reflect that the RD is directly proportional to the yield (cumulative float), and that the ash yield is directly proportional to the yield (cumulative float) as shown in Figure 22, Figure 23 and Figure 24. For the CBD ply: the IM content ranged from 1.7-1.8%, the ash yield ranged from 6.0-11.6%, the VM ranged from 5.6-5.7%, the FC ranged from 81.0-86.7% and the TS ranged from 0.94-1.08%.

A minimum yield of 24.8% of the CBD ply with an ash yield of 6.0% is obtained at an RD of 1.35g/cm³. A maximum yield of 90.5% of the CBD ply with an ash yield of 11.6% was obtained at an RD of 1.75g/cm³. The CBD ply results in Table 4 were used to plot the densimetric (RD yield) and ash yield curves of the CBD ply shown in Figure 22. The densimetric curve depicts that as the RD increases, the yield of CBD ply increases. The ash yield curve indicates that as the ash increases the yield of the CBD ply also increases. The point at which both the curves intersect is referred to as cut point; it defines the point on the curve at which the best yield and ash yield can be obtained for each ply at a specific RD (Speight, 2015). At the cut point the CBD ply has a yield of 85% and an ash yield of 10.5% at an RD of 1.65g/cm³.

Table 4: Washability analyses of the CBD, CDB, and CB plies of the Channel Sample 30B.

Sample ID	Ply	RD	Yield (%)	IM (%)	Ash (%)	VM (%)	FC (%)	TS (%)
CS30B	CBD	1.35	24.8	1.7	6.0	5.7	86.7	0.99
	CBD	1.45	69.1	1.7	8.7	5.6	84.0	0.94
	CBD	1.55	76.9	1.7	9.3	5.7	83.4	0.95
	CBD	1.65	85.1	1.7	10.5	5.68	82.2	0.99
	CBD	1.75	90.5	1.7	11.6	5.68	81.0	1.08
	CBD	sink@1.75	100	1.6	14.4	5.77	78.2	1.35
	CDB	1.35	4.7	2.4	6.3	4.7	86.7	0.61
	CDB	1.45	41.3	2.7	6.5	4.6	86.2	0.67
	CDB	1.55	83.3	2.8	7.6	4.7	85.0	0.73
	CDB	1.65	95.0	2.7	8.5	4.7	84.1	0.79
	CDB	1.75	98.1	2.7	9.0	4.8	83.6	0.83
	CDB	sink@1.75	100	2.7	9.5	4.8	83.0	0.92
	CB	1.35	4.5	4.5	6.4	4.6	84.5	1.18
	CB	1.45	13.3	5.0	6.8	4.2	84.0	1.13
	CB	1.55	55.7	4.8	9.3	5.0	80.9	1.79
	CB	1.65	85.2	4.9	9.7	4.9	80.6	1.57
	CB	1.75	92.5	4.9	10.4	5.0	79.7	1.54
	CB	sink@1.75	100	4.8	12.2	5.2	77.9	1.83

For the CDB ply: the IM content ranged from 2.4-2.8%, the ash yield ranged from 6.3-9.0%, the VM ranged from 4.6-4.8%, the FC ranged from 83.6-86.7% and the TS ranged from 0.61-0.83%. A minimum yield of 4.7% of the CDB ply with an ash yield of 6.3% was obtained at an RD of 1.35g/cm³. A maximum yield of 98.1% of the CDB ply with an ash yield of 9.0% was obtained at an RD of 1.75g/cm³. The CDB ply results in

Table 4 were used to plot the densimetric and ash yield curves of the CDB ply shown in Figure 23. The densimetric curve depicts that as the RD increases, the yield of the CDB ply increases. The ash yield curve indicates that as the ash increases the yield of the CDB ply also increases. At the cut point, the CDB ply has a yield of 95% and an ash yield of 8.5% at an RD of 1.65g/cm³.

For the CB ply: the IM content ranged from 4.5-4.9%, the ash yield ranged from 6.4-10.4%, the VM ranged from 4.2-5.0%, the FC ranged from 79.7- 84.5%, and the TS ranged from 1.13-1.79%. Within the CB ply a minimum yield of 4.5% with an ash yield of 6.4% was obtained at an RD of 1.35g/cm³. A maximum yield of 92.5% with an ash yield of 10.4% was obtained at an RD of 1.75g/cm³. The CB ply results in Table 4 were used to plot the densimetric and ash yield curves of the CB ply shown in Figure 24. The densimetric curve depicts that as the RD increases, the yield of the CB ply increases the ash yield curve indicates that as the ash increases the yield of the CB ply also increases. At the cut point, the CB ply has a yield of 85.2% and an ash yield of 9.7% at an RD of 1.65g/cm³.

The CDB ply has the best yield and ash yield in comparison to the CBD and CB plies at the same RD of 1.65g/cm³. Within the CBD, CDB, and CB plies of Channel Sample 30B, the prime and middlings products were obtained.

Channel Sample 30B

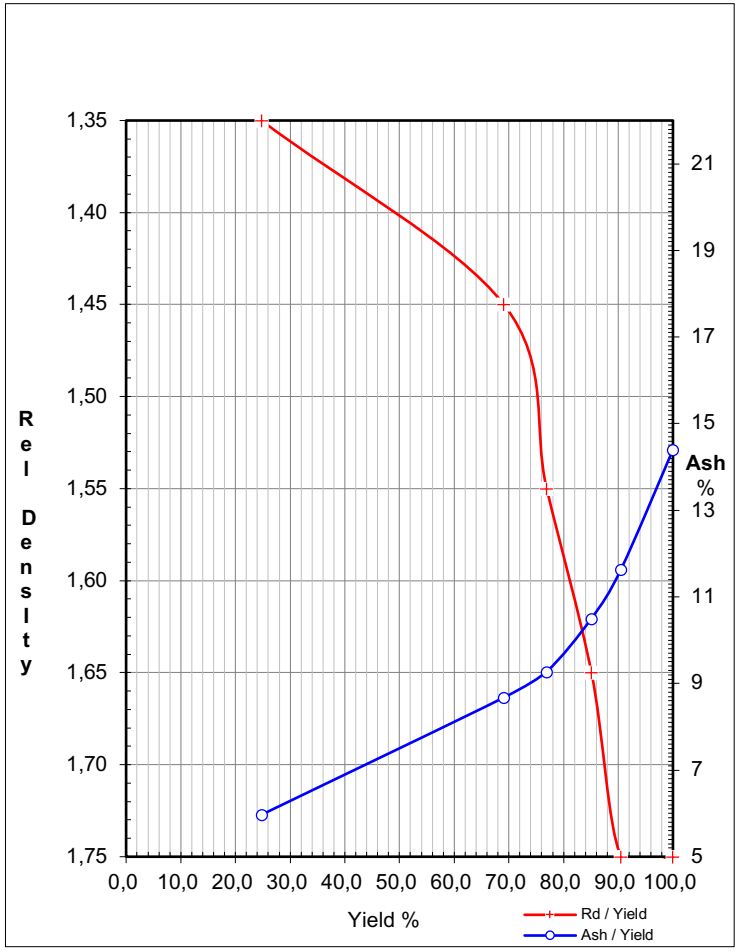


Figure 22: Graphical representation of the Ash Yield and densimetric washability curves of the CBD ply of the CS30B. Ash and RD are directly proportional to the yield of the CBD ply.

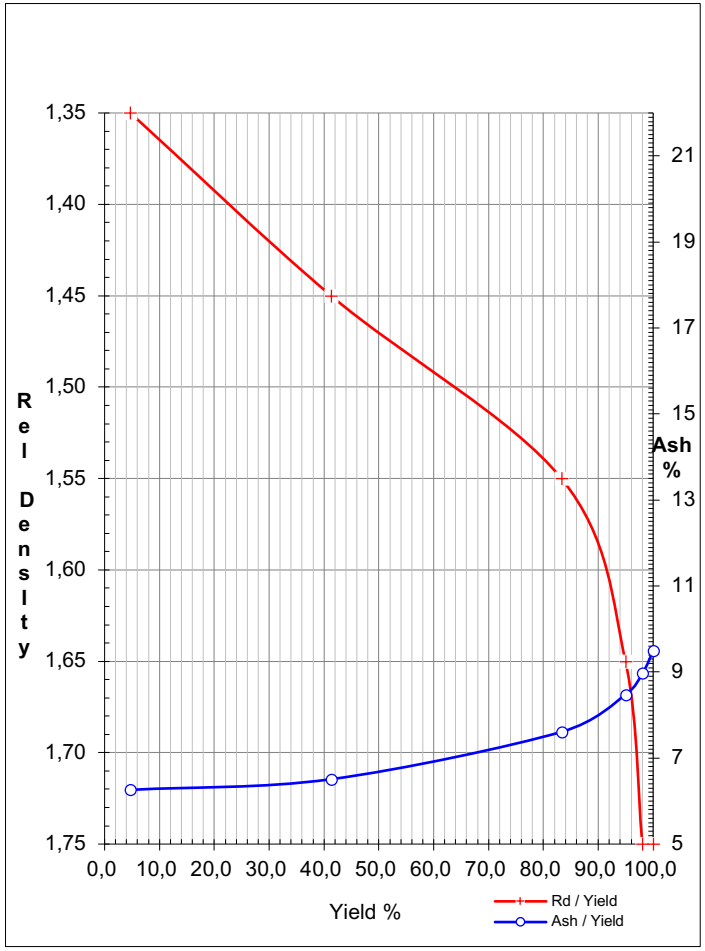


Figure 23: Graphical representation of the Ash Yield and densimetric washability curves of the CDB ply of the CS30B. Ash and RD are directly proportional to the yield of the CDB ply.

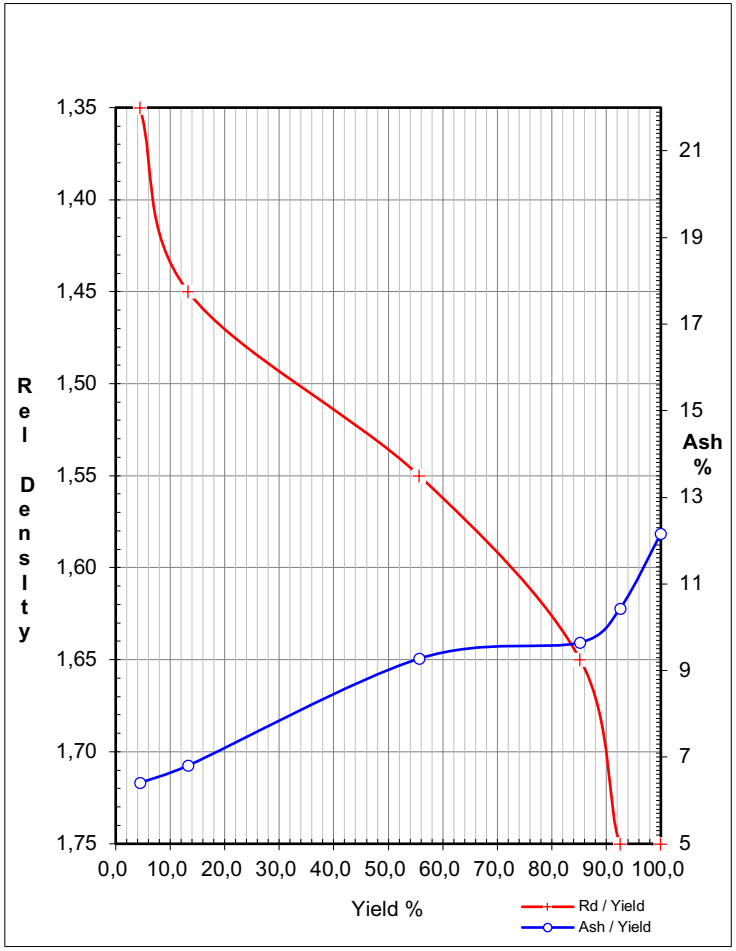


Figure 24: Graphical representation of the Ash Yield and densimetric washability curves of the CB ply of the CS30B. Ash and RD are directly proportional to the yield of the CB ply.

The results of the prime and middlings products of the CBD ply are reflected in Table 5. The densimetric and ash yield curves are presented in Figure 25. The densimetric curve depicts that as the RD increases, the yield of the CBD ply increases. The ash yield curve indicates that as the ash increases the yield of the CBD ply also increases.

Table 5: The prime and middlings products results of the CBD ply of the Channel Sample 30B.

Product	RD	Yield (%)	IM (%)	Ash (%)	VM (%)	FC (%)	TS (%)
PRIME	1.44	66.2	1.7	8.5	5.6	84.2	0.94
MIDDLINGS	1.75	24.3	1.6	20.2	5.8	72.4	1.45
WASTE		9.5	1.2	40.7	6.6	51.4	3.97

The CBD ply yielded both prime and middlings products. The prime product has a high yield in comparison to the middlings product. A yield of 66.2% of the prime product with an 8.5% ash yield was obtained at an RD of 1.44g/cm^3. It was also determined that the prime product has a moisture content of 1.7%, VM of 5.6%, FC of 84.2%, and TS of 0.94%.

A yield of 24.3% of the middlings product with a 20.2% ash yield was obtained at an RD of 1.75g/cm^3. The results of the middlings product also reflect that the ash yield does not fall within the expected range of 8.5-15.5% of the middlings product but is higher by 4.7%. It was also discovered from these results that the middlings product contained an IM of 1.6%, VM of 5.8%, FC of 84.2%, and TS of 0.94%. The remaining waste constituted a 9.5% yield with an ash yield of 40.7%. The cut point represents a low yield of 30% with a low ash yield of 6.5%.

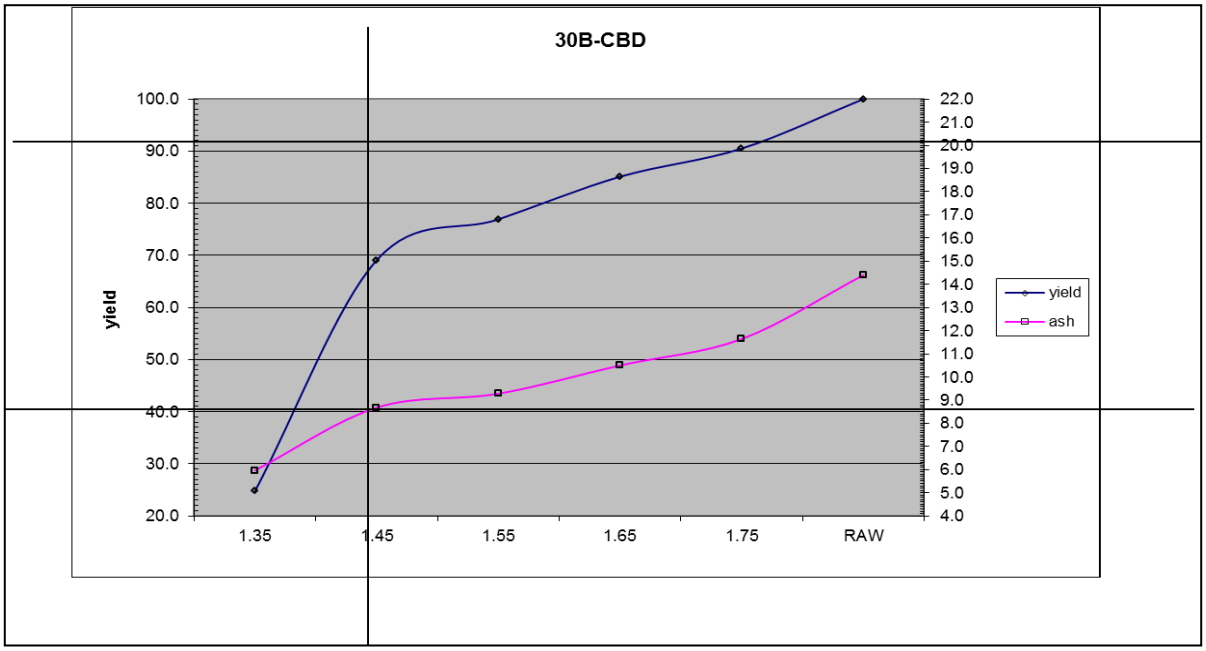


Figure 25: The densimetric and ash yield curves of the prime product of the CBD ply of the Channel Sample 30B showing the relationship between Ash Yield and RD Yield.

The results of the prime and middlings products of the CDB ply are reflected in Table 6. The densimetric and ash yield curves are presented in Figure 26. The densimetric curve depicts that as the RD increases, the yield of CDB ply increases. The ash yield curve indicates that as the ash increases the yield of the CDB ply also increases.

Table 6: The prime and middlings products results of the CDB ply of the Channel Sample 30B.

Product	RD	Yield (%)	IM (%)	Ash (%)	VM (%)	FC (%)	TS (%)
PRIME	1.65	94.9	2.7	8.5	4.7	84.1	0.79
MIDDLINGS	1.75	3.1	2.3	23.3	6.4	68.0	1.75
WASTE		1.9	1.9	36.5	7.6	54.0	5.77

The CDB ply yielded both prime and middlings products after float and sink tests were performed. The prime product has a high yield in comparison to the middlings product. The CDB ply yielded 94.9% of the prime product with an ash yield of 8.5% at an RD

of 1.65 g/cm³. It was also discovered that the prime product has an IM content of 2.7%, VM of 4.7%, FC of 84.1%, and TS of 0.79%.

The middlings product of the CDB ply has a yield of 3.1% with an ash yield of 23.3% at an RD of 1.75g/cm³. The ash yield of the middlings product reflects that it is considerably above its range of 8.5%-15.5% by 7.8%. The results also reflect that the middlings product has an IM content of 2.3%, VM of 6.4%, FC of 68.0%, and TS of 1.75%. The remaining waste has a yield of 1.9% with an ash yield of 36.5%. At the cut point the yield of CDB ply is 48% and the ash yield is 6%.

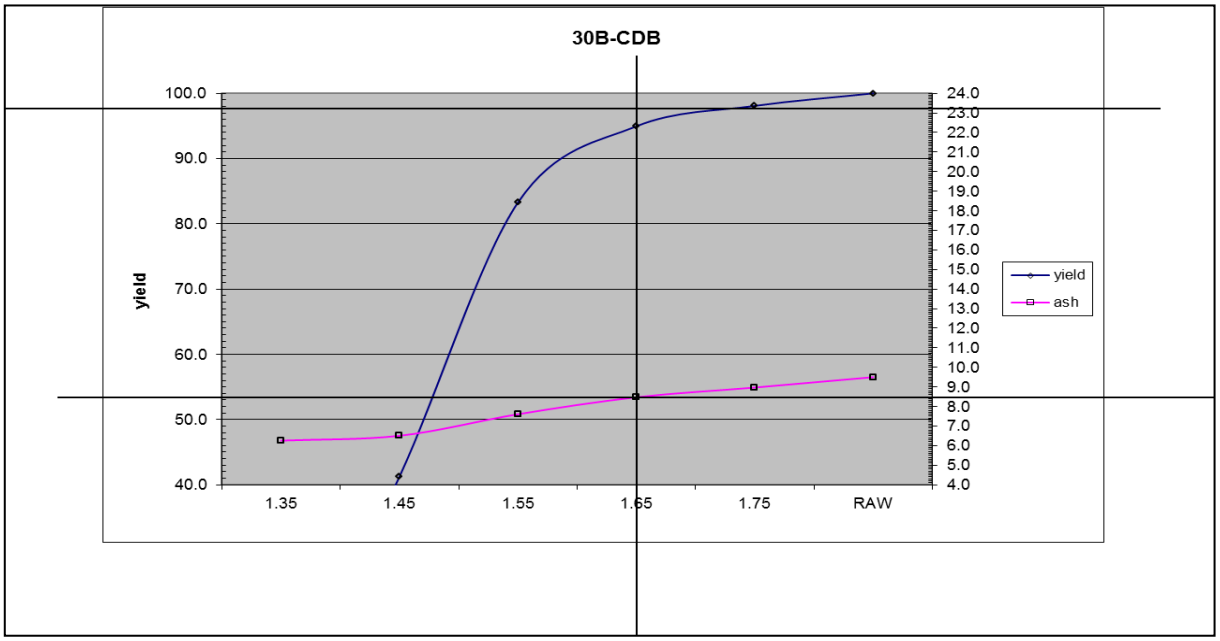


Figure 26: The densimetric and ash yield curves of the prime product of the CDB ply of the Channel Sample 30B showing a relationship between Ash Yield and RD Yield.

The results of the prime and middlings products of the CB ply are reflected in Table 7. The densimetric and ash yield curves are presented in Figure 27. The densimetric

curve depicts that as the RD increases, the yield of the CB ply increases. The ash yield curve indicates that as the ash increases the yield of the CB ply also increases.

Table 7: The prime and middlings products results of the CB ply of the Channel Sample 30B.

Product	RD	Yield (%)	IM (%)	Ash (%)	VM (%)	FC (%)	TS (%)
PRIME	1.52	42.3	4.9	8.5	4.9	81.7	1.58
MIDDLINGS	1.75	50.2	4.8	12.1	5.1	78.1	1.51
WASTE		7.5	4.0	33.6	7.8	54.6	5.44

The CB ply yielded both prime and middlings products after float and sink tests were performed. The middlings product has a high yield in comparison to the prime product. The prime product has a yield of 42.3% with an ash yield of 8.5% that was obtained at an RD of 1.52g/cm^3. It was also discovered that the prime product has a moisture content of 4.9%, VM of 4.9%, FC of 81.7%, and TS of 1.58%.

The middlings product of the CB ply yielded 50.2% with an ash yield of 12.1% that was obtained at an RD of 1.75 g/cm^3. The results also reflect that the middlings product has a moisture content of 4.8%, VM of 5.1%, FC of 78.1%, and TS of 1.51%. The remaining waste has a yield of 7.5% with an ash yield of 33.6%. A yield of 62% of CB ply and an ash yield of 9.5% is noted at the cut point.

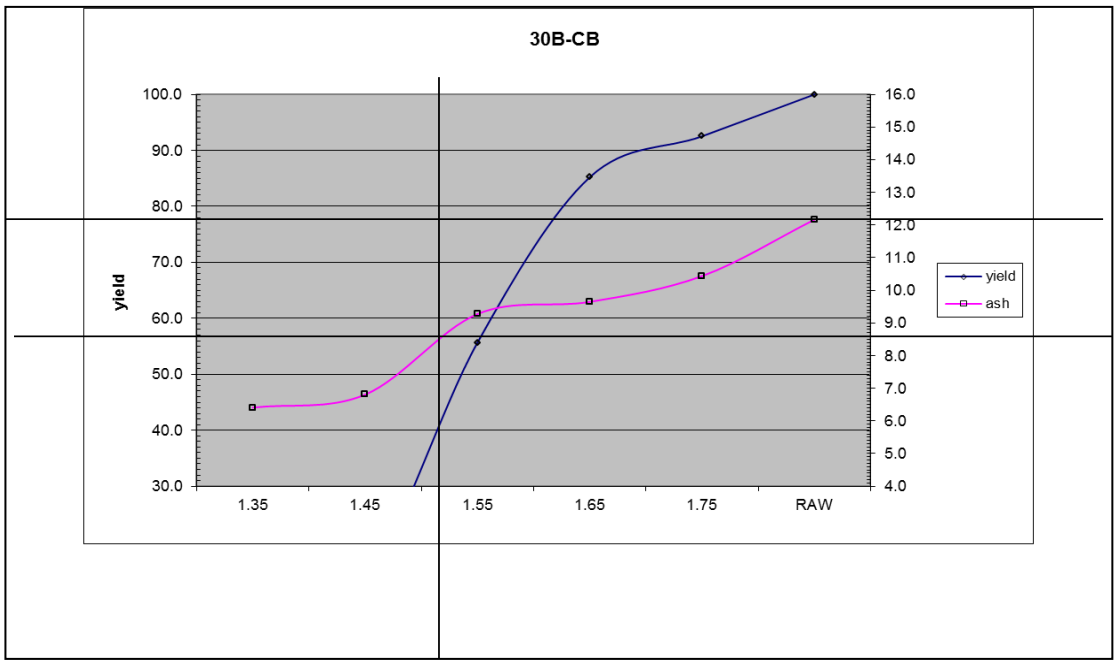


Figure 27: The densimetric and ash yield curves of the prime product of the CB ply of the Channel Sample 30B showing a relationship between Ash Yield and RD Yield.

Channel Sample 30AI

The float and sink test results of the CBD, CDB and CB plies of the Channel Sample 30AI are shown in Table 8. The float and sink tests were conducted at a wash density of 1.35-1.75g/cm³ for all plies. The results reflect that the yield is directly proportional to the RD and the yield is directly proportional to the ash yield (Figure 28, Figure 29, and Figure 30).

For the CBD ply: the IM content ranged from 2.8-2.9%, the ash yield ranged from 7.2-10.9%, the VM ranged from 5.4-5.7%, the FC ranged from 80.5-84.5% and the TS ranged from 1.05-1.25%. A minimum yield of 7.2% of the CBD ply with an ash yield of 7.2% was obtained at an RD of 1.35g/cm³. A maximum yield of 87.3% of the CBD ply with an ash yield of 10.9% was obtained at an RD of 1.75g/cm³. The CBD ply results in Table 8 were used to plot the densimetric and ash yield curves of the CBD ply shown in Figure 28. The densimetric curve depicts that as the RD increases, the yield of the

CBD ply increases. The ash yield curve indicates that as the ash increases the yield of the CBD ply also increases. At the cut point, the CBD ply has an 82% yield and a 10.2% ash yield at an RD of 1.63g/cm³.

Table 8: Washability analyses of the CBD, CDB, and CB plies for Channel Sample 30AI.

Sample ID	Ply	RD	Yield (%)	IM (%)	Ash (%)	VM (%)	FC (%)	TS (%)
CS30AI	CBD	1.35	7.2	2.8	7.2	5.4	84.5	1.10
	CBD	1.45	57.1	2.9	8.8	5.5	82.8	1.05
	CBD	1.55	74.8	2.8	9.6	5.7	81.9	1.16
	CBD	1.65	83.9	2.9	10.3	5.7	81.1	1.20
	CBD	1.75	87.3	2.8	10.9	5.7	80.5	1.25
	CBD	sink@1.75	100	2.7	14.6	5.9	76.7	1.62
	CDB	1.35	5.5	2.4	8.9	5.0	83.7	0.90
	CDB	1.45	33.4	2.1	10.2	7.1	80.7	0.73
	CDB	1.55	84.0	2.1	12.1	7.7	78.2	0.66
	CDB	1.65	96.6	2.1	13.1	7.9	76.9	0.65
	CDB	1.75	98.8	2.1	13.5	7.9	76.5	0.65
	CDB	sink@1.75	100	2.1	13.8	7.9	76.2	0.66
	CB	1.35	5.3	2.2	7.7	4.8	85.2	1.63
	CB	1.45	26.6	2.3	10.5	4.8	82.4	1.37
	CB	1.55	57.2	2.2	11.0	4.7	82.1	1.37
	CB	1.65	71.7	2.2	12.6	4.7	80.5	1.48
	CB	1.75	79.5	2.2	13.8	4.8	79.2	1.71
	CB	sink@1.75	100	2.1	19.7	4.1	74.2	4.31

For the CDB ply: the IM ranged from 2.1-2.4%, the ash yield ranged from 8.9-13.5%, the VM ranged from 5.0-7.9%, the FC ranged from 76.5-83.7% and the TS ranged from 0.65-0.90%. A minimum yield of 5.5% of the CDB ply with an ash yield of 8.9% was obtained at an RD of 1.35g/cm³. A maximum yield of 98.8% of the CDB ply with an ash yield of 13.8% was obtained at an RD of 1.75g/cm³. The CDB ply results in Table 8 were used to plot the densimetric and ash yield curves of the CDB ply shown in Figure 29. The densimetric curve depicts that as the RD increases, the yield of CDB ply increases. The ash yield curve indicates that as the ash increases the yield of the CDB ply also increases. At the cut point, the CDB ply has a 90% yield and a 12.6% ash yield at an RD of 1.57g/cm³.

For the CB ply: the IM ranged from 2.2-2.3%, the ash yield ranged from 7.7-13.8%, the VM ranged from 4.7-4.8%, the FC ranged from 79.2-85.2% and the TS ranged from 1.37-4.31%. Within the CB ply a minimum yield of 5.3% with an ash yield of 7.7% was obtained at an RD of 1.35g/cm³. A maximum yield of 79.5% with an ash yield of 13.8% was obtained at an RD of 1.75g/cm³. The CB ply results in Table 8 were used to plot the densimetric and ash yield curves of the CB ply shown in Figure 30. The densimetric curve depicts that as the RD increases, the yield of CB ply increases. The ash yield curve indicates that as the ash increases the yield of the CB ply also increases. At the cut point, the CB ply has a 64.5% yield and a 11.4% ash yield at an RD of 1.59g/cm³.

The CDB ply has the best yield and ash yield in comparison to the CBD and CB plies. The best yield and ash yield are noted at cut point for each ply. Within the CBD and

CB plies of the Channel Sample 30AI, the prime and middlings products is obtained. Only the middlings product could be obtained in the CDB ply.

Channel Sample 30AI

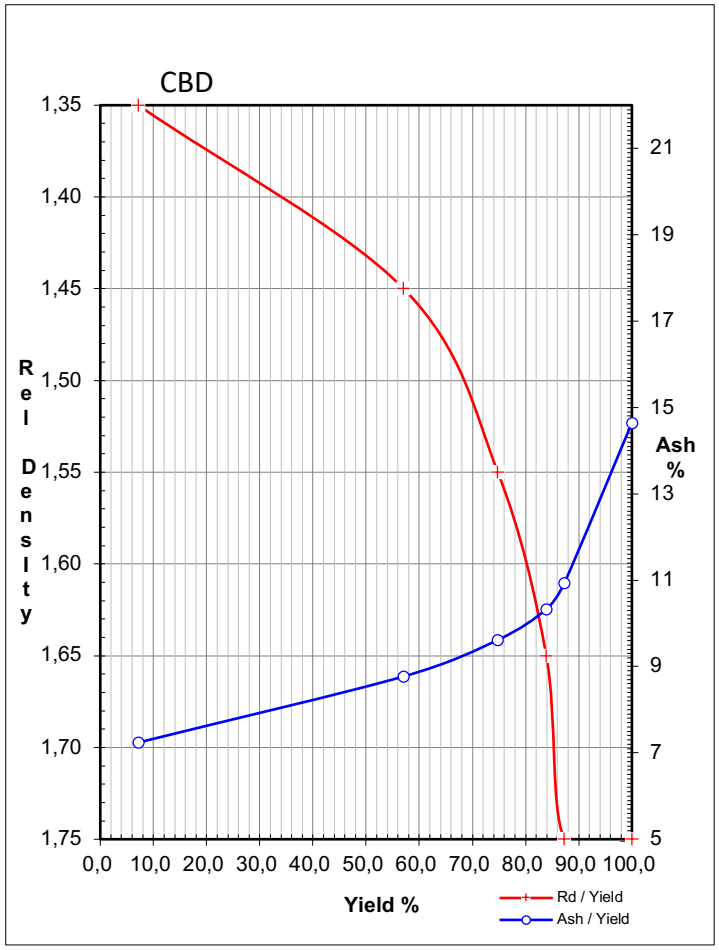


Figure 28: Graphical representation of the Ash Yield and densimetric washability curves of the CBD ply of the CS30AI. Ash and RD are directly proportional to the yield of the CBD ply.

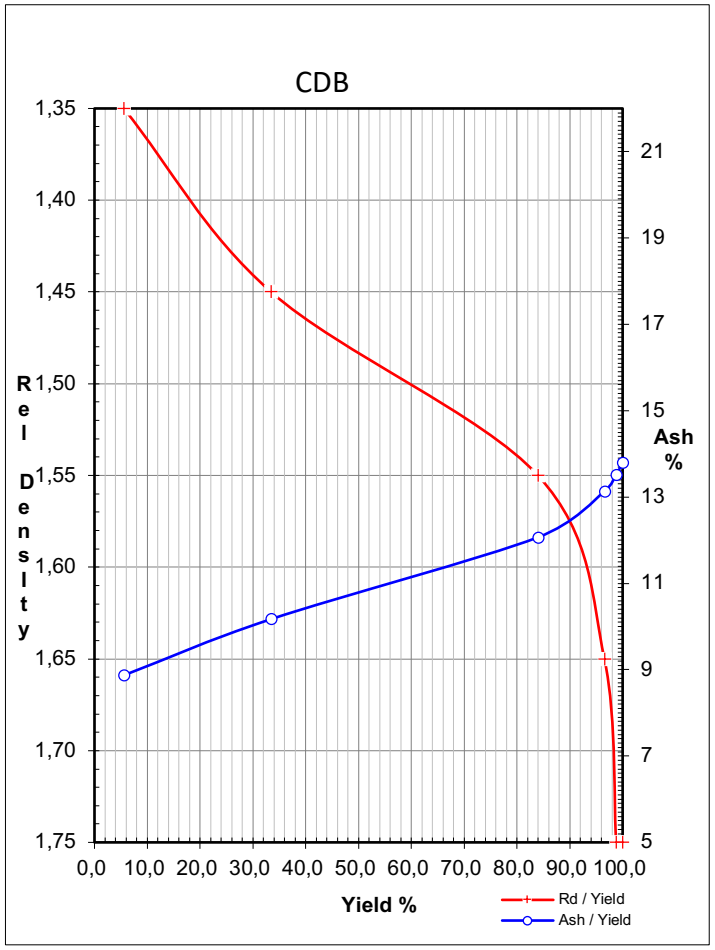


Figure 29: Graphical representation of the Ash Yield and densimetric washability curves of the CDB ply of the CS30AI. Ash and RD are directly proportional to the yield of the CDB ply.

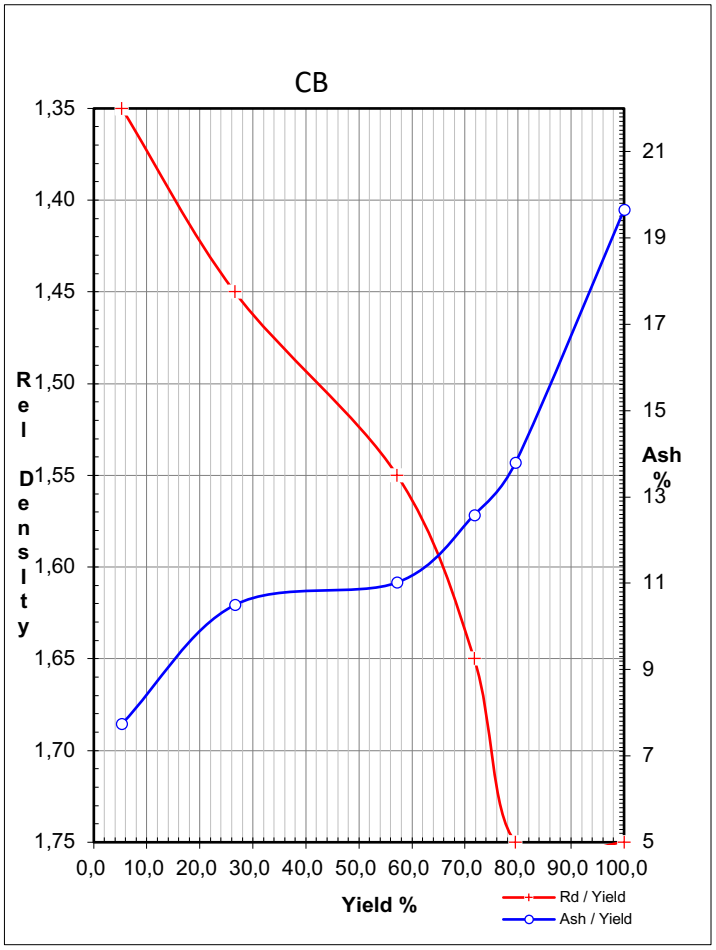


Figure 30: Graphical representation of the Ash Yield and densimetric washability curves of the CB ply of the CS30AI. Ash and RD are directly proportional to the yield of the CB ply.

The results of the prime and middlings products are represented in Table 9. Figure 31 presents the densimetric and ash yield curves of the CBD ply of Channel Sample 30AI.

Table 9: The prime and middlings products results of the CBD ply of the Channel Sample 30AI.

Product	RD	Yield%	IM%	ASH%	VM%	FC%	TS%
PRIME	1.43	48.2	2.9	8.5	5.5	83.1	1.06
MIDDLINGS	1.75	39.1	2.8	13.9	6.0	77.3	1.49
WASTE		12.7	1.8	40.1	7.4	50.6	4.11

The CBD ply yielded 48.2% of the prime product with an ash yield of 8.5% at an RD of 1.43g/cm^3. The prime product comprised 2.9% IM, 5.5% VM, 83.1% FC, and 1.06% TS. The results also reflect that the yield of the prime product of the CBD ply is high in comparison to the yield of the middlings product of the same ply.

A yield of 39.1% of the middlings product with an ash yield of 13.9% was also obtained within the CBD ply at an RD of 1.75g/cm^3. The middlings product contained 2.8% IM, 6.0% VM, 77.3% FC, and 1.49% TS. The remaining 12.7% yield constitutes waste with an ash yield of 40.1%. At the cut point the yield is 30% and the ash yield is 7.9%.

The results of the prime and middlings products of the CDB ply are represented in Table 10. Figure 32 presents the densimetric and ash yield curves of the CDB ply.

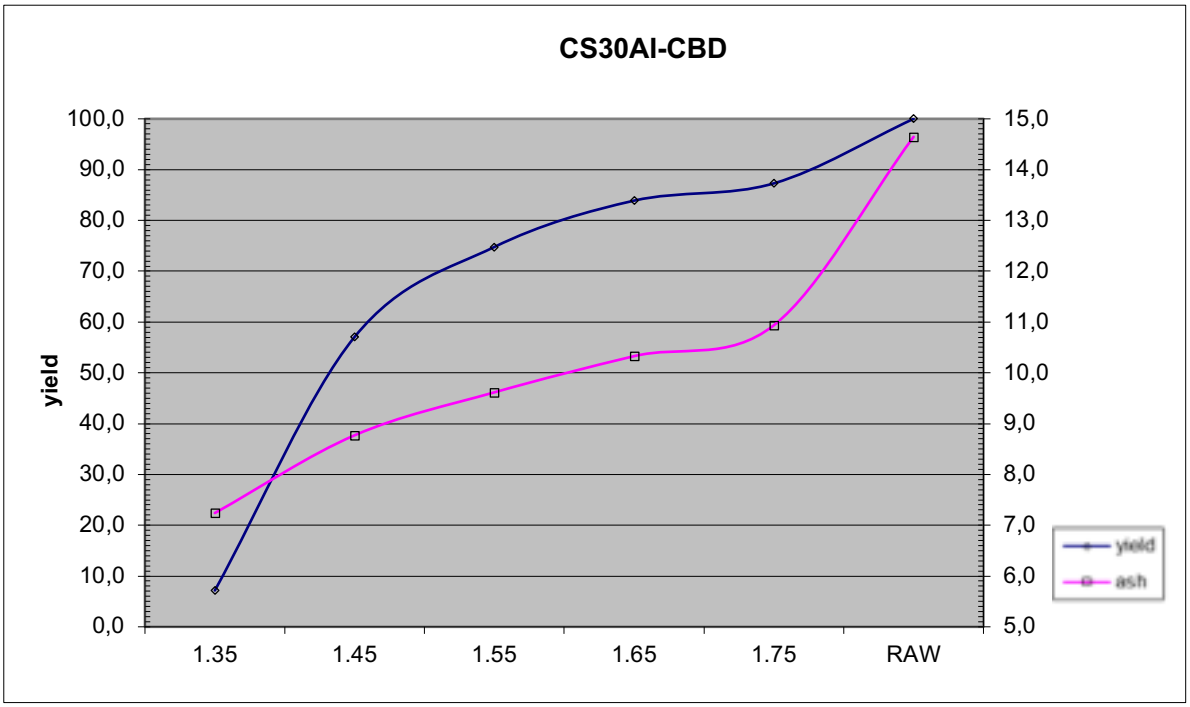


Figure 31: The densimetric and ash yield curves of the prime product of the CBD ply of the Channel Sample 30AI showing a relationship between Ash Yield and RD Yield.

Table 10: The middlings product results of the CDB ply of the Channel Sample 30AI.

Product	RD	Yield%	IM%	ASH%	VM%	FC%	TS%
PRIME		0	0	0	0	0	0
MIDDLINGS	1.75	98.8	2.1	13.5	7.9	76.5	0.65
WASTE		1.2	2.1	13.8	7.9	76.2	0.66

The results of the CDB ply reflect no yield of the prime product. The 98.8% yield of the middlings product of the CDB ply was obtained at an RD of 1.75g/cm^3 with an ash yield of 13.5%. The middlings product contained 2.1% IM, 7.9% VM, 76.5% FC, and 0.65% TS. The remaining yield of 1.2% was the waste with an ash yield of 13.8%. At the cut point the yield is 62% and the ash yield is 11.2% at an RD of 1.52g/cm^3.

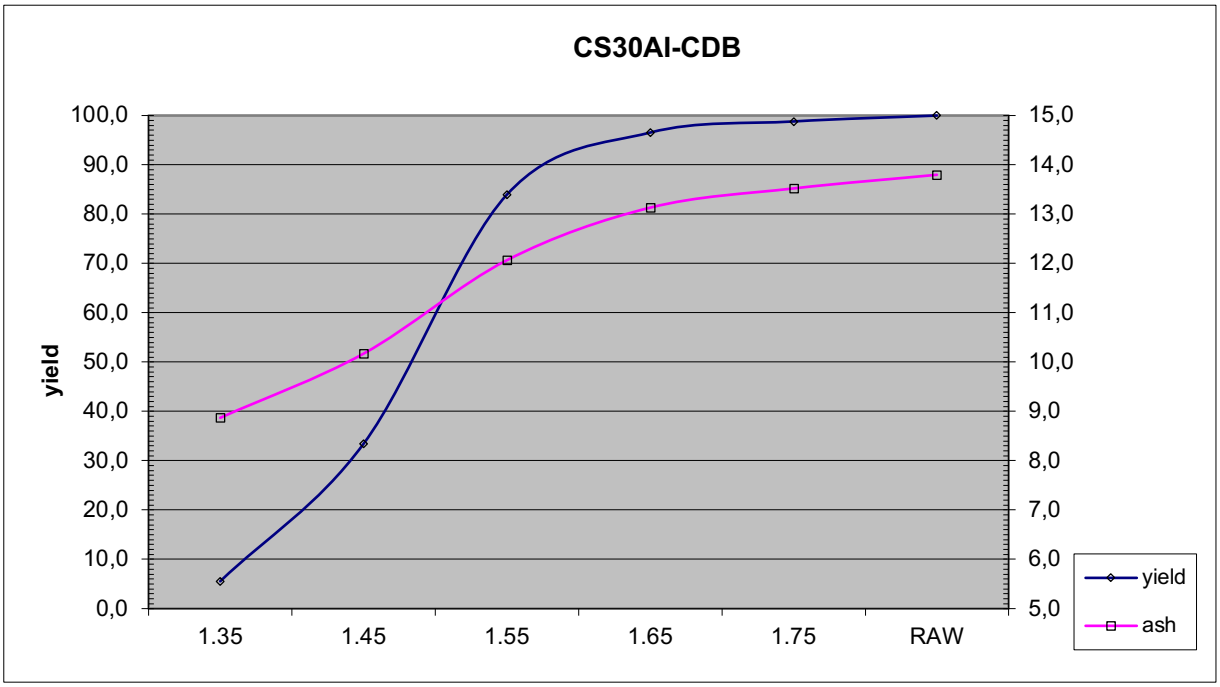


Figure 32: The densimetric and ash yield curves of the prime product of the CDB ply of the Channel Sample 30AI showing a relationship between Ash Yield and RD Yield.

The results of the prime and middlings products of the CB ply are presented in Table 11. Figure 33 presents the densimetric and ash yield curves of the CB ply.

Table 11: The prime and middlings products results of the CB ply of the Channel Sample 30AI.

Product	RD	Yield%	IM%	ASH%	VM%	FC%	TS%
PRIME	1.38	11.2	2.2	8.5	4.8	84.5	1.56
MIDDLINGS	1.75	68.4	2.2	14.7	4.8	78.3	1.74
WASTE		20.5	1.7	42.4	1.2	54.7	14.43

The CB ply reflected prime and middlings products results. The CB ply yielded 11.2% of the prime product containing an ash yield of 8.5% obtained at an RD of 1.38g/cm^3. The results reflect that the prime product contained 2.2% IM, 4.8% VM, 84.5% FC, and 1.56% TS. The prime product of the CB ply reflects a low yield compared to the middlings product of the same ply.

The results also show that the CB ply yielded 68.4% of the middlings product containing an ash yield of 14.7% obtained at an RD of 1.75 g/cm³. The middlings product contained 2.2% IM, 4.8% VM, 78.3% FC, and 1.74% TS. Both prime and middlings products contained the same amount of IM and VM. The waste-constituting 20.5% yield contained an ash yield of 42.4%.

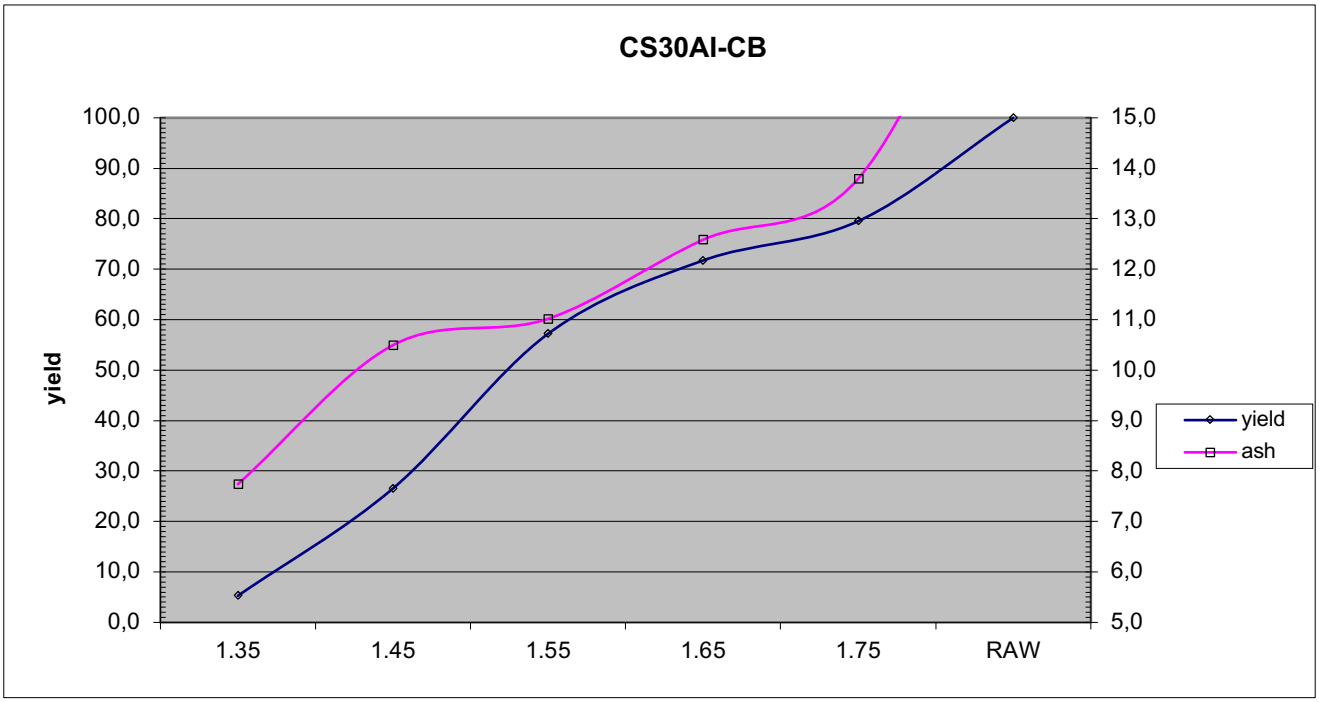


Figure 33: The densimetric and ash yield curves of the prime product of the CB ply of the Channel Sample 30AI showing a relationship between Ash Yield and RD Yield.

Channel Sample 30D

The float and sink test results of the CBD, CDB, and CB plies of Channel Sample CS30D are shown in Table 12. The float and sink tests were conducted in a wash density of 1.35-1.75g/cm³ for the CDB and CB plies. The CBD ply was washed at a density of 1.35-1.65g/cm³. The results reflect that the yield is directly proportional to the RD. The yield, therefore, increases with increasing RD. The results also reflect that the yield is directly proportional to the ash yield.

For the CBD ply: the IM ranged from 2.9-3.2%, the ash yield ranged from 6.2%-8.3%, the VM ranged from 4.4-4.9%, the FC ranged from 84.0-86.3% and the TS ranged from 1.45-1.79%. A minimum yield of 5.1% of the CBD ply with an ash yield of 6.2% was obtained at an RD of 1.35g/cm³. A maximum yield of 95.0% of the CBD ply with an ash yield of 8.3% was obtained at an RD of 1.65 g/cm³. The CBD ply results in Table 12 were used to plot the densimetric and ash yield curves of the CBD ply shown in Figure 34. The densimetric curve depicts that as the RD increases, the yield of CBD ply increases. The ash yield curve indicates that as the ash increases the yield of the CBD ply also increases. At the cut point, the CBD ply has a 96% yield and an 8.6% ash yield at an RD of 1.67g/cm³.

Table 12: Washability analyses of the CBD, CDB, and CB plies for Channel Sample 30D.

Sample ID	Ply	RD	Yield (%)	IM (%)	Ash (%)	VM (%)	FC (%)	TS (%)
CS30D	CBD	1.35	5.1	3.2	6.2	4.4	86.3	1.45
	CBD	1.45	45.6	3.0	6.9	4.8	85.2	1.61
	CBD	1.55	87.9	2.9	7.7	4.9	84.5	1.70
	CBD	1.65	95.0	2.9	8.3	4.9	84.0	1.79
	CBD	sink@1.65	100	2.8	9.1	5.0	83.2	2.32
	CDB	1.35	13.3	2.8	6.5	7.2	83.5	0.75
	CDB	1.45	41.6	2.6	8.0	7.6	81.9	0.77
	CDB	1.55	86.9	2.8	9.2	7.3	80.7	0.77
	CDB	1.65	93.2	2.7	9.9	7.4	80.1	0.78
	CDB	1.75	95.6	2.7	10.2	7.3	79.8	0.84
	CDB	sink@1.75	100	2.7	11.5	7.3	78.6	0.89
	CB	1.35	13.1	2.7	8.6	5.2	83.5	1.02
	CB	1.45	46.2	2.9	8.7	5.1	83.3	1.12

	CB	1.55	82.4	3.0	11.3	5.3	80.5	1.25
	CB	1.65	91.8	3.0	12.0	5.5	79.6	1.41
	CB	1.75	93.8	2.9	12.5	5.5	79.2	1.50
	CB	sink@1.75	100	2.9	14.2	5.5	77.4	1.47

For the CDB ply: the IM ranged from 2.6-2.8%, the ash yield ranged from 6.5-10.2%, the VM ranged from 7.2-7.6%, the FC ranged from 79.8%-83.5% and the TS ranged from 0.75-0.84%. A minimum yield of 13.3% of the CDB ply with an ash yield of 6.5% was obtained at an RD of 1.35g/cm³. A maximum yield of 95.6% of the CDB ply with an ash yield of 10.2% was obtained at an RD of 1.75g/cm³. The CDB ply results in Table 12 were used to plot the densimetric and ash yield curves of the CDB ply shown in Figure 35. The densimetric curve depicts that as the RD increases, the yield of CDB ply increases, and the ash yield curve indicate that as the ash increases the yield of the CDB ply also increases. At the cut point, the CDB ply has 93.5% yield and 9.7% ash yield at a relative density of 1.64g/cm³.

For the CB ply: the IM ranged from 2.7-3.0%, the ash yield ranged from 8.6-12.5%, the VM ranged from 5.1-5.5%, the FC ranged from 79.2-83.5% and the TS ranged from 1.02-1.50%. Within the CB ply a minimum yield of 13.1% with an ash yield of 8.6% was obtained at an RD of 1.35g/cm³. A maximum yield of 93.8% with an ash yield of 12.5% was obtained at an RD of 1.75g/cm³. The CB ply results in Table 12 were used to plot the densimetric and ash yield curves of the CB ply shown in Figure 36. The densimetric curve depicts that as the RD increases, the yield of the CB ply increases. The ash yield curve indicates that as the ash increases the yield of the CB

ply also increases. At the cut point, the CBD ply has an 88% yield and a 11.6% ash yield at an RD of 1.59g/cm³.

The CBD ply has the best yield and ash yield in comparison to the CDB and CB plies. Within the CBD and CB plies of Channel Sample 30D, only the prime product was obtained. The prime and middlings products were obtained within the CDB ply.

Channel Sample30D

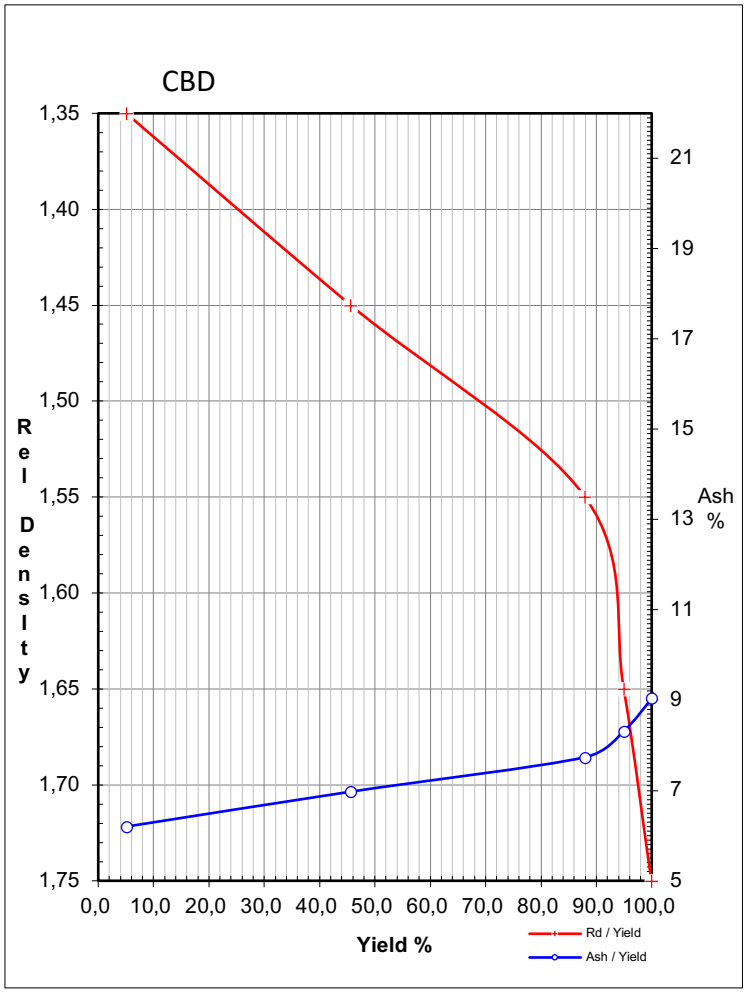


Figure 34: Graphical representation of the Ash Yield and densimetric washability curves of the CBD ply of the CS30D. Ash and RD are directly proportional to the yield of the CBD ply.

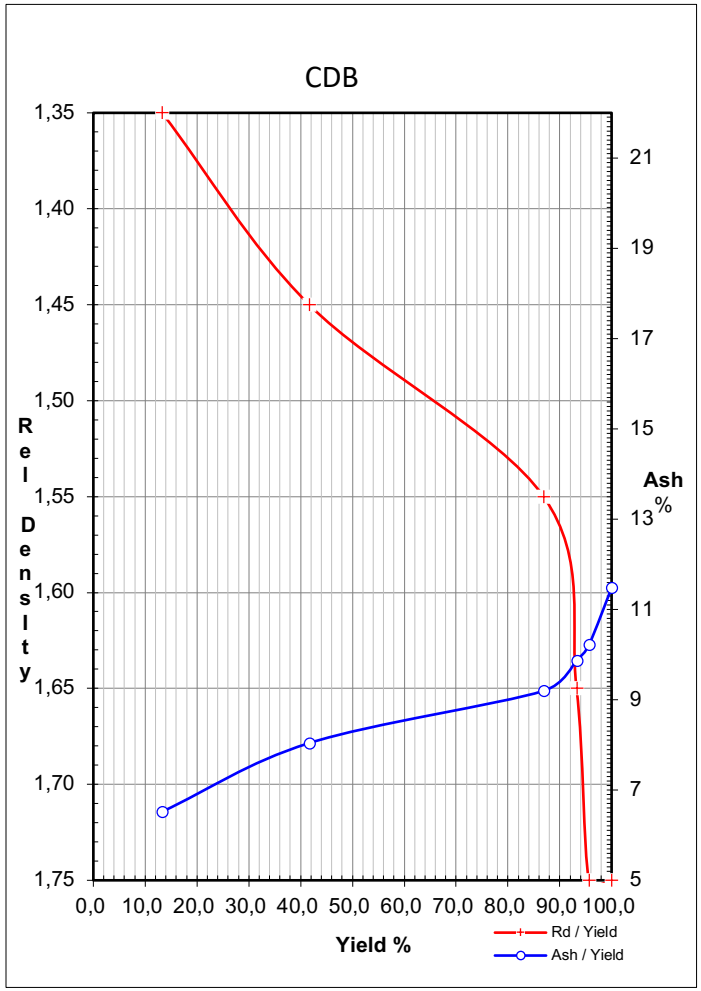


Figure 35: Graphical representation of the Ash Yield and densimetric washability curves of the CDB ply of the CS30D. Ash and RD are directly proportional to the yield of the CDB ply.

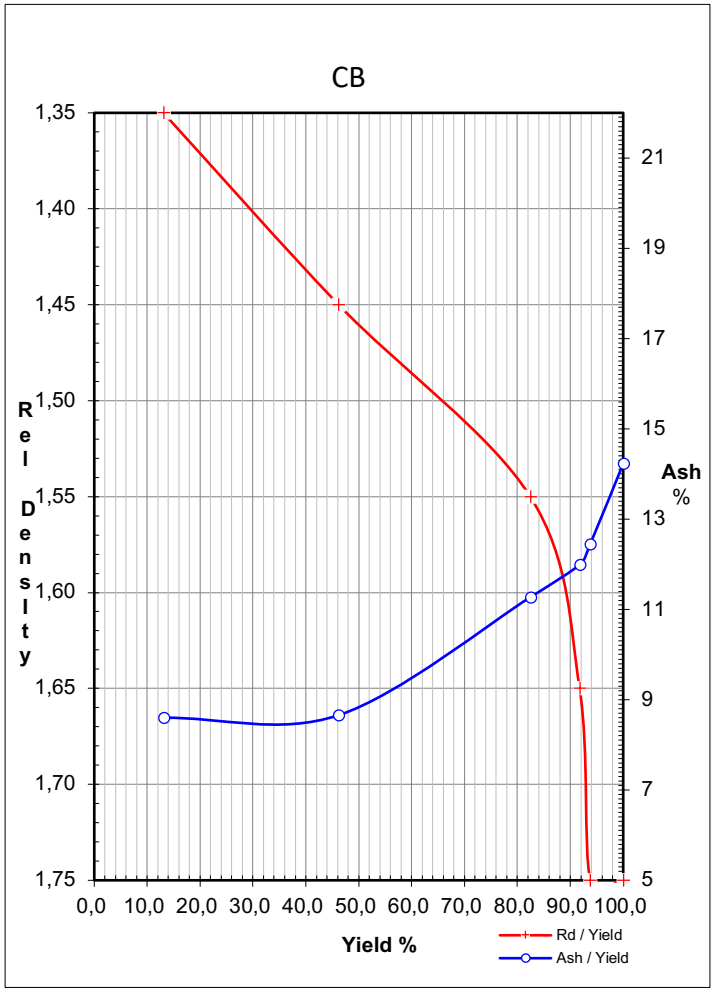


Figure 36: Graphical representation of the Ash Yield and densimetric washability curves of the CB ply of the CS30D. Ash and RD are directly proportional to the yield of the CB ply.

The results of the prime product of the CBD ply are reflected in Table 13. These results were used to plot the densimetric and ash yield curves of the CBD ply shown in Figure 37.

Table 13: The middlings product and waste results of the CBD ply of the Channel Sample 30D.

Product	RD	Yield %	IM %	Ash %	VM %	FC %	TS %
PRIME	1.65	96.2	2.8	8.5	4.9	83.8	1.92
MIDDLINGS		0	0	0	0	0	0
WASTE		3.8	2.1	23.1	7.1	67.7	12.35

The results in Table 13 indicate that only the prime product was obtained for the CBD ply of Channel Sample 30D of the Main Seam at the ZAC. A total yield of 96.2% with an ash yield of 8.5% was obtained at an RD of 1.65 g/cm^3. The CBD ply has an IM of 2.8%, VM of 4.9%, FC of 83.8% and TS of 1.92%. The remaining yield of 3.8% was the waste product with an ash yield of 23.1%. At the cut point a yield of 12% and an ash yield of 6.5% is noted.

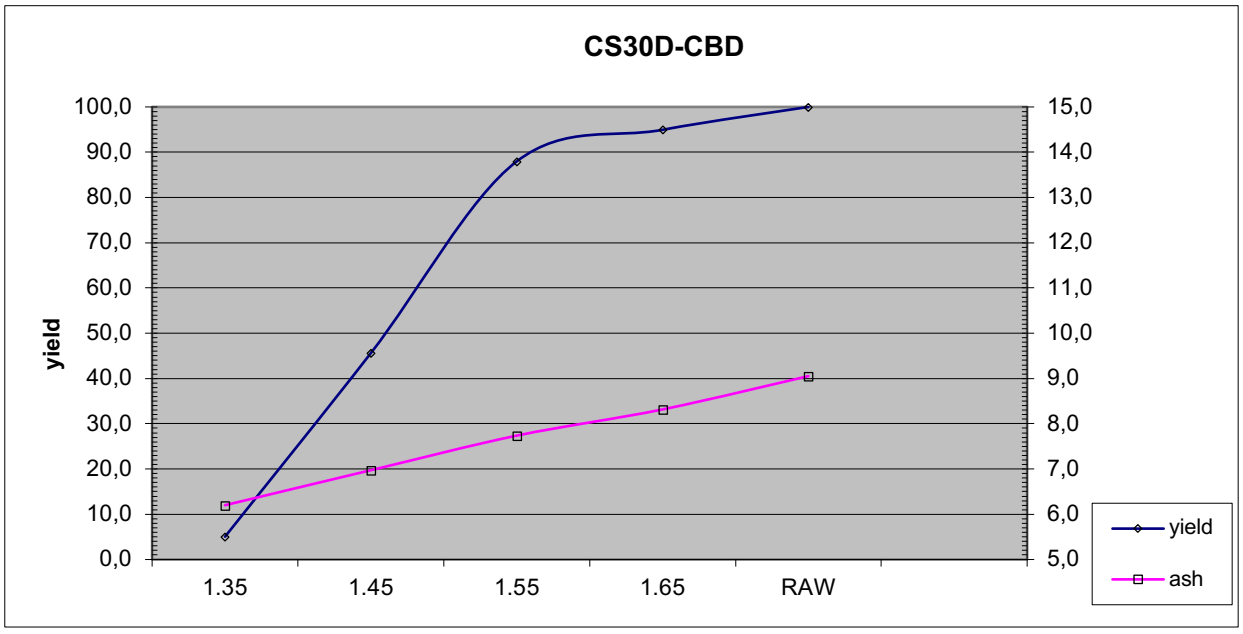


Figure 37: The densimetric and ash yield curves of the prime product of the CBD ply of the Channel Sample 30D showing a relationship between Ash Yield and RD Yield.

The results in Table 14 indicate that the prime and middlings products were yielded within the CDB ply of Channel Sample 30D of the Main Seam at the ZAC. A total yield of 50.2% of the prime product with an ash yield of 8.5% was obtained at an RD of 1.48g/cm³. The prime product of the CDB ply comprises 2.5% IM, 7.7% VM, 81.4% FC and 0.78% TS. The results also reflect that the prime product of the CDB ply was higher in comparison to the middlings product of the same ply.

The yield of 45.4% was obtained for the middlings product with an ash yield of 12.1% at an RD of 1.75g/cm³. The middlings product contains 3.0% IM, 6.9% VM, 78.0% FC, and 0.90% TS. The remaining 4.4% yield was the waste with a 39.1% ash yield. Figure 38 shows the densimetric and ash yield curves of the prime and middlings product of the CDB ply of the Channel Sample 30D. At the cut point a yield of 16% and an ash yield of 6.6% is noted.

Table 14: The prime and middlings products results of the CDB ply of the Channel Sample 30D.

Product	RD	Yield %	IM %	Ash %	VM %	FC %	TS %
PRIME	1.48	50.2	2.5	8.5	7.7	81.4	0.78
MIDDLINGS	1.75	45.4	3.0	12.1	6.9	78.0	0.90
WASTE		4.4	1.7	39.1	6.4	52.8	2.11

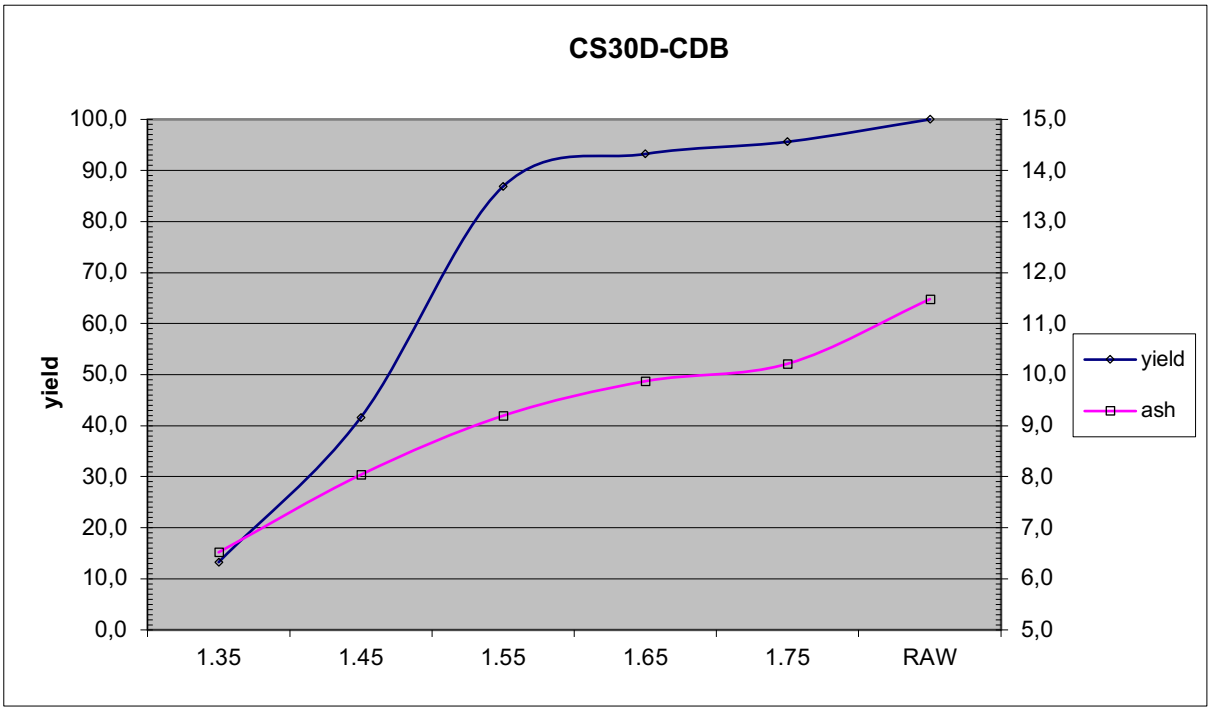


Figure 38: The densimetric and ash yield curves of the prime and middlings product of the CDB ply of the Channel Sample 30D showing a relationship between Ash Yield and RD Yield.

The results in Table 15 represent the middlings product that was obtained within the CB ply of Channel Sample 30D of the Main Seam. There was no prime product yielded within the CB ply, however, a 93.8% yield of the middlings product with an ash yield of 12.5% was obtained at an RD of 1.75g/cm^3. The middlings product contains 2.9% IM 5.5% VM, 79.2% FC and 1.50%TS. The remaining 6.2% yield was for the waste with an ash yield 14.2%. Figure 39 presents the densimetric and ash yield curves of the middlings product of the CB ply.

Table 15: The middlings product and waste results of the CB ply of the Channel Sample 30D.

Product	RD	Yield %	IM %	Ash %	VM %	FC %	TS %
PRIME		0	0	0	0	0	0
MIDDLINGS	1.75	93.8	2.9	12.5	5.5	79.2	1.50
WASTE		6.2	2.9	14.2	5.5	77.4	1.47

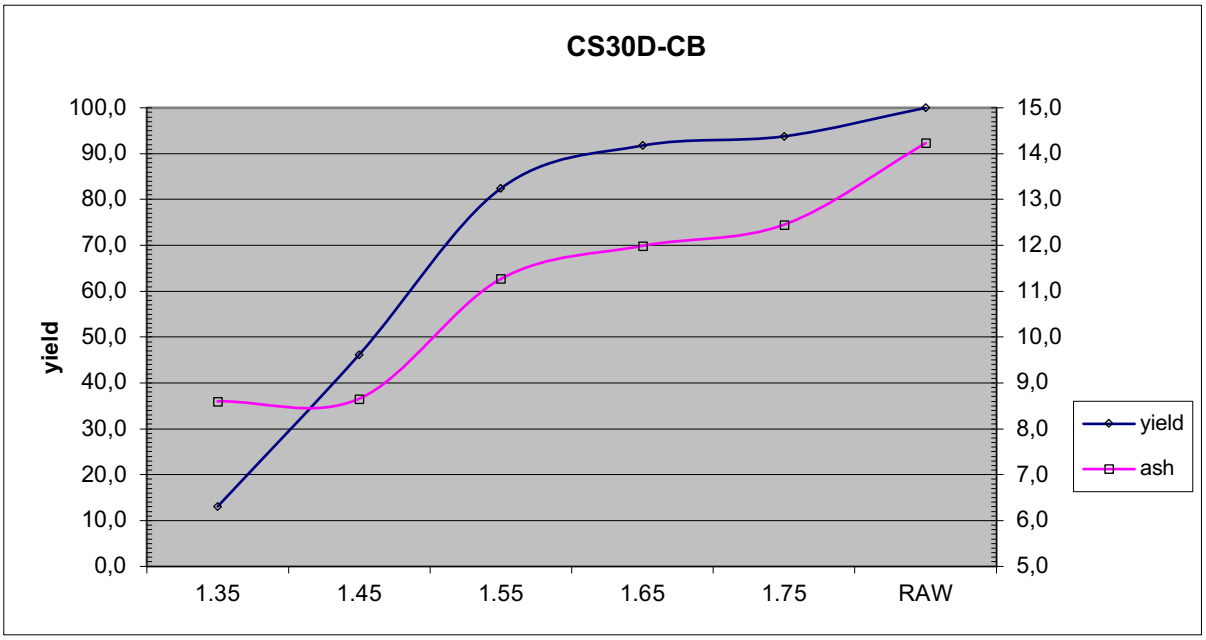


Figure 39: The densimetric and ash yield curves of the middlings product of the CB ply of the Channel Sample 30D showing a relationship between Ash Yield and RD Yield.

This section represents the results of the petrographic analyses which included maceral analysis and vitrinite reflectance analysis.

Petrography analyses

Petrographic analyses are an important tool in coal characterisation; they are used to identify different constituents that make up coal through the use of a microscope (Richards et al., 2013). The vitrinite reflectance was also measured in the CBD, CDB, and CB plies of Channel Sample 30B, Channel Sample 30AI and Channel Sample 30D of the Main Seam. Vitrinite reflectance determines the rank of the coal.

Maceral analysis

Maceral analysis was conducted on the CBD, CDB, CB plies of Channel Sample 30B, Channel Sample 30AI, and Channel Sample 30D. The results of this analysis are presented in Table 16.

The results in Table 16 indicate that the Main Seam of the Ngwabe Shaft has a high content of inertinite and vitrinite but has no liptinite. The dominant maceral group is inertinite, followed by vitrinite. The CDB ply has a high inertinite content in comparison to the CBD and CB plies. The inertinite content of the CDB ply has more than 70% volume dominated by fusinite, inert semifusinite and secretinite. Fusinite occurs in bands and lenses with a strongly developed cellular structure (Figure 40E). It appears light-grey in colour and has high reflectance values compared to all other macerals.

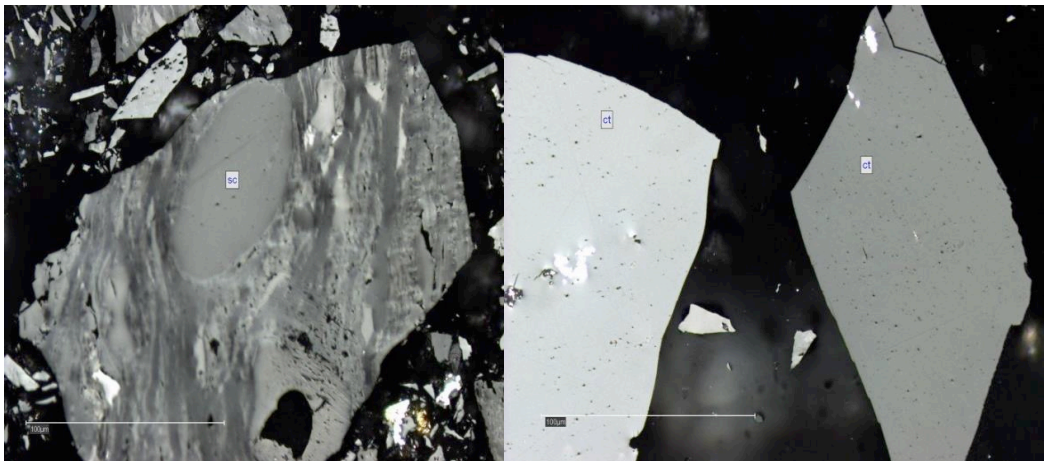
The inertinite within the CBD ply is more than 50% volume dominated by inert semifusinite (Figure 40C). The cell structure of the inert semifusinite is well developed within this ply. Its colour appears light grey, and a sharp boundary is observed between collotelinite and semifusinite (Figure 40C). The pyrite inclusions were also observed within inert semifusinite (Figure 40C). For the CB ply, the inertinite is less than 40% volume dominated by secretinite (Figure 40A). The secretinite is characterised by an oval shaped structure and is light-grey in colour as shown in Figure 40A. Only the CB ply of Channel Sample 30D indicated inertinite of more than 50% volume.

The CB ply has a high vitrinite component compared to the CBD and CDB plies. This ply has vitrinite of more than 60% volume dominated by maceral collotelinite. The maceral collotelinite appears light grey and dark in colour with cracks filled by pyrite and clay material (Figure 49D). The collotelinite and collodetrinite occurs within the CBD, CDB and CB plies of all channel samples, whereas telinite, gelinite and corprogelinite occurred occasionally in very small proportions (less than 0.4% volume) in each ply. The CBD ply has a vitrinite component of less than 40% volume. The CDB ply has vitrinite of less than 30% volume reported on a mineral matter free basis (mmf).

The mineral matter observed microscopically within the CBD, CDB, and CB plies is less than 13% volume (very low) and consists of clay, quartz, carbonates and sulphides (Figure 40D). Only in the CDB ply of Channel Sample 30AI were sulphides not observed. Carbonates were also observed in small proportions within the plies. Carbonates did not, however, occur within the CBD and CDB plies of Channel Sample 30B and the CB ply of Channel Sample 30D. Quartz occurs in very small proportions (less than 1.5% volume) but did not occur within the CDB and CB plies of Channel Samples 30B, CBD and CB plies of Channel Sample 30AI, and CDB and CB plies of Channel Samples 30D.

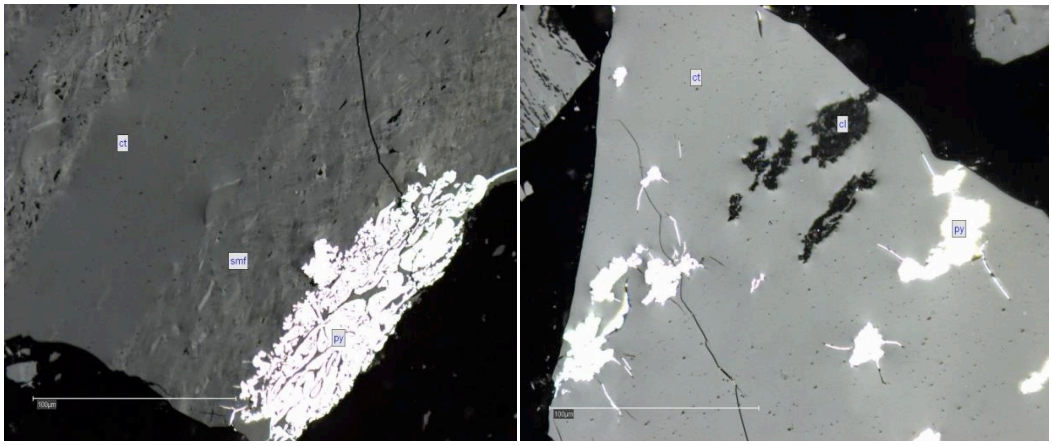
Table 16: Results of the maceral group analysis of the CBD, CDB and CB plies within the Main Seam. mmf = mineral matter free (source: Appendix 5).

	CS30B						CS30AI						CS30D					
Maceral group Totals (Vol %)	**CBD**		**CDB**		**CB**		**CBD**		**CDB**		**CB**		**CBD**		**CDB**		**CB**	
	Mm	**mmf**	**mm**	**mmf**	**mm**	**mmf**	**mm**	**mmf**	**mm**	**mmf**	**mm**	**mmf**	**mm**	**mmf**	**mm**	**mmf**	**mm**	**mmf**
Vitrinite	22.0	24.6	8.0	8.1	59.6	61.6	32.2	36.5	12.9	13.4	66.3	67.1	36.4	41.7	22.2	22.9	40.0	41.2
Inertinite	67.5	75.4	90.8	91.9	37.2	38.4	56.0	63.5	82.9	86.6	32.5	32.9	50.8	58.1	74.6	77.1	57.2	58.8
Liptinite	0.0	0.0	0.0	0.0	0.0	0.0	0.0	0.0	0.0	0.0	0.0	0.0	0.0	0.0	0.0	0.0	0.0	0.0
Mineral Matter	10.4		1.2		3.2		11.8		4.2		1.2		12.6		3.2		2.8	



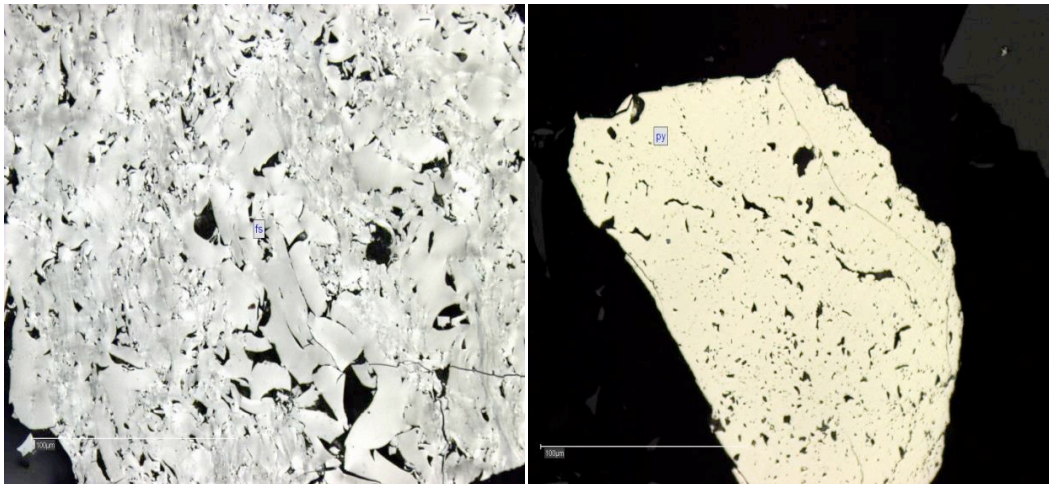
A. Secretinite.

B. Collotelinite in bright coal (left) and dull coal (right)



C. Collotelinite (ct), semifusinite (smf) pyrite (py)

D. Collotelinite, clay (cl) and pyrite (py)



E. Fusinite

F. Pyrite

Figure 40: Photomicrographs of different maceral components determined within the Main Seam (UJ petrography laboratory).

Vitrinite reflectance

The mean vitrinite reflectance (RoV%) results are presented in Table 17. The vitrinite reflectance measurements were only taken in maceral collotelinite. The vitrinite reflectance measurements were then used to plot histograms presented in Figure 41. The histograms for the CBD, CDB, and CB plies for all three channel samples depict a unimodal distribution. A unimodal distribution is a distribution reflecting a single clear peak of the most frequent value (Nazan and Faruk, 2020). The histograms of the CBD, CDB, and CB plies of Channel Sample 30D were represented as an example of a unimodal distribution. All of the histograms are presented in Appendix 6.

The vitrinite reflectance results indicate that the CB ply has a higher reflectance value in comparison to the CBD and CDB plies in all channel samples. The RoV% of the CBD and CDB plies reflected a similar RoV%, and it was noted that there is a trend from the top (CBD ply) to the bottom (CB ply) of the Main Seam. The CB ply of Channel Sample 30B reported a mean RoV% ranging from 3.54-5.15%, with an average of 4.24%. The CBD ply of Channel Sample 30B indicated a mean RoV% ranging from 2.83-4.57%, with an average of 3.64%. The CDB ply of Channel Sample 30B indicate a mean RoV% ranging from 2.51-4.91%, with an average of 3.65%.

The CB ply of Channel Sample 30AI reported a mean RoV% ranging from 2.40-5.05%, with an average of 4.02%. The CBD ply of Channel Sample 30AI indicated a mean RoV% ranging from 2.03-4.61%, with an average of 3.56%. The CDB ply of Channel Sample 30AI indicated a mean RoV% ranging from 1.83-4.83%, with an average of 3.53%. This is the only ply reflecting a minimum RoV% of less than 2%.

The CB ply of Channel Sample 30D reported a mean RoV% ranging from 3.56%-5.17%, with an average of 4.16%. The CBD ply of Channel Sample 30D reported a mean RoV% ranging from 2.37-5.17%, with an average of 3.61%. The CDB ply of Channel Sample 30D indicated a mean RoV% ranging from 2.80-4.55%, with an average of 3.61%

Table 17: Vitrinite reflectance analysis results of the CBD, CDB and CB plies.

Vitrinite Reflectance Analysis (RoV %)										
		CS30B			**CS30AI**			**CS30D**		
Ply.		**CBD**	**CDB**	**CB**	**CBD**	**CDB**	**CB**	**CBD**	**CDB**	**CB**
Vitrinite reflectance (RoV%)	**Random**	3.64	3.65	4.24	3.56	3.53	4.02	3.61	3.61	4.16
	St. dev.	0.37	0.44	0.37	0.55	0.90	0.71	0.48	0.41	0.37
	Max	4.57	4.91	5.15	4.61	4.83	5.05	5.17	4.55	5.17
	Min	2.83	2.51	3.54	2.03	1.83	2.40	2.37	2.80	3.56
	Rank Category	High Rank B	High Rank B	High Rank A	High Rank B	High Rank B	High Rank B	High Rank B	High Rank B	High Rank A

The histograms shown in Figure 41 represent unimodal distributions of the CBD, CDB and CB plies of Channel Sample 30B. The histograms for the CBD, CDB, and CB plies of Channel Sample 30AI and Channel Sample 30D are presented in Appendix 6. All three channel samples represented have a distinctive range of vitrinite reflectance measured on the collotelinite. The CBD ply of Channel Sample 30B ranged from 2.83-4.57 %, whereas the CDB ply ranged from 2.51-4.91 % and the CB ply ranged from 3.54-5.15 %. The RoV% for the CBD, CDB, and CB plies exhibit a trend and increases from the top (CBD ply) to the bottom (CDB ply) of the Main Seam

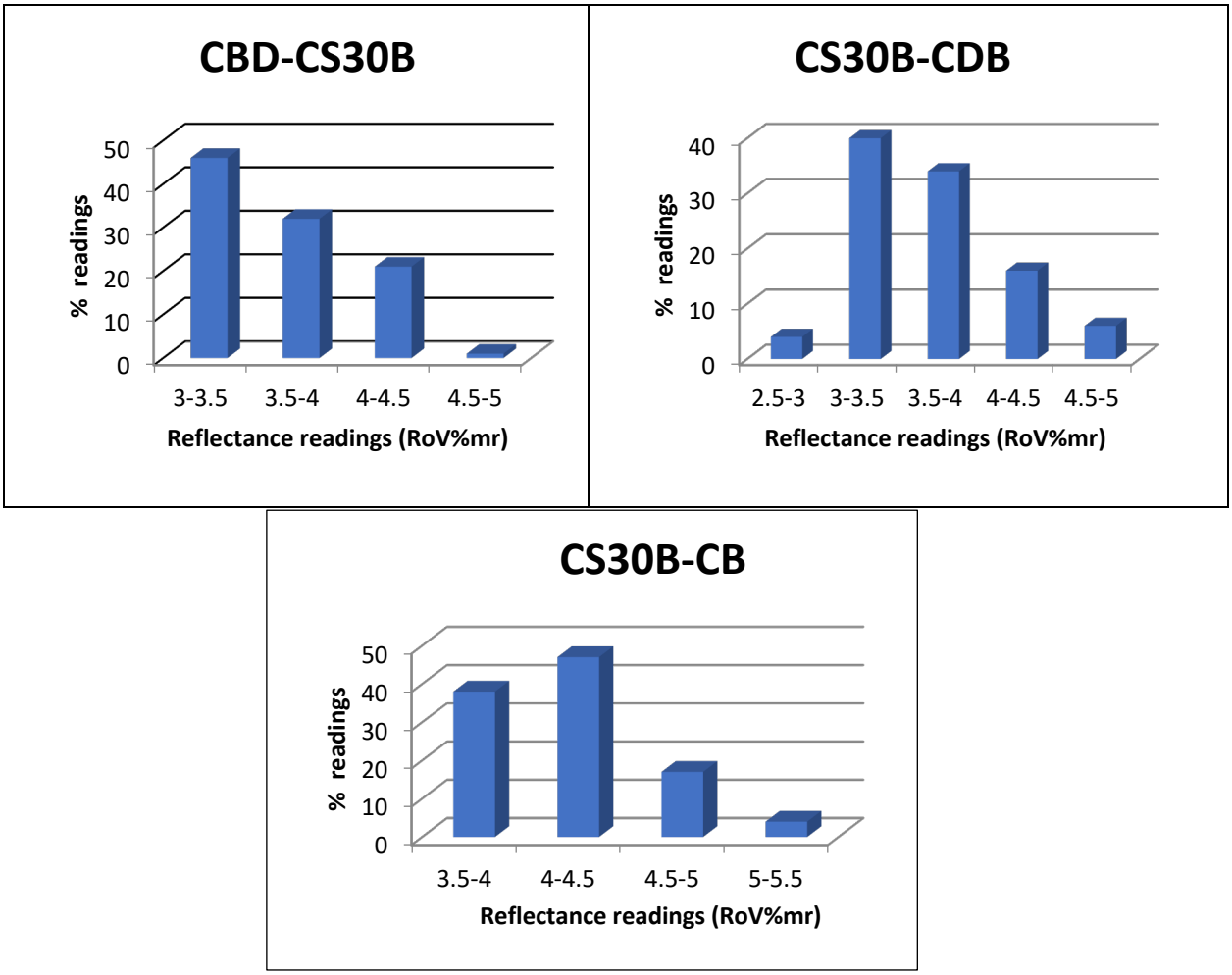


Figure 41: Unimodal distribution of the vitrinite reflectance of the CBD, CDB, and CB plies of the Main Seam

Chapter 4

Discussion and Conclusion

It is noted from the proximate and washability analysis results that the moisture content for the Coal, mainly Bright, Dull (CBD), Coal, mainly Dull, Bright (CDB), and Coal Bright (CB) plies is below 5%. All three plies reflect that the Main Seam is of a high rank, with the CDB ply having the lowest moisture content (1.4-2.6%) while the CB ply has the highest moisture content (2.9-4.2%) as shown by the proximate analysis results. Based on the moisture content, the CDB ply possesses an increased heating value compared to the CBD and CB plies.

After coal has been burnt, the non-combustible remains comprising bulk mineral matter represents ash content - thereby indicating the quality of the coal. The ash yield, volatile matter (VM), and moisture (IM) of the CBD, CDB, and CB plies as revealed by the proximate analysis is very low, indicating coal of a high quality. The CB ply has a low ash yield (7.6-12.6%) compared to the CBD and CDB plies. The CBD ply has the highest ash yield (14.2-20.7%) as indicated by the proximate analysis results. This result may be due to a thin layer of coaly shale material that occasionally occurs in this ply (Figure 21).

The petrographic results also confirmed that the CBD ply has the highest mineral matter (Table 16) in all channel samples, and therefore a high ash content. The CB ply has the lowest ash content compared to the CDB ply. The bulk mineral matter constituting clay, quartz, sulphides and carbonates was most concentrated within the CBD ply, followed by the CDB ply.

When coal is exposed to higher temperatures where moisture and ash has already been eliminated, the remaining constituents of coal represents volatile matter (VM). Coals with high VM are easily ignitable and also indicate coal of low rank, compared to coal with low VM that indicates coal of a high rank. The proximate analysis results showed that all channel samples have a VM yield that is not more than 6.8% - which is low. Within the Main Seam, the CDB ply has the highest VM yield (5.5-6.8%) and the CB ply has the lowest VM yield (4.8-5.1%).

The low VM yield indicate that the plies are representative of a high rank coal. This is also confirmed by the petrographic analysis of maceral groups showing that in all the plies liptinite is absent. In anthracite, liptinite reflectance converges with vitrinite reflectance; it thus becomes hard to recognise it in abundance of vitrinite (Suarez-Ruiz and Ward, 2008). Liptinite tends to reduce in appearance with coal's maturity stages. Therefore, in coals of lower rank with high VM, liptinite appears more clearly (Suarez-Ruiz and Ward, 2008). The structure of the inertinite appear well-developed and well preserved in all plies as reflected in Figure 40E.

Fixed carbon (FC) plays a critical role in maintaining combustion processes; it is therefore one of the key parameters in assessing the quality of coal (Aich et.al., 2020). Coals with higher FC are also known to have high calorific value and is therefore better quality coal (Rasheed et.al., 2015). It is also noted that increased FC indicates coals of high reflectance and lower hydrogen content (Richards et.al., 2013). The FC of coal generally ranges from 50-98% (Falcon, 2013). The results in Table 1 show that the FC content in all the plies is above 70% confirming that the coal is of high rank (Anthracite). The presence of inertinite macerals introduces a higher carbon and lower

VM content than vitrinite at the same rank, thus superimposing another source of carbon from that achieved by rank alone (Falcon and Ham, 1988).

The CB ply has a high FC content (78.1-84.4%) and the CBD ply has a low fixed carbon content (71.4-78.3%). The RoV% analysis represented in Table 17 also confirmed that the CB ply has higher values of reflectance which were measured in collotelinite (Figure 40B). The increased values of reflectance are due to the fact that the optical reflectance of vitrinite increases regularly and progressively with increasing rank, irrespective of the proportion of mineral and macerals present (Falcon and Ham, 1988).

Sulphur and mineral matter are naturally preserved in coal. Sulphur is generally categorised into organic and inorganic forms (Chou, 2012). At the Zululand Anthracite Colliery (ZAC) sulphur is mostly identified in cleats and fractures of coal, occurring as pyritic stringers or pyritic nodular (Figure 20). This type of sulphur can be referred to as inorganic form of sulphur. Generally the Main Seam at the ZAC has low sulphur content, but looking at each ply the CB has high sulphur content (0.91-1.56%) compared to CDB ply (0.74-1.36%) as reflected in Table 1. These trends suggest the accumulation of organic sulphur during peat formation since there was no occurrence of pyritic stringers and pyritic nodulars identified along the fractures in the CB ply. High sulphur and mineral matter in coal can pose a danger to the environment and thus, reduction of such quantities is essential before utilisation (Chou, 2012). In steel making industries metallurgical coke containing high sulphur and mineral matter is inappropriate for iron blast furnaces (Chou, 2012).

In the washability results of the CBD, CDB, and CB plies ash yield was still a critical parameter to be looked at as its content revealed how clean the coal is and how much of the ash-forming minerals were liberated. Coal was crushed into +0.5 x 25mm particle size for washability which increased the liberation of ash-forming minerals. A high ash yield indicates that there is little liberation of the ash-forming minerals within coal whereas a reduction in ash yield after coal has been washed indicates a larger percentage of ash-forming minerals being liberated (Matjie et al., 2011). The minerals in the CDB ply occur in fissures and cracks and are therefore easily liberated.

The CBD ply - as revealed by petrographic analysis - proved to be the ply with high mineral matter as reflected in Table 4. After the ply was washed, however, a reduction in ash yield was noted. The ash yield for the raw CBD ply ranged from 14.2-20.7% but for clean coal it was significantly reduced, ranging from 8.3-11.6%. Within the CBD ply better yields of 87.3-95.0% were obtained at a separation density of 1.65-1.75g/cm^3. The Relative Density (RD) Yield curves represented by Figures 22 and 24 also reflect that notable changes in the slope occurred at a separation density of 1.45g/cm^3 except for Figure 28 where a significant change in slope was noted at a separation density of 1.55g/cm^3. These changes in slope indicated that washing in these separation densities resulted in an increased yield of coal. A flat slope was noted at a separation density of 1.75g/cm^3 which indicated that all the CB ply material was recovered. The ash yield curves presented in Figures 22, 25, and 28 indicated a notable trend where changes in slope reflected points at which ash-forming minerals were no longer liberated from the CDB ply. Minerals such as pyrite occurred intimately intergrown with the organic matter, therefore making it difficult to be liberated from the ply.

The CDB ply revealed that it has the highest yield of coal that ranged from 95.6%-98.8% obtained at a separation density of 1.75g/cm^3. The raw CDB ply contained an ash yield that ranged from 8.6%-14.1%. After this ply was washed there was a slight decrease in ash yield as it then ranged from 9.0%-13.5%. The RD Yield curves represented by Figures 23, 26, and 29 reflect a consistent change in slope at a separation density of 1.55g/cm^3. The yield at this separation density was above 80%, thus indicating that a large percentage of the CDB ply sunk at 1.55g/cm^3. A sharp change in slope was noted at a separation density of 1.75g/cm^3 where all the CDB ply material sunk. A trend was noted in the ash yield and changes in the slope where an increase in ash was noted, indicating points at which the ash-forming minerals were no longer liberated.

The CB ply has the least yield of coal; it ranged from 79.5%-93.8% at a separation density of 1.75g/cm^3. The raw CB ply results revealed an ash yield that ranged from 7.6%-12.6%, whereas the washed CB ply revealed an ash yield that ranged from 10.4%-13.8%. The RD Yield curves in Figures 24, 27 and 30 of the CB ply represented significant slope changes at separation densities of 1.45g/cm^3, 1.55g/cm^3, 1.65g/cm^3 and 1.75g/cm^3. Figure 24 revealed that only 12% of the yield sunk at a separation density of 1.45g/cm^3 whereas 84% of the yield sank at a separation density of 1.65g/cm^3. A zero RD Yield slope occurred at a separation density of 1.75g/cm^3 as shown in Figures 24, 27, and 30 where all the remaining material sank, resulting in a yield of 100%.

The ash yield curves presented by Figures 24 and 30 reveal that a 100% yield was obtained with ash of less than 15%. Only the ash yield curve in Figure 27 reflected

that 100% yield has a high ash content. High ash indicates that ash-forming minerals in the CB ply are not liberated, and also that the coaly shale layer that is normally overlain by this ply might have been present. Smaller quantities of clay minerals observed through petrographic analysis as shown in Figure 40D might not have been completely liberated during the washing of the CB ply; this could also explain why the ash yield did not reduce as expected.

The prime and middlings products were recovered in the CBD ply of Channel Samples 30B and 30AI. The prime product was much higher than the middlings product in both channel samples of this ply. The prime product of the CBD ply of Channel Sample 30B reflected a yield of 66.2% as compared to the CBD ply of Channel Sample 30AI with a yield of 48.2%. A high yield of 96.2% of prime product was obtained in the CBD ply of Channel Sample 30D. The middlings product of the CBD ply of Channel Sample 30D reflected an ash yield above 15%; this may be as a result of the coaly shale layer that occasionally occurs within this ply. The Channel Sample 30D reflected that the CBD ply has a low ash yield. Thus, within this ply in this sample channel only prime product was obtained, and also significant ash-forming minerals were liberated.

The prime and middlings products of the CDB ply were obtained in both Channel Samples 30B and 30D. Only the CDB ply of Channel Sample 30AI had a middlings product. High yields for both prime and middlings products were noted in this ply compared to the CBD and CB plies. An ash yield of 23.3% was noted in Channel Sample 30B of the CDB ply. This yield might be due to contamination of the ply by the plies either overlying or underlying it.

The CB ply across all the channel samples reflected a high yield in the middlings product compared to the prime product. The middlings product yield ranged from 50.2%-93.8%. This yield proves that this ply has a product of high ash yield compared to both the CBD and CDB plies. It was noted that only the CB ply of Channel Sample 30D had no recoveries of the prime product.

Conclusion

The demand for anthracite in the near future is expected to grow, especially in the metallurgical industries (WCA, 2019). Statistics also prove this as 60% of steel production in South Africa is currently dependent on anthracite (WCA, 2019). Anthracite with least sulphur and mineral matter is most desired in the steel industry as it does not damage iron blast furnaces. Additionally, anthracite with least sulphur does not pose a threat to the environment when is being utilised, as a result such coal is desired. This increased demand and dependence triggered a need to investigate the quality of anthracite of the ZAC by characterising the Main Seam that is currently being mined.

The VM of the CBD, CDB, and CB plies within the Main Seam ranges from 4.8%-7.9%. Such VM content proves that each ply that was investigated was a high rank coal. The quality of this coal is also confirmed by petrographic analyses where the RoV% for the CBD, CDB, and CB plies is above 2% (thus indicating a high rank coal). A unimodal distribution was noted with RoV% of more than 2% that plies are of the same coal rank. It is also noted on the maceral group analysis that maceral liptinite is absent as it tends to reduce in appearance with coal maturity stages.

It is also noted from the proximate and washability results that the ash yield, IM, and VM of all the plies is low, and these geochemical characteristics confirm that coal is of high quality. Though all three plies had low ash yields, the CBD ply had a high ash yield compared to the CDB and CB plies, this is because of the increased content of ash-forming minerals in this ply. The maceral group analysis also confirmed that the CBD ply has the highest mineral matter that ranged from 10.4-12.6%. RD Yield curves from washability analysis proved that the CBD and CB plies have low yields of coal compared to the CDB ply.

At a separation density of 1.55 g/cm^3 the CDB ply yielded more than 80% in all channel samples, while the CBD and CB plies occasionally yielded 80% of coal. Better yields and ash yields of both prime and middlings products were noted in the CDB ply compared to the CBD and CB plies. The ply that has a better quality with a high yield proved to be the CDB ply. Therefore, if selective mining were to be applied at the ZAC, the CDB ply is the ply to mine.

References

Aich, S., Behera, D., Nandi, B.K. and Bhattacharya, S. 2020. Relationship between proximate analysis parameters and combustion behaviour of high ash Indian coal. International Journal of Coal Science Technology, 7, 1-12.

American Society for Testing and Materials (ASTM) D4596. 1986. Standard practice for collection of channel samples of coal in the mine. In: Annual book of ASTM standards. 5(5), 519-21.

American Society for Testing and Materials (ASTM) D5142. 2013. Standard Test Methods for Proximate Analysis of the Analysis Sample of Coal and Coke by Instrumental Procedures. Annual Book of Standards, Volume 05.06. ASTM International, West Conshohocken, Pennsylvania.

Baiyegunhi, C., Nxantsiya, Z., Pharoe, K., Baiyegunhi, T. L and Mepaiyeda, Seyi. 2019. Petrographical and geophysical investigation of the Ecca Group between Fort Beaufort and Grahamstown, in the Eastern Cape Province, South Africa. Open Geosciences. 11 (1), 313-326.

Blenkinsop, T.G. 2008. Relationships between faults, extension fractures and veins, and stress. Journal of Structural Geology, 30, 622-32.

Board, A. 2018. Clean Coal Centre. https://www.mining-technology.com/news/menar-partners-develop-anthracite-coal-project-south-africa/. [Accessed March 2021)

Bordy, E.M., Spelman, S., Cole D.I. and Mthembi, P. 2017. Lithostratigraphy of the Pietermaritzburg Formation (Ecca Group, Karoo Supergroup), South Africa. South African Journal of Geology 120(2), 293-302.

Bordy, E.M. and Prevec, R. 2015. Lithostratigraphy of the Emakwezini Formation, Karoo Supergroup, South African. South African Journal of Geology, 118(3), 307-10.

Bott, M.H.P., 1976. Formation of sedimentary basins of graben type by extension of the continental crust. Tectonophysics, 36, 77-86.

Burton, J., Caetano, T. and McCall, B. 2018. Coal transition in South Africa - Understanding the implications of a 2°C-compatible coal phase-out for South Africa. IDDRI & Climate Strategies.

Cairncross, B., 2001. An overview of the Permian (Karoo) coal deposits of southern Africa. Journal of African Earth Sciences 33, 529-562.

Cairncross, B. 2011. An overview of the Permian (Karoo) coal deposits of Southern Africa. Journal of African Earth Sciences, 33(3-4), 529-62.

Catuneanu, O., Hancox, P.J., Rubidge, B.S., 1998. Reciprocal flexural behaviour and contrasting stratigraphies: a new basin development model for the Karoo retroarc foreland system, South Africa. Basin Research 10, 417-439.

Catuneanu, O., Wopfner, H., Eriksson, P.G., Cairncross, B., Rubidge, B.S., Smith, R.M.H. and Hancox, P.J. 2005. The Karoo basins of south-central Africa. Journal of African Earth Sciences, 43(1-3), 21-53.

Chou, C.L. 2012. Sulfur in coals: A review of geochemistry and origins. International Journal of Coal Geology, 100, 1-13.

De Raaf, J.F.M., Boersma, J.R. and Van Gelder, A. 1977. Wave-generated structures and sequences from a shallow marine succession, Lower Carboniferous, Country Cork, Ireland. Sedimentology, 24, 451-83.

Diessel, C.F.K. 1992. Coal Formation and Sequence Stratigraphy. In: Coal-Bearing Depositional Systems. Springer, Berlin, Heidelberg, 461-514.

Eberhard, A. 2011. The future of South African Coal: Market, investment and policy challenges. Working Paper No. 100 Programme on Energy and Sustainable Development. Encina Hall East, Stanford University. CA 94305-6055, pp.44.

Falcon, R., Ham, A.J. 1988. The characteristics of Southern African Coals. Journal of the South African Institute of Mining and Metallurgy, 88(5), 145-161.

Falcon, R.M.S. 2013. Coal geology, types, ranks and grades. http://www.fossilfuel.co.za/conferences/2013/CoalCokeCarbon/DayOne/01-Rosemary-Falcon.pdf. [Accessed April 2021].

Galvin, K.P. 2006. Options for Washability Analysis of Coal. A literature review, South Africa. Coal Preparation, 26(4), 209-34.

Gupta, R., 2007. Advanced Coal Characterization: A Review. Energy and Fuels, 21(2), 451-60.

Hancox, P.J. and Götz, A.E. 2014. South Africa's coalfields. A 2014 perspective, South Africa. International Journal of Coal Geology, 132, 170-254.

Hatherly, B. and Sexton, J. 2013. Independent valuation of the Mbila mining area and Msebe exploration project. Report Prepared by the MSA Group (Pty) Ltd on Behalf of Zyl Mining SA (Pty) Ltd and Stantons International Securities, 42p.

Hobday, D.K. 1973. Middle Ecca deltaic deposits in the Muden-Tugela Ferry area of Natal. Transactions of the Geological Society of South Africa, 76, 309-18.

Hobday, D.K. 1977. Fluvial deposits of the Ecca and Beaufort Group in the eastern Karoo Basin. Southern Africa. In: A.D. Miall (Editor), Fluvial Sedimentology, Memorandum. Canadian Society of Petroleum. Geologists. Calgary, 5, 413-30.

Holmes, A. 1951. The sequence of pre-Cambrian orogenic belts in South and Central Africa Republic, 18th International Geological Congress. London, 14, 254-69.

International Committee for Coal and Organic Petrology (ICCP). 2001. The New Vitrinite Classification (ICCP System, 1994). Fuel, 80, 459-71.

International Organisation for Standardisation (ISO) 562. 2013. Determination of Volatile Matter in Hard Coal and Coke. Standard Test Methods for Coal Analysis. International Organisation for Standardisation, Geneva, Switzerland, 142p.

Johnson, M.R., van Vuuren, C.J., Visser, J.N.J., Cole, D.J., Wickens, H.deV., Christie, A.D.M., Roberts, D.L., 1997. The foreland Karoo Basin, South Africa. In: Selley, R.C. (Ed.), African Basins—Sedimentary Basins of the World. Elsevier, Amsterdam, 269-317.

Jourbert, M.R. 1994. Emakwezini Formation. In: M.R. Johnson (Editor), Lexicon of South African Stratigraphy, Part 1: Phanerozoic Units, South African Committee for Stratigraphy, Council for Geoscience, South Africa, 56p.

Kröner, A. 2001. The Mozambique belt of East Africa and Madagascar: significance of zircon and Nd model ages for Rodinia and Gondwana supercontinent formation and dispersal. South African Journal of Geology, 104, 151-66.

Lopez- Buendia, A.M., Whateley, M.K.G., Bastida, J. and Urquiola, M.M. 2007. Origins of Mineral Matter in Peat March and Peat Bog Deposits, Spain. International Journal of Coal Geology, 71, 246-62.

Matjie, R. M., French, D., Ward, C.R., Pretorius, P.C. and Li. Z. 2011. Behaviour of coal mineral matter in sintering and slagging of ash during the gasification process. Fuel Processing Technology, 20(8), 1426-33.

McCabe, P.J. 1984. Depositional environments of coal and coal-bearing strata. In: R.A. Rahmani and R.M. Flores (Editors), Sedimentology of Coal and Coal-Bearing Sequences: Special publication of the International association of sedimentologists, Oxford, Blackwell scientific publications, 7, 11-42.

McHugh, L. 2017. World Energy Needs: A Role for Coal in the Energy Mix, in Coal in the 21st Century: Energy Needs, Chemicals and Environmental Controls, pp. 1-29.

Nazan, Y.E., and Faruk, A. 2020. Use of petrological and organic geochemical data in determining hydrocarbon generation potential of coals: Miocene coals of Malatya Basin (Eastern Anatolia-Turkey). International Journal of Coal Science and Technology, 44(2), 1-18.

Neumann, E., Svense, H., Galerne, C.Y. and Planke, S. 2011. Multistage Evolution of Dolerites in the Karoo Large Igneous Province, Central South Africa. Journal of Petrology, 0, 1-26.

Olariu, C., and Bhattacharya, J.P. 2006. Terminal Distributary Channels and Delta Front Architecture of River-Dominated Delta Systems. Journal of Sedimentary Research, 76, 212–33.

Rasheed, M.A., Srinivasa Rao, P.L., Boruah, A., Hasan, S.Z., Patel, A., Velani, V. and Patel, K. 2015. Geochemical Characterization of Coals Using Proximate and Ultimate Analysis of Tadkeshwar Coals, Gujarat. Geosciences, 5(4), 113-19.

Richards, J.M., Naude, G., Theron, S.J. and McCullum, M. 2013. Petrological characterization of coal: An evolving science. Journal of the Southern African Institute of Mining and Metallurgy, 113, 11.

Romanov, V.V. 1968. Hydrophysics of bogs. Israel program for scientific translations, Jerusalem. 299p.

Smith, R. M. H. 1995. Changing fluvial environments across the Permian-Triassic boundary in the Karoo Basin, South Africa and possible causes of tetrapod extinctions. Palaeogeography, Palaeoclimatology, Palaeoecology, 17(1-2), 81-104.

Snyman, C.P., Botha, W.J., 1993. Coal in South Africa. Journal of African Earth Sciences 16, 171-180.

Snyman, C.P. 1998. Coal. In: M.G.C. Wilson and C.R. Anhaeusser (Editors), The Mineral Resources of South Africa. Handbook 16. Council for Geoscience 6th Edition, pp. 136-205.

South African Committee for Stratigraphy (SACS). 1980. Stratigraphy of South Africa. Part 1 (Comp. L.E. Kent). Lithostratigraphy of the Republic of South Africa, South West Africa/Namibia and the Republics of Bophuthatswana, Transkei and Venda. Handbook, Geological Survey. South Africa. 8, 1-690.

South African National Standard (SANS). 2015. Methods for the petrographic analysis of coals, part 2: Methods for preparing coal samples, 4-12p.

Speight, J.G. 2013. Handbook of Coal Analysis. Wiley, New York.

Stauffer, P.H. 1967. Grain-Flow Deposits and their Implications, Santa Ynez Mountains, California. SEPM Journal of Sedimentary Research, 37, 487-508.

Suarez-Ruiz, I., and Ward, C.R., 2008. Basic factors controlling coal quality and technological behaviour of coal. In: Applied coal petrology, I. Suarez-Ruiz and J.C. Crelling (Editors), The role of petrology in coal utilisation. Academic Press, New York, 19-59.

Turner, B.R., and Whateley, M.K.G. 1983. Structural and sedimentological controls of coal deposition in the Nongoma graben, northern Zululand, South Africa. Special publication of the International Association of Sedimentologists, 6, 457-71.

Van der Walt, B. 2012. The petrology, petrography and geochemistry of anomalous drill hole core sequences in the Highveld Coalfield, South Africa: a case study for diatreme activity. Unpublished MSc Thesis, University of Johannesburg, 265p.

Van Niekerk, J.L. 1995. Geochemistry of the dolerites and the intrusion mechanisms of two major sills in the Secunda coalfield, PhD Thesis (unpublished), University of Stellenbosch, Western Cape.

Visser, J.N.J., 1993. A reconstruction of the late Palaeozoic ice sheet on southwestern Gondwana. International Gondwana Symosium 8, 449-458.

Von Brunn, V., and Gold, D. J. C. 1993. Diamictite in the Archaean Pongola sequence of Southern Africa. Journal of African Earth Sciences (and the Middle East), 16(3), 367-374.

Ward, C.R., and Suárez-Ruiz, I. 2008. Introduction to Applied Coal Petrology. Ápplied Coal Petrology: the Role of petrology in Coal Utilization. Suárez-Ruiz, I. and Crelling, J.C. (eds.). *Academic Press,* USA, 1-18.

Whateley, M. K. G. 1980. Structural Controls of Sedimentation in the Ecca Group in Northern Zululand. MSc Thesis (unpublished), University of the Witwatersrand, Johannesburg, pp. 74-123.

World Coal Association (WCA), 2019. Coal statistics. https://www.worldcoal.com/coal/28102019/south-africa-coal-mining-report-2019 (Accessed November 2020).

Zavala, C., and Pan, S.X. 2018. Hyperpycnal flows and hyperpycnites: Origin and distinctive characteristics. Lithologic Reservoir, 30(1), 1-27.

Online sources:

www.alsglobal.com

www.golder.com

Appendices

Appendix 1: Geological Log: Drill hole NG-108

ZAC			
LOG SHEET			
B/HOLE NAME	***NG108***	***PAGE***	***1 of 23***
DRILLED BY	***DRILLCOR***		
FARM	***NONGOMA***	***DISTRICT***	***NONGOMA***

	Y	**X**	**Z**
CO ORDS	-68726.02m	3115040.52m	218.36m

END OF HOLE	***311.86***

NOTE SECTION NOT TO SCALE

SECTION	***DEPTH***	***WIDTH***	***LOSS***	***DESCRIPTION***
	0.00			
				Percussion drilled to 99.58
	99.58	*99.58*		
				Dolerite, coarsely crystalline, grey, white feldspathic phenocryst spotted with a
				diffuse base.
	109.86	*10.28*		

					Dolerite, finely crystalline, greenish grey, abundantly starry white feldspar phenocryst spotted with a sharp near horizontal intrusive base.
		111.49	*1.63*		*FLOOR OF DOLERITE SILL*
					Sandstone, coarse grained, feldspathic, micaceous, pale whitish grey, highly
					altered, recrystallised, vaguely planar cross-bedded with an erosive base.
		117.52	*6.03*		
					Sandstone, medium to coarse grained, feldspathic, micaceous, dark grey to grey,
					thickly starkly banded with occasional black silty streaks and a gradational base.
		118.89	*1.37*		
					Carbonaceous silty mudstone/ sandstone, black to grey, finely lenticularly laminated with
					a sharp base.
		119.19	*0.30*		
					Sandstone, medium grained, feldspathic, micaceous, grey to darkish grey, finely starkly

						banded with a sharp base.
			119.72	*0.53*		
						Carbonaceous silty mudstone/ sandstone, black to grey, lenticularly laminated,
						weak along planes of bedding with a sharp base.
			119.99	*0.27*		
						CONTINUED ON PAGE 2

ZAC			
LOG SHEET			
B/HOLE NAME	***NG108***	***PAGE***	***2 of 23***

SECTION	***DEPTH***	***WIDTH***	***LOSS***	***DESCRIPTION***
	119.99			
				Sandstone, medium to barely coarse grained, feldspathic, micaceous, thickly starkly
				banded to finely trough cross-stratified with a sharp base.
	120.59	*0.60*		
				Carbonaceous silty mudstone/ gritty sandstone, black to pale whitish grey,

						thickly lenticularly laminated, weak along planes of bedding with a sharp base.
			122.19	*1.60*		
						Sandstone, medium to barely coarse grained, feldspathic, micaceous, pale to dark
						grey, stratified with a sharp base.
			122.46	*0.27*		
						Carbonaceous siltstone/ sandstone, black to darkish grey, micaceous laminated with a
						sharp base.
			122.67	*0.21*		
						Sandstone, medium to barely coarse grained, feldspathic, micaceous, grey, thickly
						starkly banded with a sharp base.
			122.89	*0.22*		
						Carbonaceous silty mudstone/ siltstone, black to dark grey, finely micaceous
						laminated with a sharp base.
			122.92	*0.03*		

						Sandstone, silty to fine grained, micaceous, grey to dark grey, finely streaky
						laminated with a sharp base.
			123.45	*0.53*		
						Sandstone, medium grained, feldspathic, micaceous, grey, thickly starkly banded
						with a gradational base.
			123.78	*0.33*		
						Sandstone, coarse grained, feldspathic, micaceous, pale whitish grey, cross-
						bedded with a gradational base.
			129.84	*6.06*		
						Sandstone, fine to medium grained, feldspathic, micaceous, pale grey, finely wispy
						current laminated, abundantly rootlet flecked with a sharp base.
			131.15	*1.31*		
						CONTINUED ON PAGE 3

ZAC			
LOG SHEET			
B/HOLE NAME	***NG108***	***PAGE***	***3 of 23***

SECTION	***DEPTH***	***WIDTH***	***LOSS***	***DESCRIPTION***
	131.15			
				Sandstone, coarse grained, feldspathic, micaceous, pale whitish grey, vaguely cross-
				bedded with a channel erosive base.
	131.25	*0.10*		
				Carbonaceous silty mudstone/ siltstone, black to dark grey, finely micaceous laminated,
				lightly horizontally calcite veined with a sharp base.
	131.58	*0.33*		
				Sandstone, fine to barely medium grained, feldspathic, micaceous, grey finely
				trough cross-bedded with a sharp base.
	131.78	*0.20*		
				Carbonaceous silty mudstone/ siltstone, black to dark grey, micaceous, finely
				streaky lenticularly laminated with scattered grit lenses and a sharp base.

			132.52	0.74		
						Sandstone, coarse grained, feldspathic, micaceous, pale whitish grey, turbid,
						reworked with an erosive calcite veined base.
			132.58	0.06		
						Sandstone, fine grained, feldspathic, micaceous, darkish grey, lightly black
						silty current laminated with a sharp base.
			133.00	0.42		
						Carbonaceous silty mudstone/ siltstone, black to dark grey, micaceous laminated,
						weak along planes of bedding with a sharp base.
			133.54	0.54		
						Sandstone, fine to barely medium grained, feldspathic, micaceous, grey, finely
						black silty current laminated with a sharp base.
			134.14	0.60		
						Carbonaceous silty mudstone/ siltstone, black to darkish grey, finely micaceous,
						streaky laminated with a sharp base.

			134.74	0.60		
						Coal. Mixed, mainly bright, streaky vintrinite banded, finely horizontally
						calcite veined with a sharp base.
			134.77	0.03		
						CONTINUED ON PAGE 4

ZAC			
LOG SHEET			
B/HOLE NAME	***NG108***	***PAGE***	***4 of 23***

SECTION	***DEPTH***	***WIDTH***	***LOSS***	***DESCRIPTION***
	134.77			
				Siltstone, dark grey to black, micaceous, pellety laminated with a gradational base.
	134.96	0.19		
				Sandstone, medium grained, feldspathic, micaceous, finely and intricately
				dark grey wave ripple cross-laminated with an erosive base.

			135.25	*0.29*		
						Sandstone/ silty sandstone, grey to blackish, feldspathic, micaceous, lightly silty current
						laminated with an erosive base.
			136.16	*0.91*		
						Siltstone/ sandstone, black to grey, finely micaceous laminated with a sharp base.
			136.34	*0.18*		
						Sandstone, medium to barely coarse grained, feldspathic, micaceous, darkish grey,
						lightly finely black wispy current laminated with a sharp base.
			137.09	*0.75*		
						Carbonaceous siltstone/ mudstone/ sandstone, black to darkish grey, thickly
						3cm banded with a gradational base.
			138.03	*0.94*		
						Carbonaceous silty mudstone, black, finely micaceous laminated, lightly horizontally
						calcite veined with a sharp base.

			138.31	*0.28*		
						Sandstone, coarse to medium grained, feldspathic, micaceous, grey, finely current
						laminated with an erosive base.
			138.46	*0.15*		
						Carbonaceous silty mudstone/ siltstone/ sandstone, black to darkish grey, feldspathic,
						micaceous, lenticularly laminated with a sharp base.
			139.02	*0.56*		
						Sandstone, coarse grained, feldspathic, micaceous, grey to darkish grey and
						blackish, cross-bedded, strongly "crackle" fractured, calcite veined between
						25º to 40º with an erosive base.
			142.11	*3.09*		
						CONTINUED ON PAGE 5

ZAC			
LOG SHEET			
B/HOLE NAME	***NG108***	***PAGE***	***5 of 23***

SECTION	DEPTH	WIDTH	LOSS	DESCRIPTION
	142.11			
				Silty sandstone, dark grey to blackish, feldspathic, micaceous laminated with a
				sharp base.
	142.19	0.08		
				Carbonaceous silty mudstone, black, finely micaceous laminated with a sharp base.
	142.23	0.04		
				Sandstone, coarse grained, feldspathic, micaceous, cross-bedded to finely
				wavy wispy current laminated with an erosive base.
	144.69	2.46		
				Sandstone, medium grained, feldspathic, micaceous, grey, thickly starkly
				banded, intensely altered, recrystallised, thickly quartz calcite veined at 65º to
				78º with a sharp near horizontal intrusive base.
	150.77	6.08		ROOF OF DOLERITE SILL

						Dolerite, finely crystalline, greenish grey, steeply calcite veined with a diffuse base.
			151.70	*0.93*		
						Dolerite, medium to barely coarse crystalline, greenish grey, lightly whitish
						feldspar phenocryst spotted, dark "mafic" specked with a diffuse base. Strongly
						steeply jointed, lightly calcite veined.
			170.36	*18.66*		
						Dolerite, finely crystalline, greenish grey, lightly dark mafic flecked, 75º jointed
						with a diffuse base.
			174.94	*4.58*		
						Dolerite, cryptocrystalline, pale yellowish green with a near horizontal sharply
						intrusive base.
			175.17	*0.23*		*FLOOR OF DOLERITE SILL*
						Sandstone, fine to medium grained, feldspathic, micaceous, grey to dark grey,
						highly altered, recrystallised, quartz calcite veined with a sharp base.

			180.52	*5.35*		
						Siltstone/ silty sandstone, dark grey to grey, finely starkly banded, highly altered, baked
						with a sharp base.
			181.97	*1.45*		*CONTINUED ON PAGE 6*

ZAC			
LOG SHEET			
B/HOLE NAME	***NG108***	***PAGE***	***6 of 23***

SECTION	***DEPTH***	***WIDTH***	***LOSS***	***DESCRIPTION***
	181.97			
				Sandstone, coarse grained, feldspathic, micaceou pale whitish, lightly
				wavy wispy current laminated with a gritty erosive base.
	184.11	*2.14*		
				Sandstone, fine to barely medium grained, feldspathic, micaceous, thickly starkly
				banded to trough cross-bedded, altered with a sharp base.

			185.89	*1.78*		
						Sandstone, coarse grained, feldspathic, micaceous, pale grey, wispy current
						laminated with a gritty erosive base.
			186.27	*0.38*		
						Sandstone, medium to coarse grained, feldspathic, micaceous, pale to darkish grey,
						thickly starkly banded with a sharp base.
			187.27	*1.00*		
						Sandstone, coarse grained to gritty, feldspathic, micaceous, pale whitish grey,
						planar cross-bedded, near vertically fissure jointed, calcite veined with an erosive base.
			189.61	*2.34*		
						Sandstone, fine to medium grained, feldspathic, micaceous, grey to darkish grey, finely dark grey wispy current laminated with a near horizontal intrusive base.
			190.97	*1.18*		*ROOF OF DOLERITE SILL STRINGER*

						Dolerite, cryptocrystalline, greenish to dark grey, finely calcite laced with a sharp horizontal base.
			190.93	*0.14*		*FLOOR OF DOLERITE SILL STRINGER*
						Sandstone, fine to medium grained, feldspathic, micaceous, darkish grey, lightly stratified with a sharp base.
			192.07	*1.14*		
						Sandstone, medium to coarse grained, feldspathic, micaceous, pale grey to whitish
						with a channel erosive base.
			193.58	*1.51*		
						CONTINUED ON PAGE 7

ZAC			
LOG SHEET			
B/HOLE NAME	***NG108***	***PAGE***	***7 of 23***

SECTION	DEPTH	WIDTH	LOSS	DESCRIPTION
	193.58			
				Silty sandstone/ siltstone/ mudstone, grey to blackish, micaceous laminated with a sharp base.
	194.27	0.69		
				Sandstone, fine grained, micaceous, grey, thickly starkly banded with a sharp base.
	194.69	0.42		
				Sandstone, coarse grained, feldspathic, micaceous, lightly near horizontally stratified to wavy wispy current laminated.
	198.14	3.45		
				Siltstone, greenish grey, laminated, highly altered, baked with a sharp base.
	198.22	0.08		
				Sandstone, coarse grained, feldspathic, micaceous, pale whitish grey to dark grey, wispy current laminated with an erosive base.

			198.68	*0.46*		
						Sandstone, coarse grained, feldspathic, micaceous, pale whitish grey, finely dark grey wispy current laminated with a gritty erosive base.
			199.81	*1.13*		
						Carbonaceous silty mudstone/ siltstone, black to grey, micaceous, lenticularly laminated, laterally bioturbated with scattered whitish grit lenses and a sharp base.
			200.14	*0.33*		
						Gritty carbonaceous silty mudstone, black, finely micaceous, turbid with randomly scattered white feldspar grains and a sharp base.
			200.23	*0.09*		
						Carbonaceous silty mudstone/ siltstone/ sandstone, black to grey, finely streaky lenticularly laminated, calcite veined at 45º with a sharp base.

			200.45	*0.22*		
						Carbonaceous silty mudstone/ siltstone/ sandstone, black to grey, finely streaky lenticularly laminated, turbid, gritty with sandstone lenses, lightlylaterally bioturbated with a sharp base.
			200.61	*0.16*		
						Sandstone, fine grained, micaceous, finely wispy current laminated, altered, baked with a gradational base.
			200.84	*0.23*		*CONTINUED ON PAGE 8*

ZAC			
LOG SHEET			
B/HOLE NAME	***NG108***	***PAGE***	***8 of 23***

SECTION	***DEPTH***	***WIDTH***	***LOSS***	***DESCRIPTION***
	200.84			
				Sandstone, medium to coarse grained, feldspathi micaceous, pale to darkish grey, cross-bedded to wisp current laminated with an erosive base.

			201.37	*0.53*		
						Sandy siltstone, dark grey, micaceous, laminated, laterally bioturbated with a sharp base.
			201.51	*0.16*		
						Sandstone, coarse grained, feldspathic, micaceous, grey, cross-bedded with an erosive base.
			201.94	*0.43*		
						Sandstone, fine to medium grained, darkish grey, feldspathic, micaceous, thickly stratified with a sharp base.
			202.22	*0.28*		
						Sandstone, coarse grained, feldspathic, micaceous, pale grey, thickly horizontally stratified with a gradational base.
			202.95	*0.73*		

						Sandstone, medium to barely coarse grained, feldspathic, micaceous, dark grey, horizontally stratified to streaky current laminated with an erosive base.
			204.60	*1.65*		
						Carbonaceous silty mudstone/ siltstone, black to pale grey, micaceous, finely streaky laminated with a sharp base.
			204.81	*0.21*		
						Sandstone, medium grained, feldspathic, micaceous, grey, thickly starkly banded with a sharp base.
			205.03	*0.22*		
						Sandstone, silty to barely medium grained, micaceous, feldspathic, darkish grey to black, finely lenticularly laminated with a sharp base.
			206.40	*1.37*		
						Carbonaceous gritty siltstone, black, micaceous, turbid with randomly scattered white feldspar grit and a sharp base.

			206.59	*0.19*		
						CONTINUED ON PAGE 9

ZAC

LOG SHEET

B/HOLE NAME	***NG108***	***PAGE***	***9 of 23***

SECTION	***DEPTH***	***WIDTH***	***LOSS***	***DESCRIPTION***
	206.59			
				Sandstone, medium to coarse grained, feldspathi micaceous, grey to pale grey,
				turbid, slumped with load cast structures and a gradational base.
	206.70	*0.11*		
				Carbonaceous silty mudstone/ silty sandstone, black to grey, micaceous laminated with a
				sharp base.
	206.82	*0.12*		
				Sandstone, fine to medium grained, micaceous, feldspathic, grey, finely starkly banded with a sharp base.

			207.30	*0.48*		
						Carbonaceous silty mudstone, black, finely micaceous laminated with a sharp base.
			207.40	*0.10*		
						Sandstone, fine grained, micaceous, grey to dark grey, finely trough cross-bedded with an erosive base.
			207.60	*0.20*		
						Gritty carbonaceous silty mudstone, black, finely micaceous, turbid with randomly scattered white feldspar grit and a sharp base.
			207.90	*0.30*		
						Sandstone/ carbonaceous silty mudstone/ siltstone, grey to black, feldspathic,micaceous, trough cross-bedded to lenticularly laminated with a sharp horizontallyintrusive base. Highly altered, baked.

			208.33	*0.43*		*ROOF OF DOLERITE SILL*
						Dolerite, finely crystalline, blueish to greenish grey with a sharp horizontal base.
			210.78	*2.45*		*FLOOR OF DOLERITE SILL*
						Carbonaceous silty mudstone/ siltstone/ sandstone, black to grey, micaceous, lenticularly laminated with a sharp base.
			211.98	*1.20*		
						Gritty carbonaceous silty mudstone, black to dark grey, turbid with randomly scattered white feldspar grit and a sharp base.
			212.29	*0.31*		
						CONTINUED ON PAGE 10

ZAC			
LOG SHEET			
B/HOLE NAME	***NG108***	***PAGE***	***10 of 23***

SECTION	DEPTH	WIDTH	LOSS	DESCRIPTION
	212.29			
				Carbonaceous silty mudstone/ sandstone, black to whitish grey, gritty, micaceous, feldspathic, finely streaky lenticularly laminated, weak along planes of bedding with agradational base.
	213.53	*1.24*		
				Carbonaceous silty mudstone/ siltstone/ silty sandstone, black to grey, micaceous, finely lenticularly laminated with a sharp base.
	214.44	*0.91*		
				Sandstone, medium to coarse grained, pale grey, trough cross-bedded with a channel erosive base.
	214.52	*0.08*		
				Sandstone, pale grey, fine grained, strongly wispy carbonaceous current laminated with a sharp base.

			214.70	*0.18*		
						Sandstone/ carbonaceous mudstone/ siltstone, grey to black, micaceous, lenticularly laminated, laterally bioturbated, weak along planes of bedding with a sharp base.
			215.22	*0.52*		
						Carbonaceous silty mudstone/ siltstone, black to grey, micaceous, lenticularly laminated,laterally bioturbated with a sharp base.
			215.50	*0.28*		
						Coarse grained sandstone/ carbonaceous mudstone, grey to black, feldspathic, micaceous, thickly lenticularly intercalated with an erosive base.
			215.71	*0.21*		
						Siltstone, black, finely micaceous laminated with a gradational base.
			215.86	*0.15*		

						Sandstone, medium to coarse grained, feldspathic, micaceous, ripple cross-laminated with an erosive base.
			216.25	*0.39*		
						Carbonaceous silty mudstone, black, finely micaceous laminated with a sharp base.
			216.59	*0.34*		
						CONTINUED ON PAGE 23

ZAC

LOG SHEET

B/HOLE NAME	***NG108***	***PAGE***	***11 of 23***

SECTION	***DEPTH***	***WIDTH***	***LOSS***	***DESCRIPTION***
	216.59			
				Sandstone/ silty sandstone, black to grey, thickly 3mm banded with a sharp base.
	216.74	*0.15*		
				Sandstone, medium grained, grey, finely banded to trough cross-bedded with an erosive base.

			216.81	*0.07*		
						Carbonaceous silty mudstone/ sandstone, black to grey, micaceous, feldspathic, lenticularly laminated, weak along planes of bedding with a sharp base.
			217.16	*0.35*		
						Sandstone, medium grained, grey, feldspathic, micaceous, trough cross-bedded with an erosive base.
			217.26	*0.10*		
						Sandstone, medium grained, feldspathic, micaceous, banded to trough cross-bedded with several thin laterally bioturbated mudstone bands and a sharp base.
			217.55	*0.29*		
						Sandstone, grey, medium grained, lightly dark grey silty current laminated with an erosive base.
			217.67	*0.12*		

						Carbonaceous silty mudstone/ siltstone, black to grey, micaceous, feldspathic, thickly lenticularly laminated with a sharp base.
			217.77	*0.10*		
						Sandstone, medium grained, feldspathic, micaceous, grey, finely current laminated trough cross-bedded with scattered pyrite lenses and a sharp base.
			218.27	*0.50*		
						Carbonaceous silty mudstone/ sandstone, black to grey, micaceous, feldspathic, lenticularly laminated with a sharp base.
			218.34	*0.07*		
						Sandstone, medium grained to barely coarse grained, feldspathic, micaceous, grey to darkish grey, thickly lenticularly laminated with an erosive base.
			218.45	*0.11*		

ZAC			
LOG SHEET			
B/HOLE NAME	***NG108***	***PAGE***	***12 of 23***

SECTION	***DEPTH***	***WIDTH***	***LOSS***	***DESCRIPTION***
	218.45			
				Carbonaceous silty mudstone/ sandstone, black to grey, micaceous, feldspathic, lenticularly laminated with a sharp base.
	218.60	*0.15*		
				Sandstone, medium grained, feldspathic, micaceous, grey, trough cross-bedded with an erosive base.
	218.76	*0.16*		
				Carbonaceous silty mudstone/ siltstone, black to grey, micaceous, finely lenticularly laminated with a sharp base.
	218.82	*0.06*		
				Sandstone, coarse grained, feldspathic, micaceous, pale whitish grey cross-bedded with an erosive base.

			219.25	*0.43*		
						Carbonaceous silty mudstone, black, finely micaceous laminated with a sharp base.
			219.32	*0.07*		
						Sandstone, coarse grained, feldspathic, micaceous, pale whitish grey, massive with a few coarse pyrite lenses and an erosive base.
			221.00	*1.68*		
						Sandstone, medium to coarse grained, feldspathic, micaceous, darkish grey cross-bedded, lightly slumped with a sharp base.
			222.30	*1.30*		
						Sandstone, coarse grained, feldspathic, micaceous, pale whitish grey cross-bedded with an erosive base.
			222.42	*0.12*		

						Silty sandstone, dark grey to black, micaceous, turbid with randomly scattered white feldspar grains and a sharp base.
			222.92	*0.50*		
						Sandstone, coarse grained, gritty, feldspathic, micaceous, whitish grey with an erosive base.
			222.98	*0.06*		
						CONTINUED ON PAGE 13

ZAC			
LOG SHEET			
B/HOLE NAME	***NG108***	***PAGE***	***13 of 23***

SECTION	***DEPTH***	***WIDTH***	***LOSS***	***DESCRIPTION***
	222.98			
				Gritty silty sandstone, dark grey, turbid with randomly scattered white feldspar grit and a sharp base.

			223.16	*0.18*		
						Sandstone, coarse grained, feldspathic, micaceous, grey, cross-bedded with an erosive base.
			223.92	*0.76*		
						Carbonaceous silty mudstone, black, turbid with randomly scattered white feldspar grit and a sharp base.
			224.05	*0.13*		
						Sandstone, coarse grained, feldspathic, micaceous, whitish grey, cross-bedded with a gradational base.
			224.52	*0.47*		
						Sandstone, medium to coarse grained, feldspathic, micaceous, grey, lightly cross-bedded to wispy current laminated with a sharp base.
			227.38	*2.86*		*BOTTOM OF UNIT 0*
						TOP OF UNIT 1 WAVE RIPPLE MARKER

						Sandstone, fine to medium grained, feldspathic, micaceous, grey, lightly wave ripple cross-laminated to horizontally stratified with a gradational base.
			230.53	*3.15*		
						Sandstone, medium grained, feldspathic, micaceous, finely and intricately wave ripple cross-laminated, grey to darkish grey, intensely pyritic in basal 7cm to a sharp base.
			231.05	*0.52*		*BOTTOM OF UNIT 1*
						TOP OF UNIT 2 SLIVER ZONE
						Sandstone, coarse grained, feldspathic, micaceous, whitish grey, lightly cross-bedded with an erosive base.
			231.20	*0.15*		
						Sandstone, fine to medium grained, grey, finely streaky current laminated, abundantly rootlet bioturbated with a sharp base.

			232.30	1.10		
						CONTINUED ON PAGE 14

ZAC			
LOG SHEET			
B/HOLE NAME	***NG108***	***PAGE***	***14 of 23***

SECTION	***DEPTH***	***WIDTH***	***LOSS***	***DESCRIPTION***
	232.30			
				Sandstone, coarse grained, feldspathic, micaceous, whitish with an erosive base.
	232.34	0.04		
				Sandstone, medium grained, grey, current laminated, abundantly rootlet bioturbated with a sharp base.
	232.43	0.09		
				Sandstone, coarse grained, feldspathic, micaceous, whitish with an erosive base.
	232.50	0.07		

						Sandstone, fine to medium grained, grey, wispy current laminated, abundantly rootlet bioturbated with a sharp base.
			232.75	*0.25*		
						Sandstone, medium to coarse grained, feldspathic, micaceous, grey to dark grey, thickly starkly banded with a sharp base.
			233.08	*0.33*		
						Sandstone, medium to coarse grained, feldspathic, micaceous, turbid, abundantly rootlet bioturbated with a sharp base.
			233.54	*0.46*		
						Sandstone, coarse grained, feldspathic, micaceous, pale whitish grey cross-bedded with an erosive base.
			233.68	*0.14*		
						Silty sandstone, grey, micaceous, feldspathic, finely streaky laminated with a gradational base.

			234.30	*0.62*		
						Sandstone, coarse grained, feldspathic, micaceous, whitish to darkish grey, finely carbonaceous wispy current laminated, rootlet bioturbated with a channel erosive base.
			234.70	*0.40*		
						Sandstone, coarse grained, feldspathic, micaceous, whitish grey cross-bedded with an erosive base.
			235.46	*0.76*		
						Sandstone, medium to coarse grained, feldspathic, micaceous, finely wavywispy carbonaceous current laminated, lightly rootlet bioturbated with a sharp base.
			236.01	*0.55*		*CONTINUED ON PAGE 15*

ZAC			
LOG SHEET			
B/HOLE NAME	***NG108***	***PAGE***	***15 of 23***

SECTION	DEPTH	WIDTH	LOSS	DESCRIPTION
	236.01			
				Sandstone, coarse grained, feldspathic, micaceou whitish grey, cross-
				bedded with an erosive base.
	236.30	0.09		
				Sandstone, medium to barely coarse grained, grey, feldspathic, micaceous, intricately wave ripple cross-laminated, glauconitic with a gradational base.
	237.03	0.73		
				Sandstone, medium grained, grey, feldspathic, micaceous, reworked with laterally bioturbated black mudstone wisps and lenses to a gritty erosive base.
	237.37	0.34		
				Sandstone, medium to coarse grained, feldspathic, micaceous, grey, trough cross-bedded to lightly wispy carbonaceous current laminated with an erosive base
				.

			238.29	*0.92*		
						Sandstone/ siltstone/ mudstone, grey to black, lenticularly laminated, micaceous,feldspathic, laterally bioturbated with a sharp base.
			238.87	*0.58*		
						Sandstone, medium grained, feldspathic, micaceous, grey, ripple laminated to trough cross-bedded, glauconitic with an erosive base.
			239.36	*0.49*		
						Sandstone/ siltstone/ carbonaceous silty mudstone, grey to black, lenticularly laminated, lightly laterally bioturbated with a gradational base.
						.
			240.02	*0.66*		
						Carbonaceous silty mudstone/ siltstone/ sandstone, black to grey, micaceous, finely lenticularly laminated, laterally bioturbated, weak along planes of bedding with a gradational base.

			242.27	*2.25*		
						Sandstone, fine to medium grained, feldspathic, micaceous, grey to greenish, finely intricately wave ripple cross-laminated, glauconitic with a gritty channel erosive base.
			244.54	*2.27*		
						CONTINUED ON PAGE 23

ZAC

LOG SHEET

B/HOLE NAME	***NG108***	***PAGE***	***16 of 23***

SECTION	***DEPTH***	***WIDTH***	***LOSS***	***DESCRIPTION***
	244.54			
				Coaly carbonaceous mudstone, micro-micaceous black with a sharp base.
	244.80	*0.26*		*BOTTOM OF UNIT 2*
				TOP OF UNIT 3

						Sandstone, coarse grained, feldspathic, micaceous, pale whitish grey cross-bedded with an erosive base.
			251.98	*7.18*		
						Coal. Mixed, mainly bright, thickly vitrinite banded, blocky jointed with a sharp base.
			252.11	*0.13*		
						Sandy siltstone, micaceous, black, turbid with randomly scattered white
						feldspar grit and a gradational base.
			252.23	*0.12*		
						Sandstone, medium grained, feldspathic, micaceous, darkish grey, turbid, lightly slumped with a sharp base.
			252.80	*0.57*		
						Sandstone, coarse grained, feldspathic, micaceous, pale whitish grey cross-bedded with an erosive base.

			258.00	*5.20*		*BOTTOM OF UNIT 3*
						TOP OF UNIT 4 UPPER ANTHRACITE MARKER
						Coal. Mixed, mainly bright, finely vitrinite streaked, broken with a sharp base.
			258.30	*0.30*		
						Carbonaceous sandstone, black, feldspathic, micaceous, gritty with a sharp base.
			258.37	*0.07*		
						Sandy siltstone, black, finely micaceous laminated with a sharp base.
			258.67	*0.30*		
						Sandstone/ siltstone/ mudstone, dark grey to black, micaceous, lenticularly laminated with a sharp base.
			259.14	*0.47*		*BOTTOM OF UNIT 4*
						TOP OF UNIT 5
						CONTINUED ON PAGE 17

ZAC			
LOG SHEET			
B/HOLE NAME	***NG108***	***PAGE***	***17 of 23***

SECTION	***DEPTH***	***WIDTH***	***LOSS***	***DESCRIPTION***
	259.14			
				Sandstone, coarse grained, feldspathic, micaceou pale whitish grey cross-bedded with several grit band
	265.16	*6.02*		
				Sandstone, medium to coarse grained, feldspathic, micaceous, darkish grey, lightly wispy current laminated with an erosive base.
	265.69	*0.53*		*BOTTOM OF UNIT 5*
				TOP OF UNIT 6 PYRITIC SHALE MARKER
				Silty sandstone/ siltstone/ carbonaceous mudstone, grey to black, micaceous,
				lenticularly laminated with finely disseminated pyrite, weak along planes of bedding with a gradational base.

			266.29	*0.60*		
						Carbonaceous silty mudstone, black, finely micaceous laminated, abundantly pyrite streaked with a gradational base.
			266.91	*0.62*		
						Coaly carbonaceous mudstone, black, micaceous laminated with pyrite
						platelets on partings and a sharp base.
			267.34	*0.43*		
						Coal. Lustrous dull with minor vitrinite streaks and a sharp base.
			267.55	*0.21*		
						Carbonaceous silty mudstone, black, finely micaceous laminated with scattered pyrite specks and a sharp base.
			267.60	*0.05*		
						Sandy siltstone, black, finely micaceous laminated with a gradational base.

			268.08	*0.48*		*BOTTOM OF UNIT 6*
						TOP OF UNIT 7
						Sandstone, coarse grained, feldspathic, micaceous, pale whitish grey, cross-
						bedded with an erosive base.
			273.95	*5.87*		
						Coal. Mixed, mainly bright with mild pyrite streaks and a sharp base.
			274.20	*0.25*		*CONTINUED ON PAGE 23*

ZAC

LOG SHEET

B/HOLE NAME	***NG108***	***PAGE***	***18 of 23***

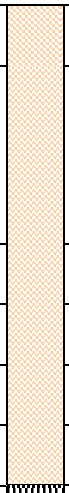
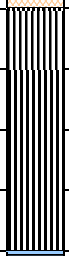
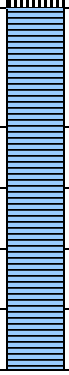
SECTION	***DEPTH***	***WIDTH***	***LOSS***	***DESCRIPTION***
	274.20			
				Carbonaceous silty mudstone, black, finely micaceou laminated with a sharp base.
	274.47	*0.27*		
				Sandstone/ siltstone/ carbonaceous mudstone, grey to black, finely streaky current laminated with a sharp base.

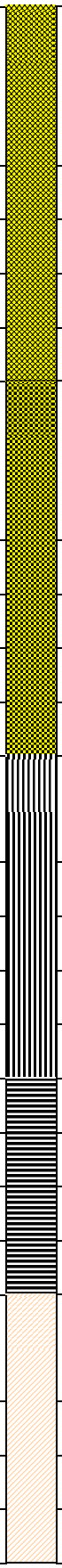
			274.83	*0.36*		
						Sandstone, medium to coarse grained, feldspathic, micaceous, grey to pale grey, cross-bedded with an erosive base.
			276.94	*2.11*		
						Carbonaceous silty mudstone/ siltstone, black to grey, streaky lenticularly laminated, micaceous with a sharp base.
			277.00	*0.06*		
						Sandstone, coarse grained, feldspathic, micaceous, grey, planar cross-bedded with an erosive base.
			278.15	*1.15*		*BOTTOM OF UNIT 7*
						TOP OF UNIT 8 ALTERNATIONS ZONE
						Sandstone/ siltstone, grey to dark grey, feldspathic, micaceous, lenticularly laminated with a sharp base.

			278.25	*0.10*		
						Coal. Mixed, mainly bright, thickly vintrinite banded, finely calcite laced.
			278.32	*0.07*		
						Coal. Lustrous dull, lightly vitrinite streaked with a sharp base.
			278.57	*0.25*		
						Carbonaceous silty mudstone/ silty sandstone, black to dark grey, micaceous, thickly banded with a sharp base.
			278.98	*0.41*		
						Sandstone, medium to coarse grained, grey, feldspathic, micaceous, thickly stratified with a sharp base.
			281.27	*2.29*		
						Carbonaceous silty mudstone, black, finely micaceous laminated with a sharp base.

			*281.33*	*0.06*		*CONTINUED ON PAGE 19*

ZAC			
LOG SHEET			
B/HOLE NAME	***NG108***	***PAGE***	***19 of 23***

SECTION			***DEPTH***	***WIDTH***	***LOSS***	***DESCRIPTION***
			*281.33*			
						Sandstone, fine to barely medium grained, grey t darkish grey, feldspathic, micaceous, streak laminated with a sharp base.
			281.43	*0.10*		
						*Coal. Dull to shaly with a sharp base.*
			281.50	*0.07*		
						*Carbonaceous silty mudstone/ siltstone, black to grey, micaceous laminated with a sharp base.*
			281.71	*0.21*		

						*Sandstone, coarse grained, feldspathic, micaceous, pale whitish grey cross-bedded to thickly stratified with an erosive base.*
			284.07	*2.36*		
						Sandstone, medium to coarse grained, feldspathic, micaceous, grey, finely black silty carbonaceous current laminated with an erosive base.
			284.40	*0.33*		
						Coal. Dull to heavy dull, shaly, steeply jointed, slightly broken with a sharp base.
			284.95	*0.55*		
						Coal. Mixed, mainly bright with a sharp base.
			285.09	*0.14*		
						Siltstone, dark grey to black, finely micaceous laminated with a gradational base.
			285.22	*0.13*		

					Sandstone, coarse grained, feldspathic, micaceous, finely streaky carbonaceous current laminated with an erosive base.
		285.25	*0.03*		
					Coal. Dull to lustrous, lightly vitrinite streaked, jointed at 55º to 60º, slightly broken with a sharp base.
		285.60	*0.35*		
					Sandstone, coarse grained, feldspathic, micaceous, grey with a black silty matrix and an erosive base.
		285.66	*0.06*		*CONTINUED ON PAGE 20*

ZAC

LOG SHEET

B/HOLE NAME	***NG108***	***PAGE***	***20 of 23***

SECTION	***DEPTH***	***WIDTH***	***LOSS***	***DESCRIPTION***
	285.66			
				Carbonaceous silty mudstone, black, finely micaceous laminated with fossil plant "hash" impressions on partings and a sharp base.

			285.96	*0.30*		
						Sandstone, fine to barely medium grained, feldspathic, micaceous, grey, finely current laminated, turbid, slumped with spectacular load cast structures and a gradational base
			286.47	*0.51*		
						Siltstone/ sandstone, black to grey, micaceous, streaky laminated to banded with a sharp base.
			286.91	*0.46*		
						Sandstone, coarse grained, feldspathic, micaceous, grey to dark grey, reworked, turbid with carbonaceous wisps and lenses, pyrite blebs, and an erosive base.
			287.30	*0.39*		
						Carbonaceous silty mudstone, black, finely micaceous laminated with a sharp base.
			288.03	*0.73*		

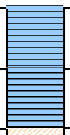
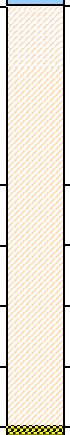
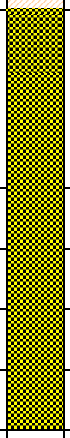
						Sandstone, fine to medium grained, feldspathic, micaceous, grey to dark grey, starkly banded to finely current laminated with a sharp base.
			288.52	*0.49*		
						Carbonaceous silty mudstone/ siltstone, black to grey, micaceous laminated with a sharp base.
			288.62	*0.10*		
						Sandstone, medium to coarse grained, feldspathic, micaceous, grey, stratified with a sharp base.
			288.87	*0.25*		
						Carbonaceous silty mudstone/ siltstone, black to dark grey, micaceous, streaky laminated with mildly scattered gritty sandstone streaks and a sharp base.
			289.38	*0.51*		
						Sandstone, coarse grained, feldspathic, micaceous, pale whitish grey with an erosive base.

			289.40	*0.02*		

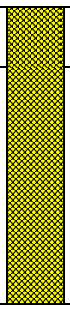
ZAC			
LOG SHEET			
B/HOLE NAME	***NG108***	***PAGE***	***21 of 23***

SECTION	***DEPTH***	***WIDTH***	***LOSS***	***DESCRIPTION***
	289.40			
				Coal. Dull to heavy dull and shaly with scattered gr and a sharp base.
	289.61	*0.21*		
				Sandstone, coarse grained, feldspathic, micaceous, carbonaceous, turbid with an erosive base.
	289.69	*0.08*		
				Coal. Lustrous dull with rare vitrinite streaks, near vertically jointed, slightly broken with a sharp base.
	289.98	*0.29*		

						Carbonaceous silty mudstone/ silty sandstone, black to dark grey, micaceous, laminated, turbid, lightly slumped with a sharp base.
			290.36	*0.38*		*BOTTOM OF UNIT 8*
						TOP OF UNIT 9 ROOF SANDSTONE
						Sandstone, coarse grained, feldspathic, micaceous, grey cross-bedded with a gradational base.
			290.66	*0.30*		
						Carbonaceous siltstone/ mudstone, black to dark grey micaceous laminated with pyrite streaks.
			290.73	*0.07*		
						Sandstone, medium to coarse grained, feldspathic, micaceous, grey with a sharp base.
			290.78	*0.05*		
						Carbonaceous silty mudstone/ siltstone, black to dark grey, micaceous laminated with a sharp base.

						
			290.88	*0.10*		
						*Sandstone, silty to medium grained, feldspathic, micaceous, grey to dark grey, lightly current laminated with a sharp base.*
			291.26	*0.38*		
						*Sandstone, medium to coarse grained, feldspathic, micaceous, grey to dark grey, thickly stratified with a sharp base.*
			291.72	*0.46*		
						CONTINUED ON PAGE 22

ZAC			
LOG SHEET			
B/HOLE NAME	***NG108***	***PAGE***	***22 of 23***

SECTION			***DEPTH***	***WIDTH***	***LOSS***	***DESCRIPTION***
			*291.72*			
						Sandstone, coarse grained, feldspathic, micaceous, pale whitish grey, planar cross-bedded with several grit bands, lightly reworked in places with mudstone wisps and lenses and an erosive base.

			295.27	*3.55*		
						Siltstone/ carbonaceous silty mudstone, dark grey to black, finely micaceous laminated with a sharp base.
			295.49	*0.22*		
						Sandstone, coarse grained, feldspathic, micaceous, pale whitish grey, starkly planar cross-bedded with an erosive ±8º base.
			297.60	*1.11*		*ROOF OF UNIT 9*
						TOP OF UNIT 10 MAIN SEAM
						Coal.
						(See detailed seam log)
			299.77	*2.17*		*BOTTOM OF UNIT 10*
						TOP OF UNIT 11
						Carbonaceous silty mudstone, black, finely micaceous laminated, fairly weak with a sharp base.

			299.82	*0.05*		
						Sandstone, fine to medium grained, feldspathic, micaceous, darkish grey, laminated with a sharp base.
			299.99	*0.17*		
						Carbonaceous silty mudstone, black, finely micaceous laminated with a sharp base.
			300.02	*0.03*		
						Sandstone, medium to coarse grained, feldspathic, micaceous, blackish to pale grey, stratified with a sharp base.
			300.97	*0.95*		
						Carbonaceous silty mudstone/ silty sandstone, black to darkish grey, micaceous laminated with a sharp base.
			301.33	*0.36*		

					CONTINUED ON PAGE 23

ZAC			
LOG SHEET			
B/HOLE NAME	***NG108***	***PAGE***	***23 of 23***

SECTION	***DEPTH***	***WIDTH***	***LOSS***	***DESCRIPTION***
	301.33			
				Sandstone, medium to coarse grained, feldspathic, micaceous, darkish grey, lightly stratified with a sharp base.
	301.65	*0.32*		
				Sandstone, coarse grained, feldspathic, micaceous, pale whitish grey with an erosive base.
	302.09	*0.44*		
				Carbonaceous silty mudstone/ siltstone, black to darkish grey, finely micaceous laminated with a sharp base.

			302.96	*0.87*		
						Sandstone, carbonaceous, black to whitish, gritty, turbid, intensely bioturbated with a gritty channel erosive base.
			303.08	*0.12*		
						Carbonaceous sandstone, black to dark grey, micaceous, lightly current laminated with a sharp base.
			303.84	*0.76*		*BOTTOM OF UNIT 11*
						TOP OF UNIT 12
						Sandstone, medium to coarse grained, feldspathic, micaceous, grey to darkish grey, lightly current laminated to cross-bedded with a gradational base.
			304.64	*0.80*		
						Sandstone, coarse grained, feldspathic, micaceous, starkly planar cross-bedded with an erosive base.
			310.04	*5.40*		*BOTTOM OF UNIT 12*

						TOP OF UNIT 13 FOOTWALL SEAM
						Coal. Dull to lustrous, lightly vitrinite streaked with a sharp base.
			310.30	*0.26*		*BOTTOM OF UNIT 13*
						TOP OF UNIT 14
						Sandstone, coarse grained, feldspathic, micaceous, pale whitish grey cross-bedded to finely wavy wispy current laminated.
			311.86	*1.56*		*End of Hole.*

Appendix 2: NG-108 Core photos



NG 108-01



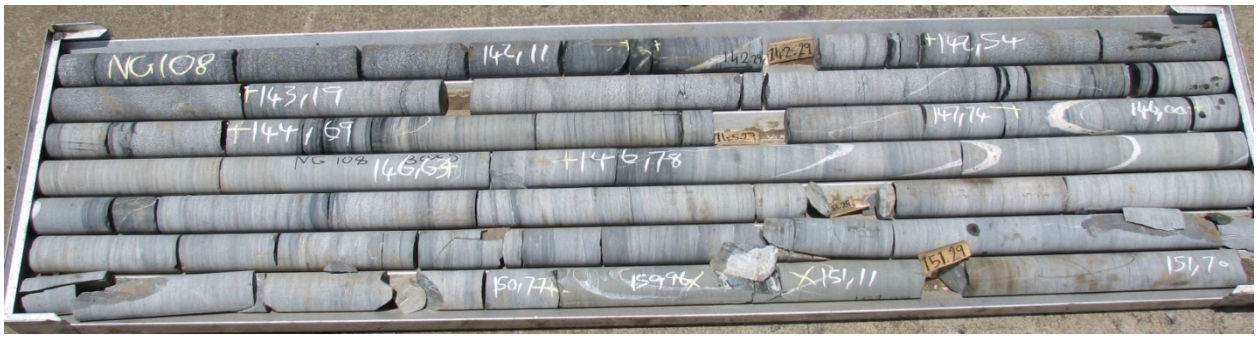
NG 108-02



NG 108-03



NG 108-04



NG 108-05



NG 108-06



NG 108-07



NG 108-08



NG 108-09



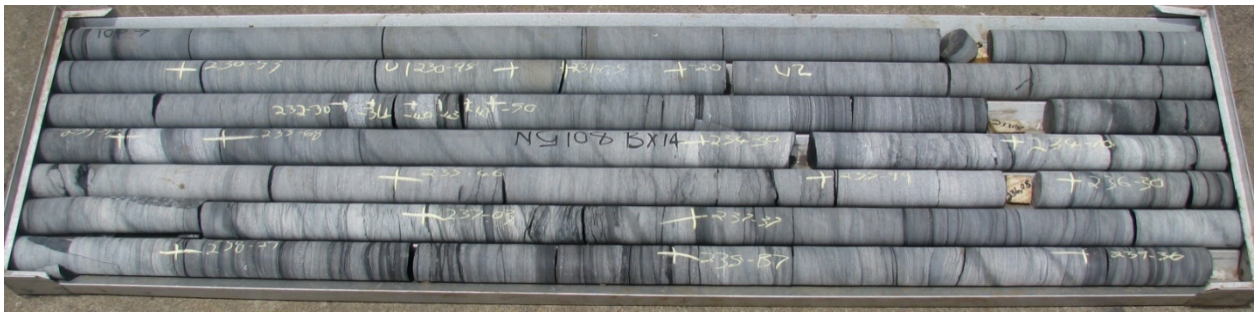
NG 108-10



NG 108-10



NG 108-11



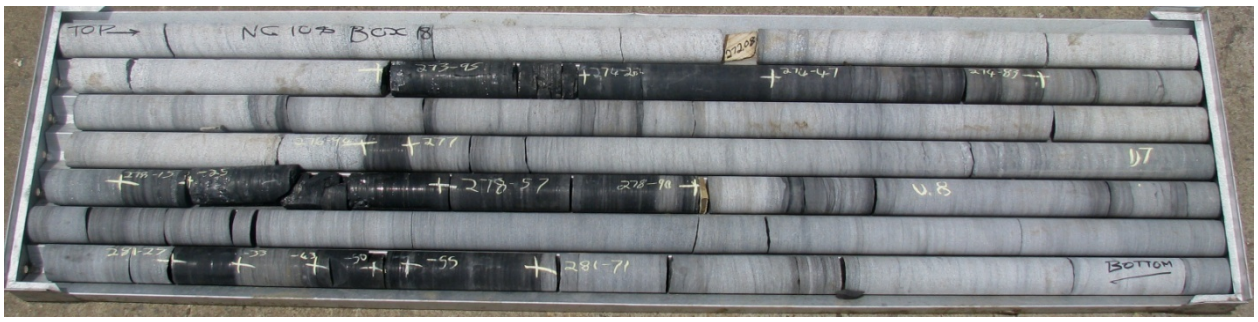
NG 108-12



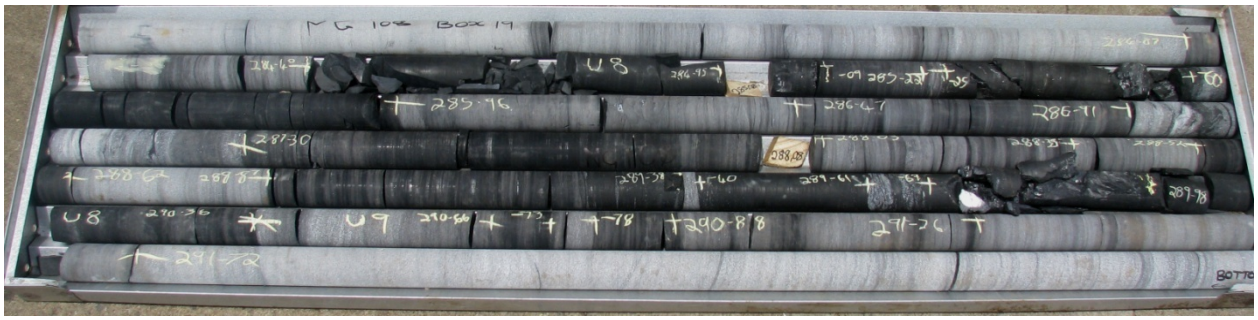
NG 108-13



NG 108-14



NG 108-15



NG 108-16



NG 108-17



NG 108-18

Appendix 3: Coal quality data and Proximate analysis data

To		Reference number:	
For Attention		Sample submitted:	**2017/08/18**
Tel:		Sample description:	
Fax:		Contact Person:	**Letho**
Cell:		Report date:	**2017/08/21**
Address \ Email:		Report status:	**Final**
		Number of pages	**1 OF 2**

TEST REPORT

			Results reported on an Air-Dry Basis							
Lab.no.	Sample name	Description	Inherent Moisture	Ash Content	Volatile Matter	Fixed carbon	Calorific Value	Total sulphur	Phos *	Total H2O
			%	%	%	Calc / %	MJ/Kg	%	%	%
121775	CS30E/03/17-CB	0.5X10MM	2.9	7.6	5.1	84.4		1.03		
121776	CS30E/03/17-CDB	0.5X10MM	2.6	8.6	5.5	83.3		0.74		
121777	CS30E/03/17-CBD	0.5X10MM	1.6	20.7	6.3	71.4		0.77		
121778	CS30EI/01/17-CB	0.5X10MM	3.0	7.7	4.8	84.5		1.56		
121779	CS30EI/01/17-CBD	0.5X10MM	2.1	14.2	5.5	78.2		1.62		
121780	CS30DI/01/17-CB	0.5X10MM	4.2	12.6	5.1	78.1		0.91		
121781	CS301/01/17-CDB	0.5X10MM	1.7	14.1	6.8	77.4		1.36		
121782	CS30DI/01/17-CBD	0.5X10MM	2.5	19.7	5.9	71.9		1.01		
121783	CS30DI/01/17-CDB	0.5X10MM	1.4	13.6	5.6	79.4		0.98		

Appendix 4: Washability analysis data

Mahlabatini District
Tel: 035 - 874 7300
Fax: 035 - 870 0807

CLIENT: CHANNEL SAMPLING
PRODUCT: CS30B (CBD)
SAMPLED DATE: 06-07-2017
REPORTING DATE: **20/07/2017**

Relative Density		FRACTIONAL Yield %	FRACTIONAL $l.H_2O$ %	FRACTIONAL Ash %	FRACTIONAL V.M. %	FRACTIONAL F.C. %	FRACTIONAL S %	FRACTIONAL Phos %	CUMULATIVE Yield %	CUMULATIVE $l.H_2O$ %	CUMULATIVE Ash %	CUMULATIVE V.M. %	CUMULATIVE F.C. %	CUMULATIVE S %	CUMULATIVE Phos %
F @	1.35	24.8	1.7	6.0	5.7	86.7	0.99		24.8	1.7	6.0	5.7	86.7	0.99	
F @	1.45	44.3	1.7	10.2	5.6	82.5	0.91		69.1	1.7	8.7	5.6	84.0	0.94	
F @	1.55	7.8	1.7	14.6	5.9	77.8	1.07		76.9	1.7	9.3	5.7	83.4	0.95	
F @	1.65	8.2	1.5	22.0	5.8	70.6	1.31		85.1	1.7	10.5	5.7	82.2	0.99	
F @	1.75	5.4	1.5	29.5	5.8	63.2	2.51		90.5	1.6	11.6	5.7	81.0	1.08	
Sink @	1.75	9.5	1.2	40.7	6.6	51.4	3.97		100.0	1.6	14.4	5.8	78.2	1.35	
Whole Coal		**100.0**	**1.6**	**14.4**	**5.8**	**78.2**	**1.35**	**0.000**	**100.0**	**1.6**	**14.4**	**5.8**	**78.2**	**1.35**	**0.000**

	Yield %	$l.H_2O$ %	Ash %	V.M. %	F.C. %	S %	Phos %
+0.5mm	98.3						
-0.5mm	1.7	2.5	18.4	5.4	73.7	3.07	
Whole Coal		**2.5**	**18.4**	**5.4**	**73.7**	**3.07**	**0.000**

Items marked with an (*) is not accredited.

TEST	METHOD
Total Moisture	ISO 589
Moisture in Analysis	SANS 5925
Ash Content	ISO 1171
Volatile Matter	ISO 562
Total Sulphur	ASTM D4239
*Sizing	ISO 1953

Mahlabatini District
Tel: 035 - 874 7300
Fax: 035 - 870 0807

CLIENT: CHANNEL SAMPLING
PRODUCT: CS30B (CDB)
SAMPLED DATE: 06-07-2017
REPORTING DATE: **20/07/2017**

Relative Density		FRACTIONAL Yield %	FRACTIONAL $l.H_2O$ %	FRACTIONAL Ash %	FRACTIONAL V.M. %	FRACTIONAL F.C. %	FRACTIONAL S %	FRACTIONAL Phos %	CUMULATIVE Yield %	CUMULATIVE $l.H_2O$ %	CUMULATIVE Ash %	CUMULATIVE V.M. %	CUMULATIVE F.C. %	CUMULATIVE S %	CUMULATIVE Phos %
F @	1.35	4.7	2.4	6.3	4.7	86.7	0.61		4.7	2.4	6.3	4.7	86.7	0.61	
F @	1.45	36.6	2.8	6.5	4.5	86.2	0.68		41.3	2.7	6.5	4.6	86.2	0.67	
F @	1.55	42.0	2.8	8.7	4.8	83.7	0.78		83.3	2.8	7.6	4.7	85.0	0.73	
F @	1.65	11.7	2.5	14.7	5.0	77.9	1.28		94.9	2.7	8.5	4.7	84.1	0.79	
F @	1.75	3.1	2.3	24.0	6.5	67.2	1.75		98.1	2.7	9.0	4.8	83.5	0.83	
Sink @	1.75	1.9	1.9	36.5	7.6	54.0	5.77		100.0	2.7	9.5	4.8	83.0	0.92	
Whole Coal		**100.0**	**2.7**	**9.5**	**4.8**	**83.0**	**0.92**	**0.000**	**100.0**	**2.7**	**9.5**	**4.8**	**83.0**	**0.92**	**0.000**

	Yield %	$l.H_2O$ %	Ash %	V.M. %	F.C. %	S %	Phos %
+0.5mm	97.0						
-0.5mm	3.0	5.7	9.1	2.1	83.1	0.84	
Whole Coal		**5.7**	**9.1**	**2.1**	**83.1**	**0.84**	**0.000**

Items marked with an (*) is not accredited.

TEST	METHOD
Total Moisture	ISO 589
Moisture in Analysis	SANS 5925
Ash Content	ISO 1171
Volatile Matter	ISO 562
Total Sulphur	ASTM D4239
*Sizing	ISO 1953

Mahlabatini District
Tel: 035 - 874 7300
Fax: 035 - 870 0807

CLIENT: CHANNEL SAMPLING
PRODUCT: CS 30B-CB
SAMPLED DATE: 06-07-2017
REPORTING DATE: **20/07/2017**

Relative Density		FRACTIONAL							CUMULATIVE						
		Yield %	I.H_2O %	Ash %	V.M. %	F.C. %	S %	Phos %	Yield %	I.H_2O %	Ash %	V.M. %	F.C. %	S %	Phos %
F @	1.35	4.5	4.5	6.4	4.6	84.5	1.18		4.5	4.5	6.4	4.6	84.5	1.18	
F @	1.45	8.8	5.3	7.0	4.0	83.8	1.10		13.3	5.0	6.8	4.2	84.0	1.13	
F @	1.55	42.4	4.8	10.1	5.3	79.9	2.00		55.7	4.8	9.3	5.0	80.9	1.79	
F @	1.65	29.6	4.9	10.4	4.7	80.1	1.14		85.2	4.9	9.6	4.9	80.6	1.57	
F @	1.75	7.3	4.7	19.7	6.0	69.7	1.25		92.5	4.8	10.4	5.0	79.7	1.54	
Sink @	1.75	7.5	4.0	33.6	7.8	54.6	5.44		100.0	4.8	12.2	5.2	77.9	1.83	
Whole Coal		**100.0**	**4.8**	**12.2**	**5.2**	**77.9**	**1.83**	**0.000**	**100.0**	**4.8**	**12.2**	**5.2**	**77.9**	**1.83**	**0.000**

	Yield %	I.H_2O %	Ash %	V.M. %	F.C. %	S %	Phos %
+0.5mm	96.8						
-0.5mm	3.2	4.3	22.1	11.4	62.3	1.06	
Whole Coal		**4.3**	**22.1**	**11.4**	**62.3**	**1.06**	**0.000**

Items marked with an (*) is not accredited.

TEST	METHOD
Total Moisture	ISO 589
Moisture in Analysis	SANS 5925
Ash Content	ISO 1171
Volatile Matter	ISO 562
Total Sulphur	ASTM D4239
*Sizing	ISO 1953

Mahlabatini District
Tel: 035 - 874 7300
Fax: 035 - 870 0807

CLIENT: CHANNEL SAMPLING
PRODUCT: CS30AI(CBD)
SAMPLED DATE: 06-07-2017
REPORTING DATE: **20/07/2017**

Relative Density		FRACTIONAL							CUMULATIVE						
		Yield %	I.H_2O %	Ash %	V.M. %	F.C. %	S %	Phos %	Yield %	I.H_2O %	Ash %	V.M. %	F.C. %	S %	Phos %
F @	1.35	7.2	2.8	7.2	5.4	84.5	1.10		7.2	2.8	7.2	5.4	84.5	1.10	
F @	1.45	49.9	2.9	9.0	5.6	82.6	1.04		57.1	2.9	8.8	5.5	82.8	1.05	
F @	1.55	17.7	2.6	12.3	6.0	79.0	1.51		74.8	2.8	9.6	5.7	81.9	1.16	
F @	1.65	9.1	3.2	16.2	5.8	74.9	1.52		83.9	2.9	10.3	5.7	81.1	1.20	
F @	1.75	3.4	2.3	26.0	7.0	64.8	2.64		87.3	2.8	10.9	5.7	80.5	1.25	
Sink @	1.75	12.7	1.8	40.1	7.4	50.6	4.11		100.0	2.7	14.6	5.9	76.7	1.62	
Whole Coal		**100.0**	**2.7**	**14.6**	**5.9**	**76.7**	**1.62**	**0.000**	**100.0**	**2.7**	**14.6**	**5.9**	**76.7**	**1.62**	**0.000**

	Yield %	I.H_2O %	Ash %	V.M. %	F.C. %	S %	Phos %
+0.5mm	99.6						
-0.5mm	0.4	2.9	28.3	8.6	60.2	1.17	
Whole Coal		**2.9**	**28.3**	**8.6**	**60.2**	**1.17**	**0.000**

Items marked with an (*) is not accredited.

TEST	METHOD
Total Moisture	ISO 589
Moisture in Analysis	SANS 5925
Ash Content	ISO 1171
Volatile Matter	ISO 562
Total Sulphur	ASTM D4239
*Sizing	ISO 1953

Mahlabatini District
Tel: 035 - 874 7300
Fax: 035 - 870 0807

CLIENT: CHANNEL SAMPLING
PRODUCT: CS30AI (CDB)
SAMPLED DATE: 06-07-2017
REPORTING DATE: **20/07/2017**

Relative Density		FRACTIONAL							CUMULATIVE						
		Yield %	$I.H_2O$ %	Ash %	V.M. %	F.C. %	S %	Phos %	Yield %	$I.H_2O$ %	Ash %	V.M. %	F.C. %	S %	Phos %
F @	1.35	5.5	2.4	8.9	5.0	83.7	0.90		5.5	2.4	8.9	5.0	83.7	0.90	
F @	1.45	27.9	2.0	10.4	7.5	80.1	0.70		33.4	2.1	10.2	7.1	80.7	0.73	
F @	1.55	50.5	2.1	13.3	8.1	76.5	0.61		84.0	2.1	12.1	7.7	78.2	0.66	
F @	1.65	12.6	1.9	20.2	9.4	68.5	0.60		96.6	2.1	13.1	7.9	76.9	0.65	
F @	1.75	2.2	1.8	30.2	8.6	59.4	0.54		98.8	2.1	13.5	7.9	76.5	0.65	
Sink @	1.75	1.2	2.1	36.6	9.6	51.8	1.77		100.0	2.1	13.8	7.9	76.2	0.66	
Whole Coal		**100.0**	**2.1**	**13.8**	**7.9**	**76.2**	**0.66**	**0.000**	**100.0**	**2.1**	**13.8**	**7.9**	**76.2**	**0.66**	**0.000**

	Yield %	$I.H_2O$ %	Ash %	V.M. %	F.C. %	S %	Phos %
+0.5mm	97.6						
-0.5mm	2.4				100.0		
Whole Coal		**0.0**	**0.0**	**0.0**	**100.0**	**0.00**	**0.000**

Items marked with an (*) is not accredited.

TEST	METHOD
Total Moisture	ISO 589
Moisture in Analysis	SANS 5925
Ash Content	ISO 1171
Volatile Matter	ISO 562
Total Sulphur	ASTM D4239
*Sizing	ISO 1953

Mahlabatini District
Tel: 035 - 874 7300
Fax: 035 - 870 0807

CLIENT: CHANNEL SAMPLING
PRODUCT: CS 30AI-CB
SAMPLED DATE: 06-07-2017
REPORTING DATE: **20/07/2017**

Relative Density		FRACTIONAL Yield %	FRACTIONAL $l.H_2O$ %	FRACTIONAL Ash %	FRACTIONAL V.M. %	FRACTIONAL F.C. %	FRACTIONAL S %	FRACTIONAL Phos %	CUMULATIVE Yield %	CUMULATIVE $l.H_2O$ %	CUMULATIVE Ash %	CUMULATIVE V.M. %	CUMULATIVE F.C. %	CUMULATIVE S %	CUMULATIVE Phos %
F @	1.35	5.3	2.2	7.7	4.8	85.2	1.63		5.3	2.2	7.7	4.8	85.2	1.63	
F @	1.45	21.3	2.3	11.2	4.8	81.8	1.31		26.6	2.3	10.5	4.8	82.4	1.37	
F @	1.55	30.6	2.1	11.5	4.6	81.8	1.36		57.2	2.2	11.0	4.7	82.1	1.37	
F @	1.65	14.5	2.3	18.8	4.9	74.1	1.95		71.7	2.2	12.6	4.7	80.5	1.48	
F @	1.75	7.8	2.3	24.9	5.6	67.2	3.79		79.5	2.2	13.8	4.8	79.2	1.71	
Sink @	1.75	20.5	1.7	42.4	1.2	54.7	14.43		100.0	2.1	19.7	4.1	74.2	4.31	
Whole Coal		**100.0**	**2.1**	**19.7**	**4.1**	**74.2**	**4.31**	**0.000**	**100.0**	**2.1**	**19.7**	**4.1**	**74.2**	**4.31**	**0.000**

	Yield %	$l.H_2O$ %	Ash %	V.M. %	F.C. %	S %	Phos %
+0.5mm	71.3						
-0.5mm	28.7	2.0	32.7	12.7	52.6	2.82	
Whole Coal		**2.0**	**32.7**	**12.7**	**52.6**	**2.82**	**0.000**

Items marked with an (*) is not accredited.

TEST	METHOD
Total Moisture	ISO 589
Moisture in Analysis	SANS 5925
Ash Content	ISO 1171
Volatile Matter	ISO 562
Total Sulphur	ASTM D4239
*Sizing	ISO 1953

Mahlabatini District
Tel: 035 - 874 7300
Fax: 035 - 870 0807

CLIENT: CHANNEL SAMPLING
PRODUCT: CS30D (CBD)
SAMPLED DATE: 06-07-2017
REPORTING DATE: **20/07/2017**

Relative Density		FRACTIONAL Yield %	FRACTIONAL $l.H_2O$ %	FRACTIONAL Ash %	FRACTIONAL V.M. %	FRACTIONAL F.C. %	FRACTIONAL S %	FRACTIONAL Phos %	CUMULATIVE Yield %	CUMULATIVE $l.H_2O$ %	CUMULATIVE Ash %	CUMULATIVE V.M. %	CUMULATIVE F.C. %	CUMULATIVE S %	CUMULATIVE Phos %
F @	1.35	5.1	3.2	6.2	4.3	86.3	1.45		5.1	3.2	6.2	4.3	86.3	1.45	
F @	1.45	40.6	3.0	7.1	4.9	85.1	1.63		45.6	3.0	7.0	4.8	85.2	1.61	
F @	1.55	42.3	2.9	8.6	4.9	83.7	1.80		88.0	2.9	7.7	4.9	84.5	1.70	
F @	1.65	7.0	2.0	15.6	5.0	77.4	2.88		94.9	2.8	8.3	4.9	84.0	1.79	
Sink @	1.65	5.1	2.1	22.9	7.1	67.9	12.22		100.0	2.8	9.1	5.0	83.1	2.32	
Whole Coal		**100.0**	**2.8**	**9.1**	**5.0**	**83.1**	**2.32**	**0.000**	**100.0**	**2.8**	**9.1**	**5.0**	**83.1**	**2.32**	**0.000**

	Yield %	$l.H_2O$ %	Ash %	V.M. %	F.C. %	S %	Phos %
+0.5mm	97.0						
-0.5mm	3.0	2.5	23.5	7.5	66.5	2.15	
Whole Coal		**2.5**	**23.5**	**7.5**	**66.5**	**2.15**	**0.000**

Items marked with an (*) is not accredited.

TEST	METHOD
Total Moisture	ISO 589
Moisture in Analysis	SANS 5925
Ash Content	ISO 1171
Volatile Matter	ISO 562
Total Sulphur	ASTM D4239
*Sizing	ISO 1953

Mahlabatini District
Tel: 035 - 874 7300
Fax: 035 - 870 0807

CLIENT: CHANNEL SAMPLING
PRODUCT: CS30D (CDB)
SAMPLED DATE: 06-07-2017
REPORTING DATE: **20/07/2017**

Relative Density		FRACTIONAL Yield %	FRACTIONAL $I.H_2O$ %	FRACTIONAL Ash %	FRACTIONAL V.M. %	FRACTIONAL F.C. %	FRACTIONAL S %	FRACTIONAL Phos %	CUMULATIVE Yield %	CUMULATIVE $I.H_2O$ %	CUMULATIVE Ash %	CUMULATIVE V.M. %	CUMULATIVE F.C. %	CUMULATIVE S %	CUMULATIVE Phos %
F @	1.35	13.3	2.8	6.5	7.2	83.5	0.75		13.3	2.8	6.5	7.2	83.5	0.75	
F @	1.45	28.4	2.5	8.8	7.7	81.1	0.78		41.6	2.5	8.0	7.6	81.9	0.77	
F @	1.55	45.2	2.9	10.3	7.2	79.7	0.76		86.9	2.8	9.2	7.3	80.7	0.77	
F @	1.65	6.4	1.9	19.1	7.6	71.4	1.03		93.2	2.7	9.9	7.4	80.1	0.78	
F @	1.75	2.4	3.4	23.6	4.7	68.4	2.88		95.6	2.7	10.2	7.3	79.8	0.84	
Sink @	1.75	4.4	1.7	39.1	6.4	52.8	2.11		100.0	2.7	11.5	7.3	78.6	0.89	
Whole Coal		**100.0**	**2.7**	**11.5**	**7.3**	**78.6**	**0.89**	**0.000**	**100.0**	**2.7**	**11.5**	**7.3**	**78.6**	**0.89**	**0.000**

	Yield %	$I.H_2O$ %	Ash %	V.M. %	F.C. %	S %	Phos %
+0.5mm	97.1						
-0.5mm	2.9	2.7	14.2	6.2	77.0	0.91	
Whole Coal		**2.7**	**14.2**	**6.2**	**77.0**	**0.91**	**0.000**

Items marked with an (*) is not accredited.

TEST	METHOD
Total Moisture	ISO 589
Moisture in Analysis	SANS 5925
Ash Content	ISO 1171
Volatile Matter	ISO 562
Total Sulphur	ASTM D4239
*Sizing	ISO 1953

Tel: 035 - 874 7300
Fax: 035 - 870 0807

CLIENT: CHANNEL SAMPLING
PRODUCT: CS 30D-CB
SAMPLED DATE: 06-07-2017
REPORTING DATE: **20/07/2017**

Relative Density		FRACTIONAL Yield %	FRACTIONAL $I.H_2O$ %	FRACTIONAL Ash %	FRACTIONAL V.M. %	FRACTIONAL F.C. %	FRACTIONAL S %	FRACTIONAL Phos %	CUMULATIVE Yield %	CUMULATIVE $I.H_2O$ %	CUMULATIVE Ash %	CUMULATIVE V.M. %	CUMULATIVE F.C. %	CUMULATIVE S %	CUMULATIVE Phos %
F @	1.35	13.1	2.7	8.6	5.2	83.5	1.02		13.1	2.7	8.6	5.2	83.5	1.02	
F @	1.45	33.1	3.0	8.7	5.1	83.2	1.16		46.2	2.9	8.7	5.1	83.3	1.12	
F @	1.55	36.2	3.0	14.6	5.6	76.8	1.41		82.4	3.0	11.3	5.3	80.5	1.25	
F @	1.65	9.3	2.9	18.4	6.8	72.0	2.86		91.8	2.9	12.0	5.5	79.6	1.41	
F @	1.75	2.0	2.5	33.4	5.0	59.1	5.50		93.8	2.9	12.5	5.5	79.2	1.50	
Sink @	1.75	6.2	2.8	41.0	5.5	50.7	1.06		100.0	2.9	14.2	5.5	77.4	1.47	
Whole Coal		**100.0**	**2.9**	**14.2**	**5.5**	**77.4**	**1.47**	**0.000**	**100.0**	**2.9**	**14.2**	**5.5**	**77.4**	**1.47**	**0.000**

	Yield %	$I.H_2O$ %	Ash %	V.M. %	F.C. %	S %	Phos %
+0.5mm	98.0						
-0.5mm	2.0				100.0		
Whole Coal		**0.0**	**0.0**	**0.0**	**100.0**	**0.00**	**0.000**

Items marked with an (*) is not accredited.

TEST	METHOD
Total Moisture	ISO 589
Moisture in Analysis	SANS 5925
Ash Content	ISO 1171
Volatile Matter	ISO 562
Total Sulphur	ASTM D4239
*Sizing	ISO 1953

Appendix 5: Petrographic analyses data and Maceral group analyses data

CLIENT:	Blessing, Wits
PROJECT:	anthracite
DATE:	31-Aug-17
JOB / SAMPLE NUMBERS:	
ANALYST:	N. Nendouvhada / Nikki Wagner
ICCP ACCREDITATION:	ICCP/SCAP-056/AB ; ICCP/CBAP/056

Table 1: MACERAL GROUP ANALYSIS (% BY VOLUME)

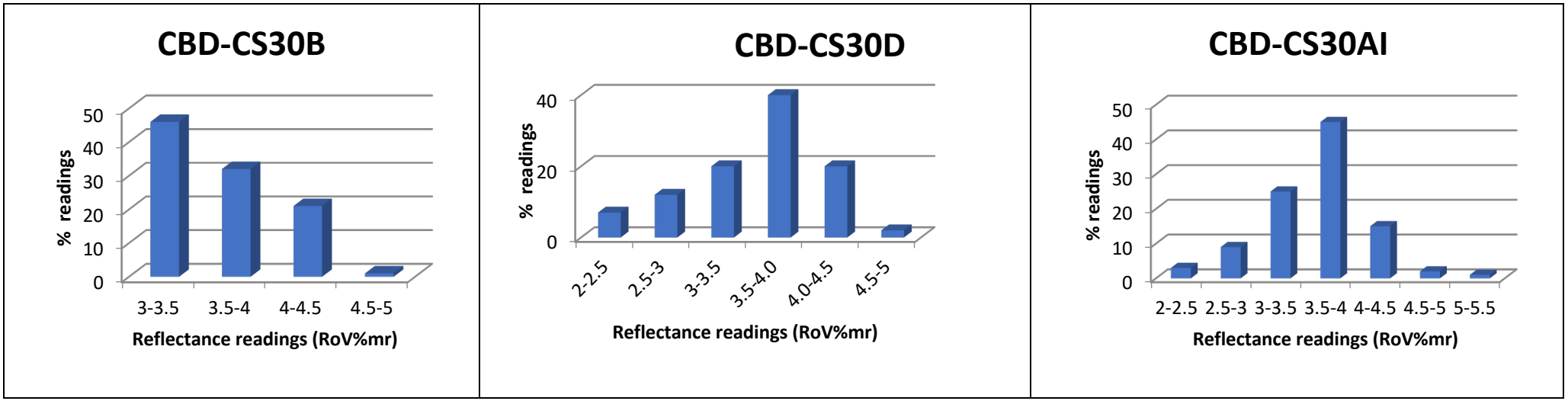
THESE RESULTS RELATE ONLY TO THE SAMPLES ANALYSED

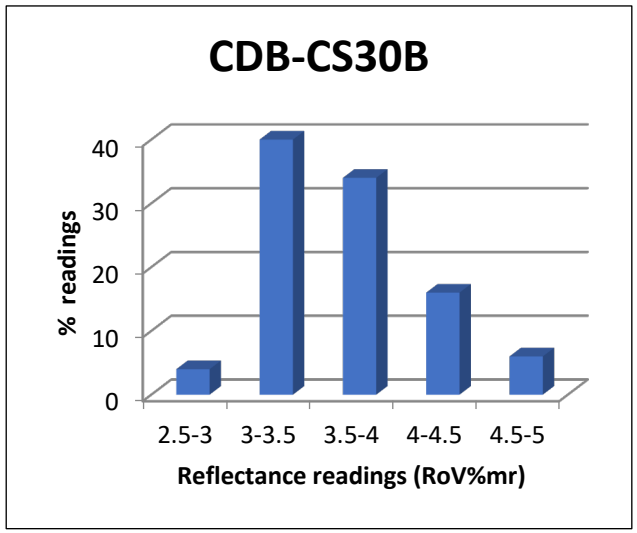
Sample no:		CBD		CDB		CB		CBD		CDB		CB		CBD		CDB		CB	
Sample identification:																			
		inc. mm	mmf	inc. mm	mmf	inc. mm	mmf	inc. mm	mmf	inc. mm	mmf	inc. mm	mmf	inc. mm	mmf	inc. mm	mmf	inc. mm	mmf
MACERAL GROUP	MACERAL (vol%)	vol%	vol%	vol%	vol%	vol%	vol%	vol%	vol%	vol%	vol%	vol%	vol%	vol%	vol%	vol%	vol%	vol%	vol%
Vitrinite	telinite	0.0	0.0	0.0	0.0	0.0	0.0	0.0	0.0	0.4	0.4	0.0	0.0	0.2	0.2	0.2	0.2	0.2	0.2
	collotelinite	17.8	19.9	6.6	6.7	50.6	52.3	24.0	27.2	12.3	12.8	54.0	54.7	30.0	34.4	18.8	19.4	36.4	37.4
	vitrodetrinite	0.0	0.0	0.0	0.0	0.0	0.0	0.0	0.0	0.0	0.0	0.0	0.0	0.0	0.0	0.0	0.0	0.0	0.0
	collodetrinite	4.0	4.5	1.2	1.2	8.4	8.7	8.2	9.3	0.2	0.2	12.2	12.4	6.0	6.9	3.2	3.3	3.2	3.3
	corpogelinite	0.0	0.0	0.0	0.0	0.0	0.0	0.0	0.0	0.0	0.0	0.0	0.0	0.2	0.2	0.0	0.0	0.0	0.0
	gelinite	0.2	0.2	0.2	0.2	0.0	0.0	0.0	0.0	0.0	0.0	0.0	0.0	0.0	0.0	0.0	0.0	0.2	0.2
	pseudovitrinite	0.0	0.0	0.0	0.0	0.6	0.6	0.0	0.0	0.0	0.0	0.0	0.0	0.0	0.0	0.0	0.0	0.0	0.0
Inertinite	fusinite	10.4	11.6	7.8	7.9	4.8	5.0	17.4	19.7	22.7	23.7	7.0	7.1	10.5	12.0	12.6	13.0	1.6	1.6
	reactive semifusinite	0.0	0.0	0.0	0.0	0.0	0.0	0.0	0.0	0.0	0.0	0.0	0.0	0.0	0.0	0.0	0.0	0.0	0.0
	inert semifusinite	30.1	33.6	43.0	43.5	18.2	18.8	14.4	16.3	35.4	37.0	21.9	22.2	26.0	29.7	50.6	52.3	27.6	28.4
	micrinite	0.2	0.2	0.0	0.0	0.2	0.2	0.0	0.0	0.0	0.0	0.0	0.0	0.0	0.0	0.0	0.0	0.0	0.0
	macrinite	0.0	0.0	0.0	0.0	0.2	0.2	0.0	0.0	0.0	0.0	0.0	0.0	0.0	0.0	0.2	0.2	0.0	0.0
	secretinite	5.4	6.0	2.8	2.8	0.2	0.2	1.4	1.6	4.8	5.0	0.0	0.0	1.7	2.0	2.8	2.9	1.2	1.2
	funginite	0.0	0.0	0.0	0.0	0.0	0.0	0.0	0.0	0.0	0.0	0.0	0.0	0.0	0.0	0.0	0.0	0.0	0.0
	inertodetrinite R	0.0	0.0	0.6	0.6	0.0	0.0	0.0	0.0	0.0	0.0	0.0	0.0	0.0	0.0	0.0	0.0	0.0	0.0
	inertodetrinite I	21.4	23.9	36.6	37.0	13.6	14.0	22.8	25.9	19.9	20.8	3.6	3.7	12.6	14.4	8.4	8.7	26.8	27.6
Liptinite	sporinite	0.0	0.0	0.0	0.0	0.0	0.0	0.0	0.0	0.0	0.0	0.0	0.0	0.0	0.0	0.0	0.0	0.0	0.0
	cutinite	0.0	0.0	0.0	0.0	0.0	0.0	0.0	0.0	0.0	0.0	0.0	0.0	0.0	0.0	0.0	0.0	0.0	0.0
	resinite	0.0	0.0	0.0	0.0	0.0	0.0	0.0	0.0	0.0	0.0	0.0	0.0	0.0	0.0	0.0	0.0	0.0	0.0
	alginite	0.0	0.0	0.0	0.0	0.0	0.0	0.0	0.0	0.0	0.0	0.0	0.0	0.0	0.0	0.0	0.0	0.0	0.0
	liptodetrinite	0.0	0.0	0.0	0.0	0.0	0.0	0.0	0.0	0.0	0.0	0.0	0.0	0.0	0.0	0.0	0.0	0.0	0.0
	suberinite	0.0	0.0	0.0	0.0	0.0	0.0	0.0	0.0	0.0	0.0	0.0	0.0	0.0	0.0	0.0	0.0	0.0	0.0
	exsudatinite	0.0	0.0	0.0	0.0	0.0	0.0	0.0	0.0	0.0	0.0	0.0	0.0	0.0	0.0	0.0	0.0	0.0	0.0
Mineral matter	clay	3.2		1.2		0.4		8		2.0		0.2		3.7		1.4		1.6	
	quartz	0.2		0.0		0.0		0		1.6		0		1.0		0.0		0.0	
	sulfide	3.8		0.0		2.8		3.6		0.2		0.8		2.3		1.2		1.2	
	carbonate	3.2		0.0		0.0		0.2		0.4		0.2		5.6		0.6		0.0	
	other	0.0		0.0		0.0		0.0		0.0		0.0		0.0		0.0		0.0	
SUMMARY TABLE																			
MACERAL GROUP	**VITRINITE**	**22.0**	**24.6**	**8.0**	**8.1**	**59.6**	**61.6**	**32.2**	**36.5**	**12.9**	**13.4**	**66.3**	**67.1**	**36.4**	**41.7**	**22.2**	**22.9**	**40.0**	**41.2**
TOTALS (vol%)	**INERTINITE**	**67.5**	**75.4**	**90.8**	**91.9**	**37.2**	**38.4**	**56.0**	**63.5**	**82.9**	**86.6**	**32.5**	**32.9**	**50.8**	**58.1**	**74.6**	**77.1**	**57.2**	**58.8**
	LIPTINITE	**0.0**	**0.0**	**0.0**	**0.0**	**0.0**	**0.0**	**0.0**	**0.0**	**0.0**	**0.0**	**0.0**	**0.0**	**0.0**	**0.0**	**0.0**	**0.0**	**0.0**	**0.0**
	MINERAL MATTER	**10.4**		**1.2**		**3.2**		**11.8**		**4.2**		**1.2**		**12.6**		**3.2**		**2.8**	
	TOTAL INERTINITE	**67.5**	**75.4**	**90.8**	**91.9**	**37.2**	**38.4**	**56.0**	**63.5**	**82.9**	**86.6**	**32.5**	**32.9**	**50.8**	**58.1**	**74.6**	**77.1**	**57.2**	**58.8**
	TOTAL REACTIVE MACERALS	**22.0**	**24.6**	**8.6**	**8.7**	**59.6**	**61.6**	**32.2**	**36.5**	**12.9**	**13.4**	**66.3**	**67.1**	**36.4**	**41.7**	**22.2**	**22.9**	**40.0**	**41.2**

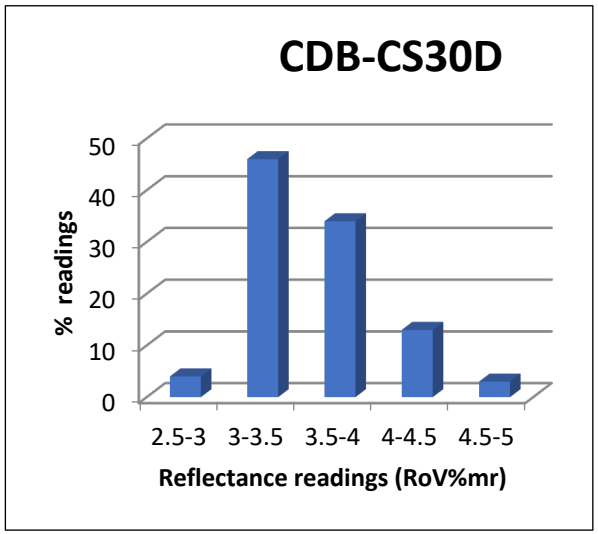
TABLE 2: VITRINITE REFLECTANCE ANALYSIS (RoV%)

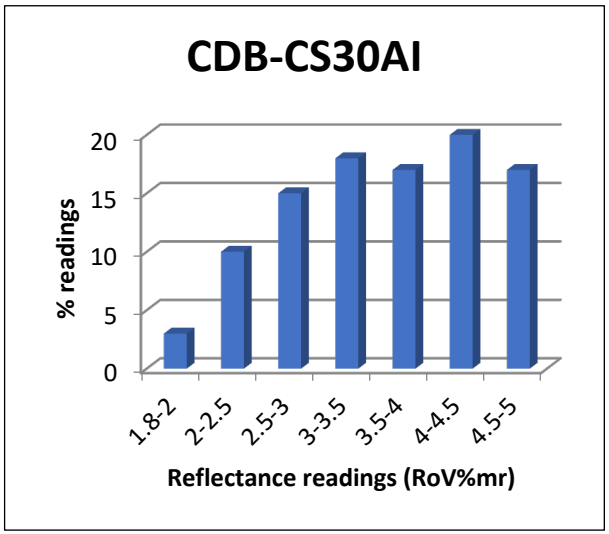
Sample no:		CBD	CDB	CB	CBD	CDB	CB	CBD	CDB	CB
Sample identification:										
Vitrinite reflectance	**Rrandom**	**3.64**	**3.65**	**4.24**	**3.56**	**3.53**	**4.02**	**3.61**	**3.61**	**4.16**
(RoV%)	st. dev.	0.37	0.44	0.37	0.55	0.9	0.71	0.48	0.41	0.37
	max	4.57	4.91	5.15	4.61	4.83	5.05	5.17	4.55	5.17
	min	2.83	2.51	3.54	2.03	1.83	2.4	2.37	2.80	3.56
	RANK CATEGORY	High rank B	High rank B	High rank A	High rank B	High rank B	High rank B	High rank B	High rank B	High rank A

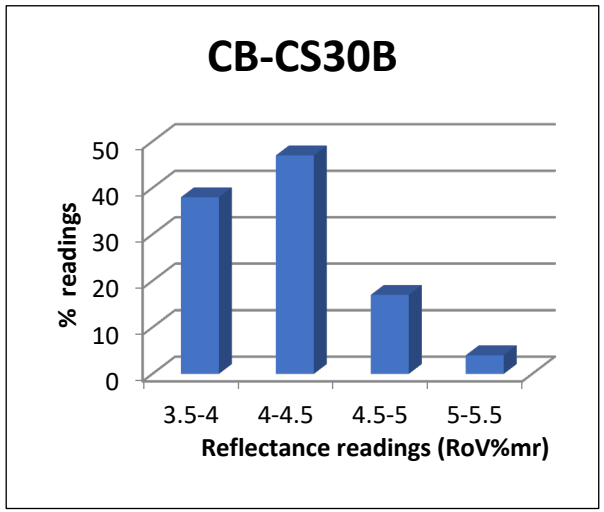
Appendix 6: Reflectance of Vintrinite analysis (RoV%) histograms

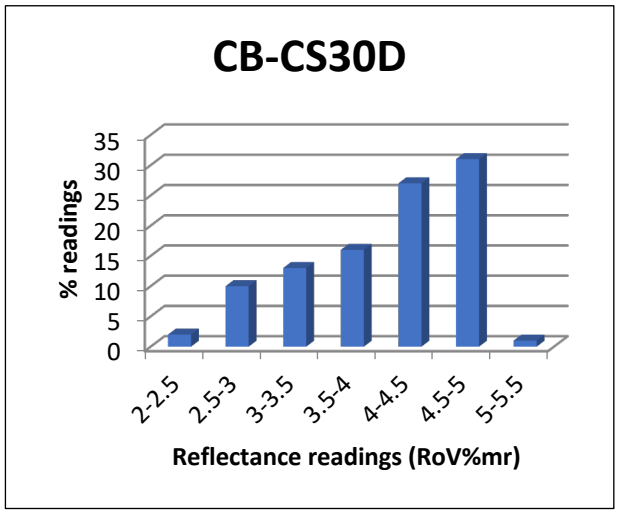


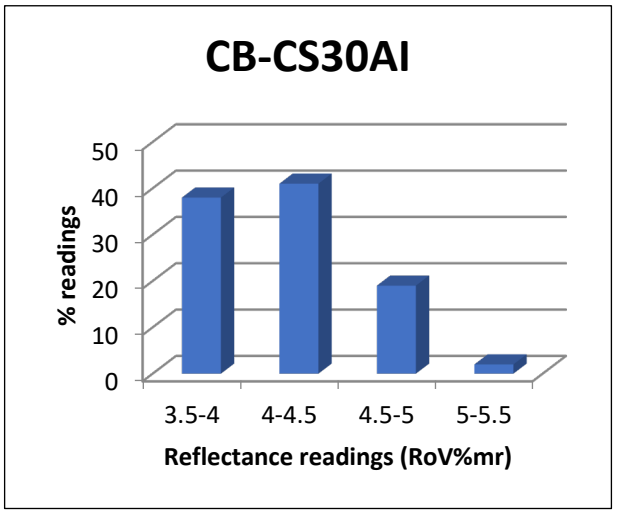

CDB-CS30B
% readings
40
30
20
10
0
2.5-3
3-3.5
3.5-4
4-4.5
4.5-5
Reflectance readings (RoV%mr)


CDB-CS30D
% readings
50
40
30
20
10
0
2.5-3
3-3.5
3.5-4
4-4.5
4.5-5
Reflectance readings (RoV%mr)


CDB-CS30AI
% readings
20
15
10
5
0
1.8-2
2-2.5
2.5-3
3-3.5
3.5-4
4-4.5
4.5-5
Reflectance readings (RoV%mr)


CB-CS30B
% readings
50
40
30
20
10
0
3.5-4
4-4.5
4.5-5
5-5.5
Reflectance readings (RoV%mr)


CB-CS30D
% readings
35
30
25
20
15
10
5
0
2-2.5
2.5-3
3-3.5
3.5-4
4-4.5
4.5-5
5-5.5
Reflectance readings (RoV%mr)


CB-CS30AI
% readings
50
40
30
20
10
0
3.5-4
4-4.5
4.5-5
5-5.5
Reflectance readings (RoV%mr)